Physics – Uspekhi **43** (8) 799 – 839 (2000)

REVIEWS OF TOPICAL PROBLEMS

PACS numbers: **21.90.+f**, **23.90.+w**, **24.90.+d**, **25.90.+k**

Exotic processes in nuclear physics

K N Mukhin, O O Patarakin

DOI: 10.1070/PU2000v043n08ABEH000802

Contents

1. Introduction **799**
1.1 Subject and content of the review; 1.2 Methodological remarks
2. History of the discovery and study of radioactivity **802**
2.1 Natural radioactivity; 2.2 Artificial radioactivity
3. The first exotic feature — nuclear isomerism **804**
4. In the footsteps of the discovery of the century **806**
4.1 Uranium fission; 4.2 Delayed neutrons; 4.3 The discovery and production of the first transuranium elements; 4.4 Spontaneous fission of uranium and transuranium elements; 4.5 Spontaneous fission of nuclei in the isomeric state; 4.6 Delayed fission
5. Proton radioactivity **811**
5.1 Retarded protons; 5.2 Isomeric proton decay; 5.3 Proton decay of a nucleus from the ground state; 5.4 Double-proton radioactivity
6. Neutron radioactivity **815**
6.1 General ideas concerning the possibility of neutron radioactivity; 6.2 Delayed double-neutron radioactivity; 6.3 Delayed triple-neutron radioactivity and tritium radioactivity
7. Cluster radioactivity **817**
7.1 The prediction of cluster radioactivity; 7.2 Carbon radioactivity; 7.3 Neon, magnesium, and silicon radioactivities; 7.4 The mechanism of cluster radioactivity; 7.5 Cluster decay of curium
8. Double β-decay **824**
8.1 Two methods for searching 2β-decay. The first experiments; 8.2 Modern 2β-decay detectors; 8.3 Results
9. Processes in nuclear physics forbidden by parity conservation law **826**
9.1 Weak nucleon – nucleon interaction; 9.2 Parity-violation effects in γ-transitions; 9.3 α-decay forbidden by parity conservation law; 9.4 Fission forbidden by parity conservation law
10. Decays of the simplest nuclei (nucleons) and the properties of the simplest antinuclei **830**
10.1 β-decay of the neutron; 10.2 Hypothetical decays of nucleons with violation of the baryon-number conservation law; 10.3 Antinucleons. Production and interaction. Decay of the antineutron; 10.4 Antideuteron, antihelium III, and antitritium
11. The last exotic feature (so far) **834**
11.1 A lyrical introduction; 11.2 Discovery of the 114th element; 11.3 Discovery of the 118th element
12. Conclusions **837**
References **838**

Abstract. This review is concerned with the modes of radioactivity and some other nuclear physics phenomena discovered comparatively a short time ago or long ago but simply less familiar that have something extraordinary about them either in terms of properties or in terms of observation (rare or even 'forbidden' occurrence, serendipitous discovery posing observational or interpretation challenges, requiring unique experimentation, or exotic in some other manner). The history of the discovery of such phenomena is presented, and their significance is discussed.

K N Mukhin, O O Patarakin Russian Research Centre 'Kurchatov Institute', Institute of General and Nuclear Physics, pl. Kurchatova 1, 123182 Moscow, Russian Federation
Tel. (7-095) 196-75 71, 196-73 63. Fax (7-095) 196-91 33
E-mail: mukhin@chen.net.kiae.su, patarak@dnuc.polyn.kiae.su

Received 24 May 2000
Uspekhi Fizicheskikh Nauk **170** (8) 855 – 897 (2000)
Translated by E Yankovsky; edited by A Radzig

1. Introduction

1.1 Subject and content of the review

The present review is devoted to the description of extraordinary, i.e. different from customary α-, β-, and γ-decays, types of radioactivity and some other processes and phenomena in nuclear physics that we will simply call exotic. The exotic features may be inherent in the new phenomenon proper. Or, alternatively, they lie in the fact that the phenomenon is expected to occur, but the related probability may be extremely low, so the phenomenon is very rare in nature and therefore difficult to observe. Or else there may be

no theoretical explanation for a phenomenon whose effect is reliably detected. Or, straight conversely, an event that has been predicted may be finally detected after long and intensive investigations as a result of employing a truly exotic method. The possibilities may be continued.

We immediately note that the title of the article does not mean that the processes and phenomena described here violate some laws of physics. For instance, all radioactive decay processes satisfy both the necessary condition ($M_n \geqslant \sum m_i$, where M_n is the mass of the radioactive nucleus, and $\sum m_i$ the sum of the masses of all the decay products, including the mass of the residual nucleus) and (except for very special cases, which will be stipulated specifically) sufficient conditions, such as the law of conservation of electric charge, the lepton- and baryon-number conservation laws, and the spatial parity conservation law (in strong and electromagnetic interactions), etc.

For a long time we wondered where to begin and what to include in the list of exotic phenomena, since many exotic features were discovered in their time among 'normal' processes of nuclear physics. For instance, isn't the conversion electron emission, where the nucleus directly transfers (i.e. without emitting an intermediate gamma quantum) its energy to an atomic electron, remarkable? And isn't the process of electron capture, where a nucleus absorbs an electron from the atomic shell, exotic? Or the production of electron – positron pairs directly at the expense of the energy of the nucleus? Or the production of such pairs by free gamma quanta, where a particle of zero mass produces a pair of particles with a total mass of about 1 MeV? Or the creation of long-range alpha particles? The list can be continued.

Most readers know all these phenomena, with the result that over the years the exotic aura has disappeared. There is, however, a further exotic phenomenon that has been around for a long time and yet is not well known to the public (the readers of *Physics – Uspekhi* include not only nuclear physicists). In 1935, a group led by Igor' V Kurchatov discovered nuclear isomerism in an isotope of bromine. This started a new avenue of research in the field of nuclear isomerism, with valuable theoretical results as a by-product, and led to the discovery of other isomeric processes less-known to the common reader. Hence our choice of the year 1935 as the 'boundary' between ordinary and exotic nuclear processes and phenomena.

Four years after the discovery of nuclear isomerism, in 1939, Otto Hahn and Fritz Strassmann discovered uranium fission, with the result that soon new exotic phenomena were detected, including phenomena in the field of radioactivity. Spontaneous uranium fission was discovered, delayed neutrons were detected and the first transuranium elements were synthesized, which, as uranium, exhibit α-, β-, and γ-radioactivity and undergo spontaneous fission. At the end of the 1940s and in the 1950s, experimental studies of the long-predicted β-decay of the neutron began. In our review we discuss this radioactive process in one of the simplest atomic nuclei.

The 1950s were marked by very important achievements in developing new experimental methods (methods that used bubble, spark, and emulsion chambers and scintillation and Cherenkov detectors), which made it possible to make many discoveries in nuclear physics and elementary particle physics, including the study of 2β-decay and the discovery of two particles closely linked to the topic of the present review. By these two particles we mean simplest antinuclei, namely, the antiproton (discovered in 1955) and the antineutron (discovered in 1956), with the second being β^+-active and both actively interacting with nucleons in the exotic process of annihilation with transformation of the mass of the nucleon – antinucleon pair into the masses and kinetic energies of some other lighter particles. Later, in the 1960s and 1970s, more complex antinuclei were discovered, i.e. the antideuteron, antihelium, and antitritium (see below).

In the 1960s, much attention was focused on the production and properties of far transuranium elements with $Z > 100$. Among the findings in radioactivity with exotic features we would like to mention the discovery in 1961 of spontaneous fission in the isomeric state, in 1962 the discovery of retarded protons, in 1966 of delayed nuclear fission, and in 1970 of isomeric proton decay.

The years 1964, 1970, and 1978 saw, sequentially, the discoveries of *electromagnetic* (γ-decay) and two *strong* nuclear-physics processes (α-decay and fission) forbidden by the spatial parity conservation law, i.e. proceeding via the weak interaction. Delayed double-neutron, triple-neutron, and tritium radioactivities were discovered in, respectively, 1979, 1980, and 1984.

A sensational discovery in the field of proton radioactivity was made in 1982, namely, proton emission from the ground state of a nucleus (an analog of α-decay). The year 1983 saw the discovery of delayed double-proton radioactivity. No smaller sensation was the chain of discoveries of spontaneous emission of nuclei heavier than the α-particle, so-called cluster radioactivity (another analog of α-decay). These started in 1984, when spontaneous emission of $^{14}_{6}$C nuclei was detected, followed by the discoveries of the emission of $^{24}_{10}$Ne nuclei in 1985, the emission of $^{28}_{12}$Mg and $^{32}_{14}$Si nuclei in the late 1980s, and the emission of a $^{34}_{14}$Si nucleus in the late 1990s. The last event was crucial in determining the mechanism of cluster decay.

Finally, the latest discoveries of exotic nuclear properties were made in 1998 – 1999, where in experiments with extremely complicated approaches and techniques the long-predicted 114th element was detected. The decay products of this element and the element itself exhibited α-decay and spontaneous fission with anomalously long half-lives (for this part of the Periodic Table). Similar experiments led to the discovery of the yet heavier 118th element.

In our review we will not touch on the properties of elementary particles (muons, π-mesons, and strange, charmed, and beautiful particles), although there is no doubt that such particles possess many exotic features. We may, however, devote another article to them. The only exception, as noted earlier, will be made for the neutron and the proton (and also for their antiparticles, the antiproton and the antineutron), which may be considered as the simplest nuclei (antinuclei). In addition to the ordinary β-decay of neutron, which was discovered in experiments half a century ago but still astonishes physicists with an ever increasing number of exotic features, we shall examine the hypothetical processes of neutron and proton decay that occur contrary to the baryon-number conservation law. A similar exotic phenomenon that occurs in violation of the lepton-number conservation law will be examined when we describe neutrinoless double β-decay. Experiments that would reveal the existence of such processes prohibited in the Standard Model are extremely difficult to conduct. It suffices to say that only one event that is suitable for further processing is registered in a week of such experiments. For all the processes

mentioned in this paragraph we will give the latest data available.

The historical approach used in the material we have just discussed is really inconvenient for writing an article. The thematic approach is more appropriate. Hence, the plan of the review is as follows. To simplify the exposition of the main material on exotic radioactivity, we start with a historical survey (Section 2) of the discoveries and research in the field of 'normal' natural and artificial radioactivities. We touch very briefly on the main laws of α-, β-, and γ-decay, including the known exotic features mentioned earlier.

The exposition actually starts with Section 3, where we discuss nuclear isomerism. Section 4 describes the discovery of uranium fission, delayed neutrons, the first transuranium elements, spontaneous fission, isomeric spontaneous fission, and delayed nuclear fission. In Section 5 we discuss proton and double-proton radioactivities, including proton decay from the ground and isomeric states of a nucleus and emission of retarded protons and proton pairs. Section 6 is devoted to neutron radioactivity. There we discuss the possibility of detecting emission of a neutron from the ground state of a nucleus with a measurable half-life and tell the stories of delayed double- and triple-neutron decays and of delayed tritium radioactivity (which are closely related due to the similarity in the methods that led to the discovery of these phenomena). Cluster radioactivity, i.e. emission of fragments heavier than alpha particles by nuclei, is described in Section 7, while Section 8 is devoted to the phenomenon of double β-decay (two-neutrino and neutrinoless). In Section 9 we report on the processes of emission of γ-radiation, α-decay, and fission forbidden by the parity conservation law. Section 10 is devoted to the decays (real and hypothetical) of the two simplest nuclei, the neutron and the proton, and also to the properties of simplest antinuclei, while in Section 11 we tell the story of the discovery of the 114th and 118th elements. We conclude our review with Section 12.

It goes without saying that in a fairly small article written for the nonspecialist it is impossible to fully cover such a broad spectrum of topics. Therefore, the attentive reader is sure to detect certain reticences and inconsistencies in the narrative and perhaps find the style of writing superfluously unscientific. The only excuse here can be that we attempted to write an article suitable for a journal that covers all sorts of areas of physics, i.e. the material must be understandable to a wide circle of readers interested in physics irrespective of their narrow specialization. Those readers that would like to get a fuller picture of the discoveries covered in this review are advised to read the original articles and monographs cited in each section.

1.2 Methodological remarks

(1) In Section 1.1 we listed about two dozen radioactive processes. Some of the processes involve nuclei in the ground state, while the other process have to do with nuclei in excited states. There are four groups of radioactive processes, and within each group the processes are characterized by common parameters.

The first group incorporates all radioactive processes that occur (and have been actually observed) for nuclei in the ground state. These are α-, β-, and proton decays, the emission of heavy fragments ($^{14}_{6}$C, $^{24}_{10}$Ne, $^{28}_{12}$Mg, $^{32}_{14}$Si, and $^{34}_{14}$Si), and spontaneous nuclear fission. The main characteristic features of the radioactive processes belonging to this group (except for the ground state of the initial nucleus) are the spontaneous nature of the emission of the elementary particles or nuclear fragments, the change in composition of the nuclei (i.e. A and/or Z), and the exponential law of activity decay with a definite half-life $T_{1/2}$. Modern methods make it possible to measure $T_{1/2} \geqslant 10^{-12}$ s. Only this group of radioactive processes is considered to possess 'true' radioactivity in popular-science literature covering problems of general physics.

The second group consists of a wide variety of delay processes occurring with highly excited atomic nuclei that emerge as a result of a preceding $\beta^{\pm}$-decay process. Among these is the emission of delayed α-particles, protons and neutrons, proton and neutron pairs, neutron triples and tritium, and delayed fission. The half-life of such two-stage processes is determined by that of the first stage, the β-decay, which follows an exponential law, since the second stage proceeds very rapidly with $\tau \approx 10^{-15}$ s (the charged particles usually escape over the Coulomb barrier). This group of radioactive processes results in a change of both the composition and energy of the excited nucleus.

Radioactive processes belonging to the third (small) group involve nuclei with long living (metastable) isomeric levels. At present only three types of isomeric transitions are known: the hindered (or unfavored) γ-transition, often accompanied by the conversion electron emission, isomeric proton decay, and isomeric spontaneous fission. The half-life of the isomeric processes is determined by the lifetimes of the metastable state. Isomeric proton decay and isomeric spontaneous fission are accompanied by a change in composition and excitation energy of the radioactive nucleus, while the isomeric γ-transition is accompanied by a change in only the nuclear excitation energy.

Finally, the fourth, least populated, so to say, group consists of a single radioactive process which, however, is extremely widespread. The process was discovered more than a century ago and is γ-decay. By this process the nuclei get rid of the excess excitation energy in almost all the radioactive processes listed above. The rate of γ-decay is determined by the differences of the excitation energies and spins of the initial and final states of the nucleus. Naturally, in γ-decay only the excitation energy of the nucleus changes, while the composition remains the same.

(2) Earlier we said that in some papers (and books) only processes belonging to the first group are considered as radioactive. (The reader will recall that in this group the nuclei are in the ground state.) Of course, such a viewpoint may be considered correct since it is a question of convention.[1] We believe, however, that such a convention is somewhat artificial and lacks logic. Indeed, (i) the α-particles and protons emitted by a nucleus in an excited state are no worse than the α-particles and protons emitted from the ground state; (ii) if γ-decay is excluded from radioactive processes,

[1] It is desirable, however, that the convention be kept throughout a single publication. For instance, in *Fizicheskaya Entsiklopediya* (Physics Encyclopedia) in 5 Vols, Eds A M Prokhorov et al. (Moscow: Bol'shaya Rossiĭskaya Entsiklopediya, 1988 – 1998) the article on radioactivity deals only with processes involving nuclei in the ground state (although γ-decay is mentioned). The same viewpoint is expressed in the article on alpha decay, but long-range α-particles are included in radioactive processes (although, as is known, such particles are emitted from the excited states of nuclei). Only the article on proton radioactivity is consistent in a way, since here radioactive processes not only incorporate proton decay from the ground state but also isomeric proton decay and the emission of retarded protons and proton pairs.

then we must exclude β-decay, since both have the same prehistory: the nucleus contains neither γ-quanta nor electrons (neither in the ground state nor in excited states). Electrons and γ-quanta *arise* in the nucleus at the moment they are emitted and do not *escape* from the nucleus. So how can we say that the nucleus *decays*? In a word, in the present review we do not adhere to this convention, since otherwise we would have to exclude from radioactive processes about one dozen processes that satisfy all the criteria for radioactivity except a single (the ground state), and this seems to us not a very important evidence.

Indeed, all processes belonging to the second, third, and fourth groups (as well as those belonging to the first) proceed spontaneously, are described by an exponential law (delayed processes are described by an exponential law in the first stage), are characterized by a definite half-life, are accompanied by the emission of elementary particles and nuclear fragments, and lead to changes in the composition and/or excitation energy of the radioactive nucleus.

In addition to what we have just said we can bring in many arguments in favor of considering all the processes of the second, third and fourth groups as radioactive. Here are some of these arguments.

(a) The fact that the scientists who discovered γ-decay in the 19th century named it one of the three types of radioactivity hardly needs additional arguments. Suffice it to note that to exclude γ-decay from radioactive processes on the grounds that such decay involves only nuclei in excited states is illogical, to say the least, since γ-decay of a nucleus in the ground state is simply *forbidden* by the energy conservation law. In this sense (from the viewpoint of the energy conservation law) all radioactive processes involving nuclei in the ground state are *allowed* because the mother nucleus has a larger mass than the masses of the decay products, i.e. is also, as in the case of emission of γ-radiation, in a higher ('excited') energy state.

(b) The various types of delayed neutron radioactivity (the emission of one, two, or three delayed neutrons) were discovered using *neutron* detectors (see Section 6).

(c) Isomeric radioactive processes were also discovered in experiments, independently from theory (which, incidentally, was developed later). Here, in the case of an isomeric γ-transition the two states of the nucleus (the ground and the metastable) differ so much in some *nuclear* properties that they appear to be two different nuclei rather than the ground and excited states of a single nucleus.

(3) The above shows that there is no real difference between the radioactivity of nuclei in the ground and excited states. In view of this we use other indications to group our material. For instance, in Section 5 devoted to proton radioactivity we consider proton decay, isomeric proton decay, retarded protons, retarded proton pairs, and even the hypothetical double-proton radioactivity. However, we stress once more that today a process is considered radioactive if its half-life $T_{1/2}$ is no shorter than 10^{-12} s, with the lower bound being greater by a factor of 1000 than the decay time of the compound nucleus that forms in a nuclear reaction proceeding by the Bohr mechanism. Such temporal 'demarcation' excludes the possibility of classifying the instantaneous ($\sim 10^{-15}$ s) process of decay of a compound nucleus with the escape of protons and neutrons as a radioactive process. A similar and rather ambiguous situation may arise, for example, when the nuclei emitting retarded protons are themselves formed in the process of a nuclear reaction accompanied by the escape of prompt 'evaporative' protons, while the retarded protons have such high energies that they also escape (after β-decay) instantly (above the Coulomb barrier). The fact that $T_{1/2} = 10^{-12}$ s is chosen as the lower bound for half-lives of radioactive processes excludes the possibility of an ambiguous interpretation of the results of experiments.

(4) We make another remark of a methodological nature by simply stating a strange fact that must be taken into account.

Earlier we said that all delayed radioactive processes involve daughter nuclei formed after the β-decay of the main nuclei constituting the target under investigation. Nevertheless, the properties of the emitted delayed particles are, in contrast to logic, associated in tables of nuclear properties with those of the target nuclei. For instance, the characteristics of the delayed neutrons actually emitted by $^{11}_{4}$Be nuclei are listed in tables of the characteristics of $^{11}_{3}$Li target nuclei, from which the $^{11}_{4}$Be nuclei are formed as a result of β^--decay.

Similarly, the retarded protons that are actually emitted by $^{13}_{7}$N nuclei are listed in tables for the target's mother nucleus $^{13}_{8}$O, which via β^+-decay is transformed into a $^{13}_{7}$N nucleus that then emits a proton, etc. Often the notation for such a reaction is somewhat absurd as, for example, in the case of $^{8}_{3}$Li, which is indicated to decay into two α-particles. But if we consider that there is actually a two-stage process

$$^{8}_{3}\mathrm{Li} \xrightarrow{\beta^-} {}^{8}_{4}\mathrm{Be} \longrightarrow 2^{4}_{2}\mathrm{He}\,,$$

then the apparent contradiction with the charge conservation law disappears. We remark again that nothing can now be done with such a system of notation. Come to think of it, it may be even convenient that we have it. For instance, the $^{8}_{4}$Be nucleus mentioned earlier is unstable and hence does not appear in tables whatsoever.

2. History of the discovery and study of radioactivity

2.1 Natural radioactivity

More than a century ago Antoine Becquerel, studying the phosphorescence of uranium salts, detected the darkening of photographic plates wrapped in paper together with a uranium salt previously not exposed to sun light [1]. In an additional experiment Becquerel showed that the effect he discovered is observed not only with salts of uranium but also with metallic uranium, i.e. is a property of that element. The discovered effect of spontaneous emission by uranium of a new, previously unknown, type of radiation was named radioactivity.

Several years later Pierre and Marie Curie discovered two new radioactive elements, polonium ($_{84}$Po) and radium ($_{88}$Ra), whose activity was found to be 10^7 times higher than that of uranium [2]. Still later on four more radioactive elements were discovered in nature: radon ($_{86}$Rn), actinium ($_{89}$Ac), thorium ($_{90}$Th), and protactinium ($_{91}$Pa). At first these seven elements and the radioactive products of their decay exhausted the list of radioactive elements found in nature if one ignores the β-active isotope of potassium ($^{40}_{19}$K) and several α-active isotopes of rare-earth elements discovered later (see below).

The study of the properties of radioactive radiation started by M Curie, who discovered a heavy component that

is rapidly stopped by matter [3], and continued by Ernest Rutherford, who investigated the deviation of emitted particles in electric and magnetic fields [4], showed that the new radiation has three components which were at that time called α-, β-, and γ-rays.

Subsequently, it was established that α-rays are helium nuclei ($^4_2$He) moving at a speed of about 10^9 cm s^{-1} and are absorbed by a layer of aluminium several micrometers thick; β-rays are electrons moving at a speed close to that of light ($c = 3 \times 10^{10}$ cm s^{-1}) and are absorbed by a layer of aluminium about 1 mm thick; finally, γ-rays constitute highly penetrating electromagnetic radiation. The source of all three types of radioactive radiation is the atomic nucleus: α-decay occurs because of the strong interaction, β-decay because of the weak interaction, and emission of γ-radiation because of the electromagnetic interaction. Radioactive nuclei can emit α- and β-rays when they are in either the ground or an excited state, while γ-radiation is emitted exclusively by nuclei in excited states.

Both α- and γ-radiation are monochromatic, while β-radiation has a continuous energy spectrum (together with the electron the nucleus emits an electron antineutrino $\tilde{\nu}_e$ that carries away a fraction of the energy). Before emission, α-particles are formed from the nucleons of the nucleus. Electrons, antineutrinos, and γ-quanta are not present in the nucleus in finished form, but are produced at the moment of emission. In addition to emitting γ-quanta, the nucleus in an excited state can transfer its energy directly (without pre-emission of a γ-quantum) to an orbital electron (internal conversion) and, if the excitation energy exceeds $2m_ec^2 \approx 1$ MeV (where m_e is the electron mass), use it to produce an electron–positron pair.

The number N of radioactive nuclei changes with the passage of time according to the radioactive decay law (exponentially):

$$N(t) = N_0 \exp(-\lambda t)\,, \tag{1}$$

where $N(t)$ and N_0 are the numbers of nuclei at instants of time t and $t = 0$, respectively, and λ is the probability of decay per unit time (the decay constant). The mean lifetime of a radioactive nucleus is $\tau = 1/\lambda$, and the mean half-life is $T_{1/2} = \tau \ln 2 \approx 0.69\tau$.

The way in which a radioactive process follows its course is practically independent of the effects of the surrounding medium.[2] The probability of the process is determined by the intensity of the respective interaction (strong, electromagnetic, or weak), the amount of energy released in the process (increases with the energy), the difference in spins of the initial and final nuclei (decreases with increasing difference) and, in the case of α-decay, by the height of the Coulomb barrier (decreases with increasing height). The half-lives for α-radiation vary from 10^{-7} s to 10^{17} y, for β-radiation from 10^{-2} s to 10^{16} y, and for γ-radiation from 10^{-19} s to 10^{10} y.

The main characteristic feature of α-decay is that the process is described by the Geiger – Nuttall law [5], according to which

$$\log \lambda = A \log T_\alpha + B\,, \tag{2}$$

where λ is the probability of α-decay, T_α the kinetic energy of an α-particle, and A and B are constants. By virtue of this law, the above huge range of half-lives for α-radiation corresponds to a quite small range of kinetic energies of α-particles (1.8 – 9 MeV).[3]

The main reason for the existence of long half-lives, i.e. comparatively low probabilities (for the strong interaction) of α-decay, is the presence of a Coulomb barrier for the escaping α-particles. In classical physics such a barrier totally prohibits α-decay, but in quantum mechanics the barrier becomes slightly penetrable due to the tunnelling effect.

The wave-mechanical theory of α-decay was built in 1928 by Gamow [6] and, independently, by Condon and Gurney [7] in the (semiclassical) WKB approximation. According to this theory, the penetrability D of the Coulomb barrier can be estimated by the formula

$$\begin{aligned} D &= \exp\left[-\frac{2}{h}\int_R^{r_T}\sqrt{2m_\alpha\frac{2Ze^2}{r} - T}\,\mathrm{d}r\right] \\ &\approx \exp\left[-\frac{2}{h}\sqrt{2m_\alpha(V_C - T)}R\right], \end{aligned} \tag{3}$$

where h is the Planck constant, R the radius of the nucleus, $r_T = 2Ze^2/T$, m_α is the mass of the α-particle, Z the charge of the nucleus, T the kinetic energy of the α-particle, and V_C the height of the Coulomb barrier. The formula's structure suggests that the penetrability of the Coulomb barrier is extremely low for low-energy α-particles, which on the whole explains the long half-lives for α-radiation.

In addition to the penetrability D of the barrier, the theory of α-decay allows for what is known as the pre-exponential factor $K = vP$, where P is the probability of formation of an α-particle from the nucleons of the mother nucleus near the surface of the nucleus (this formation factor is difficult to calculate), and $v = v/2R$ is the collision frequency of an α-particle with the barrier in the tunnelling process (v is the speed of the α-particle). Thus, the α-decay constant λ is $\lambda = KD = vPD$.

The very long lifetimes for β-decay are explained by the extreme weakness of the interaction responsible for this process (the *weak* interaction), while the very wide range of lifetimes can be explained by the proportionality of the probability of β-decay to the fifth power of the energy ($\lambda = 1/\tau \sim E_\beta^5$). In the case of γ-radiation, the broad range of lifetimes can be explained by the fact that the probability of this process is strongly dependent on the released energy E and the difference ΔI of the spins of the nucleus in the excited and ground states. For small E and large ΔI, the probability of emission of γ-radiation may become lower than the probability of internal conversion.

The radioactive processes described above are collectively called natural radioactivity. The isotopes of heavy radioactive elements found in nature are systematized in three radioactive families (series), with the first members in these families being the thorium isotope $^{232}_{90}$Th (the thorium family), the uranium isotope $^{238}_{92}$U (the uranium family), and the uranium isotope $^{235}_{92}$U (the actinouranium family). The nature of the change in the composition of nuclei that occurs in the radioactive decays clearly shows that all members of the radioactive families are described by the formulas $A = 4n$, $A = 4n + 2$, and $A = 4n + 3$, respectively, where A is the mass number,

[2] In view of the specific feature of electron capture (an electron from the atom is captured by the nucleus), the decay constant for electron capture may weakly depend on the chemical properties of the medium.

[3] Long-range α-particles may have an energy up to 11.65 MeV (^{212}Po).

and n an integer. There are very few radioactive isotopes among the low-Z and medium-Z elements found in nature. Examples of such isotopes are the scarce ($\sim 0.01\%$) β-active potassium isotope $^{40}_{19}$K, whose half-life is $T_{1/2} = 1.28 \times 10^6$ y, the α-active samarium isotopes $^{147}_{62}$Sm ($T_{1/2} = 1.06 \times 10^{11}$ y) and $^{148}_{62}$Sm ($T_{1/2} = 8 \times 10^{15}$ y), and the neodymium isotope $^{144}_{66}$Nd ($T_{1/2} = 5 \times 10^{15}$ y). In all, there are about 300 natural radioactive nuclei.

2.2 Artificial radioactivity

Many more radioactive nuclei (about 2000) have been produced artificially in nuclear reactions over the entire range of the Periodic Table, starting with the first element, hydrogen (which has a β-active isotope, tritium $^3_1$H), and 'ending' with superheavy transuranium elements, for each of which 10 to 15 radioactive isotopes have been synthesized (see Section 4.3). Here, two entirely new elements (which have long been predicted) were discovered: astatine ($_{85}$At) and francium ($_{87}$Fr), and the fourth radioactive family, the neptunium family, which filled the gap in the formulas with $A = 4n + 1$. The first member of this family is assumed to be the long-lived isotope of the first transuranium element, neptunium $^{237}_{93}$Np, although this nucleus is formed in a chain of short-lived nuclei:

$$^{241}_{94}\mathrm{Pu} \xrightarrow{\beta} {}^{241}_{95}\mathrm{Am} \xrightarrow{\alpha} {}^{237}_{93}\mathrm{Np}\,.$$

Incidentally, the same is true of the first members of the other families.

The idea of producing artificial radioactive nuclei consists in purposefully changing the nucleon composition of a stable nucleus that meets the condition $N_\mathrm{n}/N_\mathrm{p} \approx 1$ for low-Z nuclei or $N_\mathrm{n}/N_\mathrm{p} \approx 1.5$ for high-Z nuclei, where N_n is the number of neutrons in the nucleus, and N_p the number of protons. By bombarding a stable nucleus with protons (or heavy ions or α-particles) or neutrons we can create an excess of protons or neutrons in the nucleus, in view of which the new nucleus becomes energetically unstable with respect to radioactive decay. Note that stable nuclei can become radioactive if they are excited by bombarding them with γ-quanta or if the excited states in them are created due to the preceding β-decay. In Section 9.3, we will become familiar with the α-activity of the stable oxygen nucleus $^{16}_8$O, which is formed in an excited state after β-decay of the nucleus $^{16}_7$N.

The first to discover artificial radioactivity were Frederic Joliot and Irene Curie [8, 9], who, while studying the reaction

$$\alpha + {}^{27}_{13}\mathrm{Al} \rightarrow {}^{30}_{15}\mathrm{P} + \mathrm{n}\,, \tag{4}$$

discovered residual positron radioactivity in $^{30}_{15}$P *after irradiation had been stopped*:

$$^{30}_{15}\mathrm{P} \rightarrow {}^{30}_{14}\mathrm{Si} + \mathrm{e}^+ + \nu_\mathrm{e}\,. \tag{5}$$

Similarly, Enrico Fermi produced several dozen artificial β^--active nuclei via (n, γ)-reactions [10]:

$$(A, Z) + \mathrm{n} \rightarrow (A + 1, Z) + \gamma\,, \tag{6}$$

$$(A + 1, Z) \xrightarrow{\beta^-} (A + 1, Z + 1) + \mathrm{e}^- + \tilde{\nu}_\mathrm{e}\,. \tag{7}$$

Formulas (5) and (7) show that β^+-decay lowers and β^--decay raises the charge of the initial nucleus by one unit. The same effect as β^+-decay is produced by the third type of β-decay, discovered in 1937 by L Alvarez [11]: electron capture by the nucleus from the atomic shell (usually K-shell) of the atom to which the nucleus belongs, which proceeds as follows

$$(A, Z) + \mathrm{e}^- \rightarrow (A, Z - 1) + \nu_\mathrm{e}\,. \tag{8}$$

And although this discovery happened two years later than the boundary we placed between ordinary and exotic phenomena and by itself is extremely exotic (the nuclear process was discovered as a result of observing characteristic X-ray radiation, which is an atomic phenomenon), we do not discuss it in this review since we assume it to be well known. On the other hand, the much-less-known fourth type of β-activity, the double β-decay, will be reviewed separately in one of the sections devoted to exotic radioactivity (Section 8).

One more remark is in order. When artificial radioactive nuclei are produced by the reactions (4)–(8), the nuclei are usually landed in excited states, with the result that not only γ-transition become possible at all times but also α- and β-decay, as well as the peculiar cascade two-stage radioactive processes of a delayed and isomeric nature, which will be discussed in separate sections of the present review.

Our historical survey of the discovery and study of natural and artificial radioactivities turned out to be brief and incomplete, but this was deliberate. A more detailed description of this material can be found, if necessary, in the book by one of the authors (see Ref. [12]) and in the works cited therein.

3. The first exotic feature — nuclear isomerism

In 1935, i.e. at the beginning of research on artificial radioactivity, Igor' Kurchatov and his collaborators made the important discovery of nuclear isomerism in bromine, a discovery that started a whole new field of research [13]. The history of this discovery is unique and instructive, and for this reason we will discuss it here in greater detail.

From the times of Fermi's experiments in artificial β^--activity it was known that, when irradiated with neutrons, natural bromine becomes β-active, with the β-activity characterized by two half-lives, $T^{(1)}_{1/2} = 18$ min and $T^{(2)}_{1/2} = 4.4$ h. Since bromine occurs naturally as a mixture of two stable isotopes $^{79}_{35}$Br and $^{81}_{35}$Br, this result seemed quite natural: when one of the two stable isotopes captures a neutron it becomes the radioactive isotope $^{80}_{35}$Br with the half-life $T^{(1)}_{1/2}$, while when the other stable isotope captures a neutron it becomes the radioactive isotope $^{82}_{35}$Br with the half-life $T^{(2)}_{1/2}$:

$$\left({}^{79}_{35}\mathrm{Br} + {}^{81}_{35}\mathrm{Br}\right) + \mathrm{n} \rightarrow \left({}^{80}_{35}\mathrm{Br} + {}^{82}_{35}\mathrm{Br}\right) + \gamma\,, \tag{9}$$

$$\left({}^{80}_{35}\mathrm{Br} + {}^{82}_{35}\mathrm{Br}\right) \xrightarrow{\beta^-} \left({}^{80}_{36}\mathrm{Kr} + {}^{82}_{36}\mathrm{Kr}\right), \qquad T^{(1)}_{1/2} + T^{(2)}_{1/2}\,. \tag{10}$$

However, after Kurchatov and his coworkers did their experiments, this entirely plausible picture had to be changed. As a result of irradiating bromine, three instead of two half-lives were detected: the old ones (18 min and 4.4 h) and a new one, 34 h. But if the two known stable isotopes of bromine, $^{79}_{35}$Br and $^{81}_{35}$Br, which produce the radioactive isotopes $^{80}_{35}$Br and $^{82}_{35}$Br in the (n, γ)-reaction, are responsible for the first two half-lives, what is responsible for the third half-life?

The simplest answer to this question lies in the assumption that a radioactive selenium isotope is produced in an (n, p)-reaction

$$_{35}\mathrm{Br} + \mathrm{n} \rightarrow {}_{34}\mathrm{Se} + \mathrm{p} \tag{11}$$

or that a radioactive arsenic isotope is produced in an (n, α)-reaction

$$_{35}\mathrm{Br} + \mathrm{n} \rightarrow {}_{33}\mathrm{As} + \alpha\,. \qquad (12)$$

However, the truth of such an assumption was ruled out by the very procedure of the radiochemical experiment, in which the possibility of appearance of selenium or arsenic isotopes was checked. When salts of stable selenium or arsenic were added to the radioactive solution and ensuing deposition was accomplished, no activity was recorded in the sediment. Activity appeared only in solutions and sediments containing bromine.

Therefore, only three hypotheses could be proposed that answered the above question: (1) bromine has a third stable isotope; (2) a third radioactive isotope of bromine, $^{78}_{35}\mathrm{Br}$, is produced in the (n, 2n)-reaction

$$^{79}_{35}\mathrm{Br} + \mathrm{n} \rightarrow {}^{78}_{35}\mathrm{Br} + 2\mathrm{n}\,, \qquad (13)$$

and (3) one of the two known radioactive isotopes, $^{80}_{35}\mathrm{Br}$ or $^{82}_{35}\mathrm{Br}$, has two half-lives.

The first hypothesis seemed highly unlikely to be true from the start if one takes into account the regularities governing the systematics of stable nuclei with an odd proton number Z. Later the existence of the third stable bromine isotope was rejected by the mass-spectroscopy method. The second hypothesis was ruled out by subsequent experiments with slow neutrons, in which activity with the third half-life also appeared, while the (n, 2n)-reaction involving bromine could proceed only with fast neutrons. What remained was the third hypothesis, according to which one of the two known radioactive bromine isotopes had two half-lives. But which isotope has two half-lives and which two half-lives of the three discovered are shared by this particular isotope?

The answers to these questions were obtained in experiments on irradiating bromine with γ-quanta. The result was the production of two radioactive bromine isotopes $^{78}_{35}\mathrm{Br}$ and $^{80}_{35}\mathrm{Br}$:

$$\left(^{79}_{35}\mathrm{Br} + {}^{81}_{35}\mathrm{Br}\right) + \gamma \rightarrow \left(^{78}_{35}\mathrm{Br} + {}^{80}_{35}\mathrm{Br}\right) + \mathrm{n}\,, \qquad (14)$$

which decay according to the following schemes

$$^{78}_{35}\mathrm{Br} \xrightarrow{\beta^+} {}^{78}_{34}\mathrm{Se}, \quad {}^{80}_{35}\mathrm{Br} \xrightarrow{\beta^-} {}^{80}_{36}\mathrm{Kr}\,, \qquad (15)$$

where in this case, too, the β-activity had three half-lives instead of two: 6.4 min, 18 min, and 4.4 h. By comparing the results of experiments on the irradiation of bromine with neutrons and γ-quanta one can conclude that both experiments yield the similar two half-lives 18 min and 4.4 h, and the same radioactive isotope $^{80}_{35}\mathrm{Br}$, to which these two half-lives belong. Notice that one of these periods was 'taken away' from $^{82}_{35}\mathrm{Br}$, to which it had been erroneously assigned, with the result that the third half-life, 34 h, must be assigned to this isotope. It is amazing how complicated the problem of deciphering the radioactivity of bromine turned out to be!

Let us go back to the isotope $^{80}_{35}\mathrm{Br}$. The fact that it was found to have two half-lives, $T_{1/2} = 18$ min and $T_{1/2} = 4.4$ h, implies that this nucleus is produced in reaction (9) not only in its ground state characterized by β-decay with $T_{1/2} = 18$ min but also in a long-lived (metastable) excited isomeric state, which is responsible for the β-decay with the second half-life $T_{1/2} = 4.4$ h.

The simplified radioactive-decay scheme for the $^{80}_{35}\mathrm{Br}$ nucleus is displayed in Fig. 1a (the more exact one is depicted in Fig. 1b). The excited nucleus $^{80}_{35}\mathrm{Br}^*$ produced through

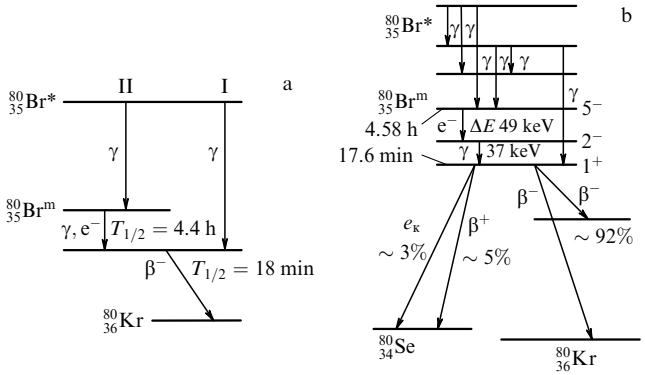

Figure 1. Level diagrams for the $^{80}_{35}\mathrm{Br}$ nucleus: simplified (a), and more exact (b).

reaction (9) can decay by two modes (I and II). By mode I, the nucleus rapidly (in $\sim 10^{-13}$ s) passes to its ground state, and from this state it emits an electron and an antineutrino with $T_{1/2} = 18$ min. By mode II, the $^{80}_{35}\mathrm{Br}^*$ nucleus rapidly passes to the metastable (long-lived and isomeric) state $^{80}_{35}\mathrm{Br}^{\mathrm{m}}$, and then slowly (with $T_{1/2} = 4.4$ h) passes to its ground state with subsequent β-decay (with the same half-life $T_{1/2} = 4.4$ h).

Soon after, nuclear isomerism was discovered in some isotopes of other elements, and this started a systematic investigation into the laws governing nuclear isomerism. What was important here, including the contribution to building the theory of isomerism, was the experimental proof obtained by Kurchatov's group that an isomeric transition of a nucleus occurs mainly not because of emission of γ-radiation but owing to the conversion electron emission.

The theory of nuclear isomerism was developed in 1936 by C Weizsacker [14], who explained the nature of this phenomenon by the fact that the isomeric nucleus has a metastable level with a larger spin I compared to that of the ground state (in our example involving bromine, $\Delta I = 4$) and low excitation energy (in the same example, $E \approx 0.1$ MeV). The theory suggests that in such cases the emission of γ-radiation is strongly hindered and the transition from the isomeric state occurs mainly by virtue of the conversion electron emission.

Today more than a hundred isomeric nuclei are known, with half-lives varying from 2.8×10^{-10} s to 5000 y. Among radioactive isomeric nuclei there are not only those with two half-lives but also those with three half-lives. The nuclear isomerism of β-stable nuclei manifests itself in the form of the hindered γ-emission and/or emission of internal conversion electrons knocked out of the K or L atomic shell.

The systematic study of the properties of isomeric nuclei led to the discovery of isomery islands, i.e. concentration of isomeric nuclei in certain regions of variation of the neutron and proton numbers in the nuclei. This discovery became a very strong argument in favor of one of the most popular models of the atomic nucleus, the nuclear shell model. The most successful variant of this model (with spin–orbit coupling) was suggested in 1949 by M Goeppert-Mayer [15]. The model correctly predicted many properties of the ground states of nuclei, such as spin and parity, and the distinctive stability of nuclei containing what became known as magic numbers of nucleons (2, 8, 20, 28, 50, 126 and, possibly,[4] 114 and 184). Incidentally, the name magic came from the exotic

[4] See Section 11.

properties of the nuclei corresponding to such numbers. This aspect, however, lies outside the scope of the present review.

The importance of the discovery of nuclear isomerism cannot be too strongly emphasized. Actually, the discovery started a chain of discoveries of new radioactive processes. In Section 4.5 we discuss a new type of nuclear isomerism observed in spontaneous fission, namely, shape isomerism; in Section 5.2 we deal with isomeric proton decay, and in Section 6.1 we mention the hypothetical possibility of isomeric neutron decay.

4. In the footsteps of the discovery of the century

New discoveries of exotic nuclear properties were just around the corner. Only several years after the discovery of nuclear isomerism the superexotic phenomenon of uranium fission was uncovered, and soon after three most important findings in the field of radioactivity were made practically at the same time: delayed neutrons were detected, spontaneous uranium fission was discovered, and the first artificial transuranium elements, which were found to be radioactive (just as uranium is), were produced. More than that, in the process of investigating the properties of the two latter phenomena (but much later), spontaneous fission in the isomeric state and delayed fission were detected. (Note the peculiar succession in the names, and in the essence as well, in relation to the preceding discoveries of nuclear isomerism, spontaneous fission, and delayed neutrons.) Below we will discuss all these findings, but now let us turn to their prehistory.

4.1 Uranium fission

In 1939, Hahn and Strassmann [16] made the unparalleled discovery of uranium fission, a discovery that laid the grounds for studying this remarkable phenomenon. As is known, the utilization of this discovery led to all the good and bad things due to which the past century was called the atomic century.

Interestingly, the discovery of nuclear fission could have been made five years earlier when Fermi conducted a large body of systematic experiments in which all the elements of the Periodic Table were irradiated with neutrons and the artificial β^--activity of the irradiation products was studied (see Section 2.2). The story goes as follows.[5] In bombarding uranium, Fermi *did not observe* the fission fragments of ^{235}U because studying β-activity and seeking to get rid of the interfering α-background noise he covered the β-active samples with a thin absorbing layer which proved to be opaque for the fission fragments.

Due to this unfortunate mistake, Fermi's interpretation [17] of the results of experiments on uranium irradiation followed the standard scheme, which was discussed in Section 2.2 on artificial radioactivity. According to this scheme, a uranium isotope captures a neutron and transforms into a heavier β-unstable isotope of the same element, which after β-decay is turned to one of the isotopes of the first *transuranium* 93rd element, which in turn may become the 94th element, and so on. The result is a chain of radioactive elements. And this is not a single chain, since uranium has several isotopes. This was exactly the case of Fermi's experiments — several radioactive chains were observed in them.

[5] One of the authors of the present review heard this story from a physicist who was already actively doing nuclear research at the time of E Fermi.

However, this interpretation of Fermi's experiments raised doubts in the minds of some radiochemists, who did not find the properties of the uranium irradiation products to correlate with those of transuranium elements. On the contrary, the products had properties inherent to elements belonging to the middle of the Periodic Table. For instance, in 1938, Curie and Savitch [18] proved that the properties of one such product are similar to those of lanthanum. The final solution to this puzzle was found by Hahn and Strassmann in their work cited earlier (see Ref. [16]). As a result of precise radiochemical analysis, the two researchers discovered an element belonging to the middle of the Periodic Table among the products of irradiation of uranium with neutrons, viz. barium. This had such a strong effect on the researchers that in their paper they wrote that although as chemists they are sure of their results, as physicists they cannot but be amazed.

A correct interpretation of the Hahn and Strassmann's experiment was soon made by Meitner and Frisch [19], who proposed the hypothesis of instability of heavy nuclei with respect to changes in shape, in view of which a uranium nucleus excited by the capture of a neutron can disintegrate into two roughly equal parts, the fission fragments.

Figure 2 schematically shows that initially, when the nucleus changes its shape from spherical to ellipsoidal and its surface area grows, the energy W of the nucleus also increases by W_f (the height of the Coulomb barrier) but then, due to Coulomb repulsion of the poles of the forming dumbbell-shaped nucleus, the energy sharply drops as the fission energy Q is released. For the nucleus to disintegrate into two fragments, the sum of the binding energy ε_n and the kinetic energy T_n of the captured neutron must be larger than the height W_f of the Coulomb barrier ($\varepsilon_n + T_n > W_f$). If the excitation is weaker, the nucleus only oscillates, changing its shape from spherical to ellipsoidal and back.

In their paper, Meitner and Frisch predicted among other things that in addition to barium there should be krypton among the uranium fission products, since $Z_{Ba} + Z_{Kr} = Z_U$ ($56 + 36 = 92$). The validity of this prediction was corroborated by Hahn and Strassmann [20], who also mentioned the possibility of neutron emission in the fission process.

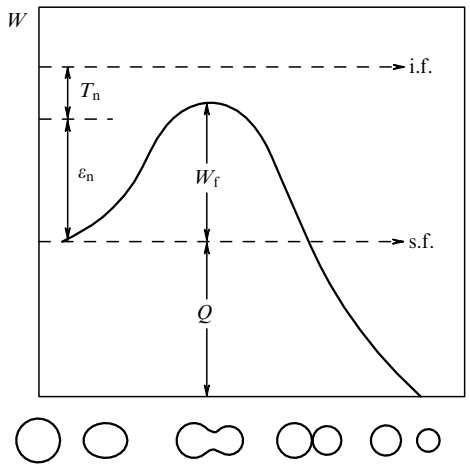

Figure 2. Dependence of the potential energy W of a fissioning nucleus on its shape: ε_n and T_n are the binding energy and the kinetic energy of the captured neutron; W_f is the height of the Coulomb barrier, and Q the fission energy. The arrows show the induced fission (i.f.) and spontaneous fission (s.f.) schemes.

Clearly, if Meitner and Frisch's hypothesis is true, the fission reaction must have the following properties:

(1) The energy release must very high, $Q \approx 200$ MeV. This value follows from the difference between the average binding energies of a nucleon in the uranium nucleus and in the nuclei of fission fragments.

(2) The dominant part of the fission energy must be released in the form of the kinetic energy of fission fragments. This follows from the existence of a strong Coulomb repulsion between the fragments produced in the fission process.

(3) The fission fragments must have a high ionizing power and a very small range in condensed matter. This follows from the fact that at the moment of their formation the fission fragments are not neutral atoms but ions with an effective positive charge $Z \approx 20$. (It is for this reason that Fermi did not notice the fission fragments in his experiments with a thin absorber of α-particles.)

(4) The fission fragments must be β-active and can emit neutrons, both instantaneous and delayed (after β-decay). This follows from the difference in the ratio of the numbers of neutrons, N_n, and protons, N_p, for uranium and fragments: $(N_n/N_p)_U = 1.6$, $(N_n/N_p)_{Ba} = 1.45$.

(5) In addition to the ability to undergo induced fission (i.f.) initiated by neutrons (or other particles) that supply an amount of excitation energy to the nucleus greater than the height W_f of the Coulomb barrier, uranium and some other nuclei can undergo spontaneous fission (s.f.). This follows from the existence of a small probability of quantum-mechanical tunnelling of the fission fragments through the potential barrier (of height W_f).

(6) In addition to fission, the capture of neutrons by the uranium nucleus may lead (by the Fermi scheme) to the formation of transuranium elements.

Very soon all these features of the fission reaction were proved to exist by experiments, while the validity of Meitner and Frisch's hypothesis was proved theoretically. In the same year of 1939, Frenkel [21] and, independently, Bohr and Wheeler [22] used the liquid drop model to develop a quantitative theory of nuclear fission from which it followed, among other things, that fission of the low-abundance uranium isotope ^{235}U can be initiated by neutrons of any energies, including thermal neutrons (i.e. for this isotope $\varepsilon_n > W_f$; see Fig. 2), while the fission of the main isotope ^{238}U can be initiated only by fast neutrons (this isotope can also capture a neutron without fission).

Experimental corroboration of the fact that the energy release in uranium fission is very high was obtained in 1939 by Frisch [23] and Joliot [24], of the emission of instantaneous fission neutrons by von Halban et al. [25], and of the emission of delayed fission neutrons by Roberts et al. [26]. Spontaneous uranium fission was discovered in 1940 in Igor' Kurchatov's laboratory by Petrzhak and Flerov [27]. At roughly the same time (1939–1940), Zel'dovich and Khariton [28] published a number of papers on the theory of nuclear chain reactions. In Sections 4.2–4.6 we will discuss in greater detail some of the aspects of the above works related to the theme of the present review.

4.2 Delayed neutrons

Earlier we said that fission neutrons were discovered in 1939 by von Halban et al. [25]. Today it is well known how important this discovery was for accomplishing a chain nuclear fission reaction. However, the properties of these *instantaneous* fission neutrons do not lie within the scope of the present article, since these neutrons are not products of radioactive decay, i.e. they are not characterized by measurable half-lives but are emitted almost instantly (in roughly 10^{-15} s) by excited fission fragments overloaded with neutrons in the process of 'evaporation'.

Delayed neutrons were a different matter. They were first discovered by Roberts et al. [26], who found that the average emission time for these neutrons was 12.5 s. A detailed study of the properties of delayed neutrons was carried out in 1942 by Snell and his collaborators (the results were published in 1947 in Ref. [29]). The researchers found that the fraction of these neutrons with respect to instantaneous neutrons amounts to about 0.6%, and the moment of emission lags behind by 0.2 s to roughly 1 min. Delayed neutrons play an important role in the process of regulating the rate of the chain reaction in reactions with a small (less than 1.006) multiplication factor.

Later, delayed neutrons were found not only near fission products but also near many other excited neutron-rich nuclei artificially produced by various nuclear reactions. The mechanism of emission of such neutrons is very simple and amounts to the following (Fig. 3). The excitation energy of the neutron-rich nucleus (A, Z) is usually removed by emitting γ-radiation and by β-decay accompanied by the formation of the daughter nucleus $(A, Z+1)$, which can also be produced in an excited state. It may so happen that the excitation energy W of the new nucleus is higher than the energy ε_n of separation of the neutron from this nucleus (the binding energy $\varepsilon_n < W$), with the result that the nucleus $(A, Z+1)$ acquires a new mechanism (in addition to the subsequent β-decay and emission of γ-radiation) of deexcitation: the emission of a neutron n with the kinetic energy $T_n = W - \varepsilon_n$. And since the possibility of emitting a neutron emerges only after β-decay preceding it and the neutron itself escapes almost instantly due to the absence of an electric charge, the emission of the neutron lags behind precisely by the time characterizing the β-decay process, i.e. $T_{1/2}^{(n)} = T_{1/2}^{(\beta)}$. This conclusion was corroborated in special experiments that made it possible to chemically extract a specific product with a unique half-life $T_{1/2}^{(n)}$ out of a collection of decay products with many various half-lives for the delayed neutrons, and to measure the half-life of the β-radiation, $T_{1/2}^{(\beta)}$, for that product. Indeed, it turned out that $T_{1/2}^{(\beta)} = T_{1/2}^{(n)}$.

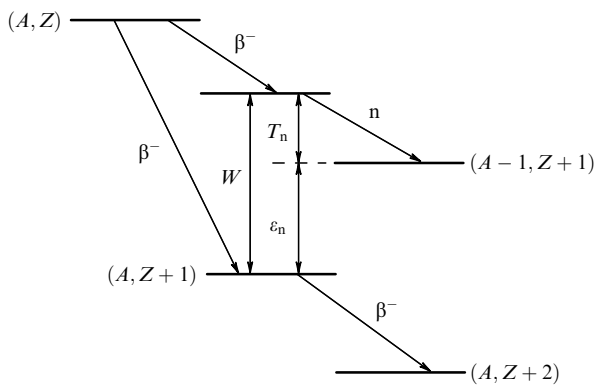

Figure 3. Diagram illustrating the emission of delayed neutrons: (A, Z) is the initial β-active nucleus; $(A, Z+1)$ the daughter nucleus with an excitation energy W exceeding the neutron binding energy ε_n, and T_n the kinetic energy of the delayed neutron n.

The energy diagram of the process of delayed neutron emission (the escape from a specific level of the nucleus) shows that their energy spectrum is discrete (in contrast to the continuous spectrum of the instantaneous fission neutrons). Measurements have corroborated this conclusion and yielded values for the kinetic energy of delayed neutrons emitted by fission fragments in the range from 0.25 to 0.62 MeV. Today more than 70 emitters of delayed neutrons with $T_{1/2}^{(n)}$ from 0.009 to 78 s are known.

4.3 The discovery and production of the first transuranium elements

As noted earlier, in 1934 already in his experiments on the irradiation of uranium with neutrons Fermi assumed that he had discovered elements in the Periodic Table after uranium, i.e. the 93rd, 94th, etc. elements. Actually, as we have already said, he observed (without knowing it) the β-activity of the ^{235}U fission fragments. Nevertheless, the discovery of the first transuranium element was made in 1940 by McMillan and Abelson [30], who used Fermi's approach: a ^{238}U nucleus captures a neutron and is turned to a β-unstable isotope ^{239}U that after β-decay transforms into an isotope of the first transuranium element, neptunium:

$$^{238}_{92}\mathrm{U}(\mathrm{n},\gamma)^{239}_{92}\mathrm{U} \xrightarrow{\beta^-} {}^{239}_{93}\mathrm{Np} \xrightarrow{\beta^-} . \qquad (16)$$

The new element in this chain was identified by its half-life, 2.35 days, which, in addition to the half-lives of $^{239}_{92}$U and the fission fragments, was observed for the irradiated uranium target but not for the fission fragments escaping the target. Another neptunium isotope, $^{238}_{93}$Np, was found when $^{238}_{92}$U was bombarded with 16-MeV deuterons:

$$^{238}_{92}\mathrm{U}(\mathrm{d},2\mathrm{n})^{238}_{93}\mathrm{Np} \xrightarrow{\beta^-} . \qquad (17)$$

Today eleven isotopes of neptunium are known in all (two of these are isomers).

The 94th element, plutonium $_{94}$Pu, was discovered in 1940 (the results were published later) by Seaborg et al. [31] in the reaction (17) together with neptunium ^{238}Np which transforms into $^{238}_{94}$Pu as a result of β-decay:

$$^{238}_{93}\mathrm{Np} \xrightarrow{\beta^-} {}^{238}_{94}\mathrm{Pu} \xrightarrow{\alpha} . \qquad (18)$$

The plutonium isotope is α-active and is used for manufacturing isotope current sources. Notice that the 93rd and 94th elements got their names after the planets Neptune and Pluto, which follow the planet Uranus as we move away from the Sun.

So far 15 isotopes of plutonium have been found. The best-known of these is $^{239}_{94}$Pu discovered in 1940 by Kennedy et al. [32] (the paper was received for publication in May, 1941 but was voluntarily withheld from publication until the end of the war). The nuclear properties of this isotope are close to those of $^{235}_{92}$U which can be disintegrated by thermal neutrons, in view of which both elements have been widely used in the construction of nuclear reactors. However, being close in their nuclear properties, the methods used to produce them are quite different. ^{235}U is produced by separating the isotopes of natural uranium, in which there is only one part in 140 of ^{235}U, while ^{239}Pu is produced at special radiochemical plants. The preparation for producing plutonium is probably the most remarkable exotic feature of the discovery and production of the first transuranium elements. The matter is that the plants for producing kilograms of plutonium were designed at a time when chemists had only 500 μg of plutonium salts produced as a result of bombarding hundreds of kilograms of uranium on a cyclotron. The process took many months to complete, and the entire complex radiochemistry attending the production of plutonium was developed by micromanipulations in vessels 0.1 – 1 mm in diameter when viewing through a microscope.

The 95th element americium ($_{95}$Am) and 96th element curium ($_{96}$Cm) were discovered in 1944, the 97th element berkelium ($_{97}$Bk) in 1949, and californium ($_{98}$Cf) in 1950. As a result of analyzing the heavy products of a thermonuclear explosion (uranium isotopes overloaded with neutrons, which were successively transformed into elements from number 93 to number 100 as a result of a chain of β-decays), einsteinium ($_{99}$Es) and fermium ($_{100}$Fm) were discovered in 1952. In 1965, the element mendelevium ($_{101}$Md) was discovered, over the period from 1957 to 1966 (for a long time no consistent results were achieved) the element nobelium ($_{102}$Nb), and in 1961 the element lawrencium ($_{103}$Lr), which is the last member of the actinide group (see below). For the subsequent transactinide elements (analogs of $_{72}$Hf, $_{73}$Ta, etc.), the following names have been approved: rutherfordium $_{104}$Rf, dubnium $_{105}$Db, seaborgium $_{106}$Sg, bohrium $_{107}$Bh, hassium $_{108}$Hs, and meitnerium $_{109}$Mt. The remaining transuranium elements, including the recently discovered elements 114 and 118 (see Section 11) for the time being are designated by the Z number of their charge.

We do not have the space here to discuss in greater detail the very interesting topic of the properties of transuranium elements. Only two specific features that must be taken into account when studying such elements will be mentioned. The first is that all the elements beginning with $_{90}$Th and ending with $_{103}$Lr belong to the actinide group, i.e. have very similar chemical properties, which makes it extremely difficult to study them (compare this with the similar situation in the case of the lanthanide group). The second is that transuranium elements exhibit all principal modes of radioactivity (α- and β-decay, spontaneous fission), and the laws governing each type help to study the properties of these elements. Some of these properties are discussed in the next section.

4.4 Spontaneous fission of uranium and transuranium elements

Spontaneous nuclear fission is not an exotic phenomenon in the sense that its discovery was not unexpected — the phenomenon was predictable, and the search for it was purposeful. The exotic angle here was different: the search was for a new radioactive process involving uranium, whose probability was 10^{10} times lower than that for the α-decay of uranium.

Such a result was arrived at by studying the mechanism of spontaneous nuclear fission by analogy with α-decay. If spontaneous fission occurs, there must be a Coulomb barrier W_f for the emerging fragments (see Fig. 2), whose penetrability can be estimated by a formula similar to (3):

$$D \approx \exp\left(-\frac{2}{h}\sqrt{2MW_\mathrm{f}}\,d\right), \qquad (19)$$

where M is the reduced mass of the fragments, W_f the height of the Coulomb barrier (fission barrier), and d the width of the barrier (fragment radius). Since the values of W_f and M in Eqn (19) are much larger than in the case of α-decay, the

barrier's penetrability for the spontaneous fission fragments proves to be extremely low, with the resulting half-life $T_{1/2}^{\text{s.f.}} \approx 10^{20}$ y, which made the discovery of this phenomenon practically impossible. Fortunately, this estimate happened to be overvalued by a factor of 10^4, but even the simpler problem of detecting a single event of spontaneous fission against the background of a million α-particles emitted in the same time proved to be very difficult as well.

Spontaneous fission of uranium was discovered in 1940 by Petrzhak and Flerov [27], who worked in Kurchatov's laboratory. To observe this phenomenon, a multilayer ionization chamber whose plates were covered by a thin film of uranium oxide was built (Fig. 4a). The fission fragments generated ionization pulses in the chamber, which were recorded by the mechanical counter after being amplified. The shape of the ionization pulses and their amplitude distribution proved to be identical to the respective parameters of pulses formed in induced fission initiated by neutrons. The results of a series of control experiments suggested that the observed effect could not be produced by cosmic rays or induced noise in the amplifier or the superposition of many α-particle pulses, i.e. spontaneous fission was indeed responsible for this effect. The scale of the detected effect can be estimated if one realizes that in the first experiment six pulses (on the average) of spontaneous fission were recorded each hour. This made it possible to estimate the experimental value of the half-life at $T_{1/2}^{\text{s.f.}} = (4 \pm 1) \times 10^{16}$ y, which is sufficiently close to the modern value.

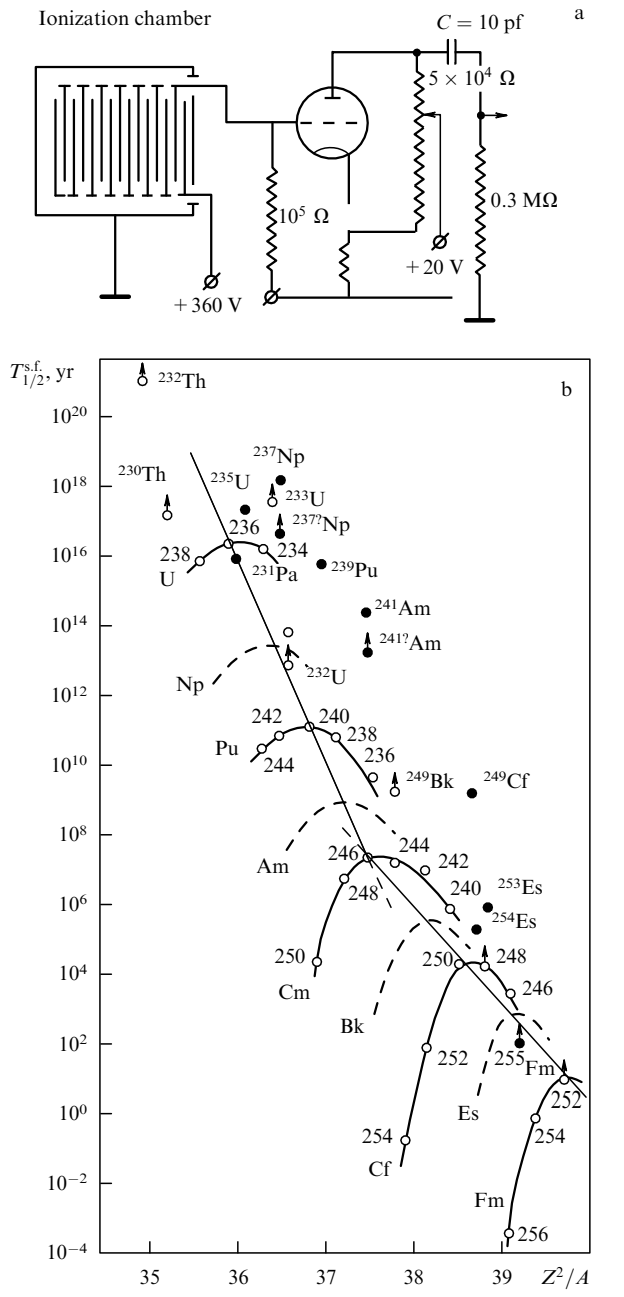

Figure 4. Discovery and investigation of spontaneous fission: (a) scheme of Petrzhak and Flerov's experiment, and (b) dependence of $T_{1/2}^{\text{s.f.}}$ of transuranium elements on the fissionability parameter Z^2/A.

In its properties, spontaneous uranium fission is very close to induced fission for low excitation energies of the fissioning nucleus. Specifically, the emission of fission neutrons (instantaneous and delayed) was also discovered in the case of spontaneous uranium fission, and a similar curve for the fragments' mass distribution was obtained.

Today, spontaneous fission is known to exist for several dozen isotopes of heavy elements, starting with $^{232}_{90}$Th, for which $T_{1/2}^{\text{s.f.}} > 10^{21}$ y at $T_{1/2}^{\alpha} = 1.4 \times 10^{10}$ y, and ending with the far transuranium elements, for which the half-lives amount to small fractions of a second. For even–even nuclei there is the following approximate relationship

$$\ln T_{1/2}^{\text{s.f.}} \approx a - b\frac{Z^2}{A}\,, \tag{20}$$

where a and b are coefficients, Z is the charge of the nucleus, A the mass number, and Z^2/A is what is known as the fissionability parameter (Fig. 4b). This relationship makes it possible to approximately estimate the half-lives of transuranium elements and the limits of possible existence of nucleon-stable nuclei (when $T_{1/2}^{\text{s.f.}}$ becomes equal to the nuclear time), which proves to correspond to $Z = 120-125$.

Equation (20) predicted the half-lives of the first transuranium elements fairly well, but for the heaviest nuclei it was discovered to yield highly undervalued half-lives $T_{1/2}^{\text{s.f.}}$, which can be attributed to the existence of an island of fairly stable nuclei near the end of the Periodic Table with $Z \sim 114$ and $N \sim 184$, although at $Z = 107$ the half-life of spontaneous fission is still extremely short ($\sim 10^{-2}$ s). At the beginning of 1999 there were reports from Dubna (Russia) about the synthesis of two isotopes of element 114 in the reactions

$$^{48}_{20}\text{Ca} + ^{242,\,244}_{94}\text{Pu} \rightarrow ^{287,\,289}114 + 3\text{n}\,. \tag{21}$$

Both isotopes proved to be α-active and decayed in 14 and 30 s, respectively. Similar α-activity is exhibited by the isotope $^{293}118$ of the 118th element, discovered at Berkeley (USA) in the same year (1999), and the third isotope of the 114th element, $^{288}114$, discovered at Dubna (see Section 11 for more details).

4.5 Spontaneous fission of nuclei in the isomeric state

In 1961, Polikanov et al. [33] and Perelygin et al. [34], while synthesizing the 104th element, unexpectedly discovered a new remarkable type of spontaneous nuclear fission with an extremely short half-life $T_{1/2}^{\text{s.f.}} = 0.014$ s. The experiments involved the internal beam of the multiply charged heavy-ion accelerator U-300 used to study the control reactions of

the interactions of $^{22}_{10}$Ne, $^{16}_{8}$O, and $^{11}_{5}$B ions with $^{238}_{92}$U nuclei, needed for synthesizing the 104th element. In the course of the experiment, the reaction products that were formed as a result of the interactions between the ions and the target nuclei landed on a rotating disk, and the fission fragments emitted by the products were recorded by two ionization chambers located at a distance from each other (in the direction of the disk's rotation), which made it possible to determine the half-life of the spontaneous fission.

Since exceptionally short activity was also observed in the reaction of the $^{11}_{5}$B and $^{238}_{92}$U nuclei, whose total charge is 97, the carrier of this activity could be one of the isotopes of the transuranium elements starting with $_{93}$Np and ending with $_{97}$Bk. However, the origin of the activity could not be connected to the spontaneous fission of the above-mentioned elements in the ground state since all known isotopes of the elements have very long half-lives, $T^{\text{s.f.}}_{1/2} > 10^7$ y. Hence, the researchers assumed that the source of the discovered activity is the isomeric (i.e. long-lived excited) state of the nucleus. Flerov et al. [35] were able to identify the isomeric nucleus by bombarding the target with ions lighter than $^{11}_{5}$B. The americium isotope $^{244}_{95}$Am proved to be this isomer. Later on spontaneous fission from the isomeric state was discovered for other americium isotopes, and still later this was done for many isotopes of other transuranium elements. Today more than three dozen spontaneously fissioning isomeric nuclei are known for elements starting with $_{92}$U and ending with $_{97}$Bk, with half-lives ranging from 2×10^{-9} to 1.4×10^{-3} s. However, deeper investigations into the properties of these isomers met with serious difficulties.

The quite natural effort to explain the discovered phenomenon by the laws of ordinary nuclear isomerism known from 1935 (see Section 3) was a failure. It turned out that such an interpretation leads at once to four puzzles. Firstly, the ratio of half-lives for spontaneous fission in the ground and isomeric states was too large. For $^{244}_{95}$Am, it amounts to $T^{\text{gr}}_{1/2}/T^{\text{isom}}_{1/2} = 10^4$ y/0.014 s $\approx 10^{23}$, while for other isomeric nuclei which have much shorter $T^{\text{isom}}_{1/2}$ than that of $^{244}_{95}$Am, this ratio reaches a value of roughly 10^{26}. Within the scope of ordinary nuclear isomerism (a level in a potential well bounded by the fission barrier) there is no explanation of such behavior. For the half-lives of the isomeric fission to be so short, there must be a much lower barrier. Secondly, the average value of the excitation energy, obtained through special experiments to determine the energy of isomeric states, was comparatively large, 3 MeV, which is highly atypical of ordinary nuclear isomerism. Thirdly, the results of other experiments suggested that the isomeric levels are characterized by low values of spin, which also contradicts the ideas about ordinary nuclear isomerism. Finally, it seemed amazing that in the conditions described above (high excitation energy and small spin) the observed emission of γ-quanta was strongly hindered.

A possible explanation of the nature of the new type of isomerism was given in 1966 by Flerov and Druin [36] and substantiated in 1967 by Strutinsky [37]. The idea is based on the assumption that the probability of spontaneous fission depends on the shape of the fissioning nucleus (shape isomerism), and the substantiation is done by introducing what is known as shell corrections (i.e. corrections that follow from the nuclear shell model; see Section 3) into the calculations of the curve reflecting the change of the potential energy of the nucleus and depicted in Fig. 2, which was obtained using the liquid drop model (see Section 4.1). Shell corrections take into account the dependence of the potential energy of the nucleus on the ratio of the numbers of neutrons and protons in the nucleus. In examining heavy fissioning nuclei that undergo strong deformations in the fission process, these corrections lead to a new potential energy curve not with one minimum and one maximum as in Fig. 2 but with two minima and two maxima, so that there are two energies of excitation above the ground state, $W^{(1)}_{\text{f}}$ and $W^{(2)}_{\text{f}}$ (the so-called double-humped curve, see Fig. 5a).

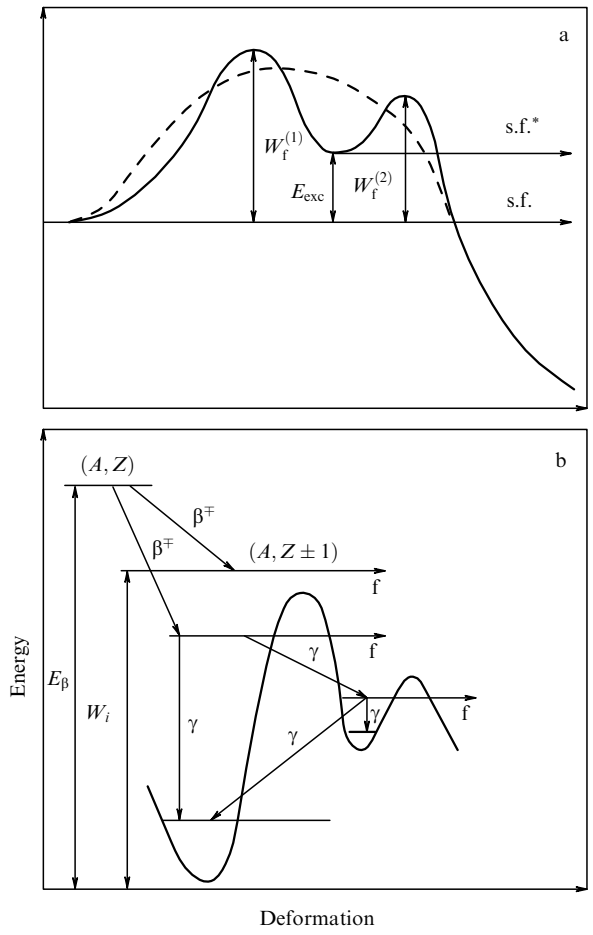

Figure 5. Diagrams for spontaneous fission in the isomeric state (a) and delayed fission (b): $W^{(1)}_{\text{f}}$ and $W^{(2)}_{\text{f}}$ are the heights of the first and second barriers, E_{exc} is the excitation energy of the nucleus in the second minimum, s.f and s.f.* are the spontaneous fissions from the ground and isomeric states; (A, Z) stands for the mother radioactive nucleus, E_β is the energy of the β-transition, W_i is the excitation energy of the daughter nucleus $(A, Z \pm 1)$, $\beta^{\mp}$ and γ are the possible β- and γ-transitions, and f indicates the possible variants of delayed fission.

Such a shape for the fission barrier makes it possible to give a qualitatively transparent interpretation of the new type of nuclear isomerism as shape isomerism. The first minimum corresponds to the long-lived ground state of the nucleus, while the second corresponds to the short-lived isomeric state. Figure 5a shows that the probability of ordinary spontaneous fission (s.f.) is determined by a broad and high potential barrier of height $W^{(1)}_{\text{f}}$ (the dashed curve in Fig. 5a), with the result that it is characterized by very long half-lives, while the probability of isomeric spontaneous fission (i.s.f.) is much higher, since it is determined by the position of the isomeric level in the second potential barrier bounded by a narrow and

low barrier of height $W_f^{(2)}$. Estimates of the penetrability of these barriers lead to values of the half-life ratios for spontaneous fission from the ground and isomeric states that are close to those obtained through experiments.

This model of shape isomerism also explains other features of spontaneous fission from the isomeric state of the nucleus. Specifically, the fact that the γ-transition accompanying isomeric spontaneous fission is hindered may be explained by the presence of a broad and high barrier between the two minima that the wave function of the isomeric nucleus must overcome for a γ-quantum to be emitted, i.e. in the transition from the isomeric state (second minimum) to the ground state (first minimum).

The fact that in the transition from the ground to the isomeric state the nucleus undergoes strong deformation is corroborated by the results of subtle experiments in determining the intrinsic quadrupole electric moments of isomeric nuclei, which suggest that these nuclei have a prolate ellipsoid shape with a 2-to-1 axis ratio. Unfortunately, due to the limited size of the present review we cannot discuss in greater detail these and other experiments that verify the shape isomerism hypothesis. The interested reader is advised to refer to Polikanov's monograph [38].

4.6 Delayed fission

In the process of studying isomers of spontaneous fission one more discovery was made. In 1966, Flerov and coworkers discovered (see Ref. [39]) fission fragments with a half-life $T_{1/2} = 2.6$ min for $^{234}_{94}$Pu nuclei produced as a result of electron capture by $^{234}_{95}$Am. Such a half-life is totally atypical for spontaneous fission from an isomeric state. Note that the isomeric nucleus $^{244}_{95}$Am has the maximum half-life for this phenomenon ($T_{1/2} = 1.4 \times 10^{-3}$ s), while all other isomeric nuclei have half-lives that are by many orders of magnitude shorter.

Similar results with half-lives in the minute range were obtained for $^{238}_{92}$U ($T_{1/2} \approx 1$ min), $^{232}_{94}$Pu ($T_{1/2} = 1.4$ min), $^{240}_{96}$Cm ($T_{1/2} \approx 5$ min), and $^{246}_{98}$Cf ($T_{1/2} \approx 8$ min) nuclei. The study of this new phenomenon was done at Dubna on the multiply charged heavy-ion accelerator U-300 with an energy of several tens of megaelectronvolts. The fission fragments were recorded by solid-state track detectors insensitive to α-particles (see Sections 7.2 and 7.3).

As an example, we investigate the chain of reactions in which fission fragments of $^{246}_{98}$Cf with $T_{1/2} \approx 8$ min were detected:

$$^{238}_{92}\mathrm{U}(^{14}_{7}\mathrm{N}, 6\mathrm{n})^{246}_{99}\mathrm{Es} \xrightarrow{\mathrm{e}} {}^{246}_{98}\mathrm{Cf} \xrightarrow{\mathrm{s.f.}} . \qquad (22)$$

The bombardment of $^{238}_{92}$U was done with $^{14}_{7}$N ions with energies ranging from 92 to 94 MeV, which corresponded to the maximum of the excitation function for this reaction; the $^{246}_{99}$Es nuclei produced were transformed via electron capture to $^{246}_{98}$Cf nuclei, which fissioned. Measurements of the half-life for the electron capture by $^{246}_{99}$Es yielded a value $T_{1/2}^{(e)} \approx 7.7$ min, which is close to the half-life measured for the fission fragments of $^{246}_{98}$Cf. This and some other indications made it possible to conclude that the new phenomenon must be interpreted as fission of the nucleus $^{246}_{98}$Cf delayed by the time of electron capture by $^{246}_{99}$Es (compare this with the emission of delayed neutrons discussed in Section 4.2).

A detailed study of similar phenomena suggested that delayed fission can occur not only after capture by the mother nucleus of an orbital electron but also as a result of other β-transformations (β^+- or β^--decays) with the mother nucleus. The possible modes of delayed fission are depicted in Fig. 5b. Here (A, Z) is the mother β-active nucleus, the horizontal lines under $(A, Z\pm1)$ stand for the levels of the excited daughter nucleus with an excitation energy W_i, the arrows labelled $\beta^\pm$ indicate the possible $\beta^\pm$-transitions, those labelled γ indicate the possible γ-transitions, and those labelled f indicate the possible variants of delayed fission.

The difficulty in observing delayed fission is due to the requirement that the following obvious conditions be met simultaneously. First, the probability of competing fissions of the mother nucleus (A, Z) by mechanisms that differ from β-decay (spontaneous fission, α-decay, and emission of γ-radiation) must be low. Second, the probability of populating the levels of the fissioning nucleus $(A, Z\pm1)$ in the preceding β-decay must be fairly high. Third, the probability of processes that compete with fission and deexcite the nucleus $(A, Z\pm1)$, i.e. emission of delayed nucleons or γ-radiation, must be low. Finally, insurmountable difficulties often emerge due to the smallness of the effect if one wishes to make the most convincing experiment involving the coincidence circuit to simultaneously register delayed fission and the preceding β-decay.

At present sufficiently many nuclei are known that undergo delayed fission, and the delay effect has been discovered not only for neutron-deficient nuclei experiencing electron capture or β^+-decay but also, somewhat later (1976), for the neutron-rich nuclei ^{234}Pa, ^{236}Pa, and ^{238}Pa that emit (also with half-lives in the minute range) electrons before fission [40, 41]. Research into delayed fission helps the study of the properties of neutron-rich and neutron-deficient nuclei, e.g. to find the parameters of their fission barriers. For more details about delayed fission the interested reader should refer to Kuznetsov's review [42].

5. Proton radioactivity

In Section 2.2 we noted that when artificial radioactive nuclei are produced in the reactions (α, n), (p, n) or through bombardment with heavy ions, neutron-deficient nuclei are produced and that the common way in which these nuclei deexcite is through β^+-decay or electron capture. Here, the energy of β-decay increases and the half-life decreases with decreasing ratio N_n/N_p, where N_n is the number of neutrons in the nucleus, and N_p the number of protons. The decrease in this ratio also causes a reduction in the energy of separation of the proton from this nucleus (the binding energy ε_p), while the nuclei themselves move closer to the proton instability limit $\varepsilon_p = 0$ (after this limit has been passed the nuclear forces cannot hold the excess protons because of the relatively strong Coulomb repulsive forces).

Near the proton instability limit one can expect the emergence, in addition to β^+-decay and electron capture, of several extraordinary modes of radioactivity, which we combined under the general name of proton radioactivity. Below we will study (in order of increasing exoticism) the emission of retarded protons, isomeric proton decay, proton decay of a nucleus from the ground state, and various modes of double-proton radioactivity (including hypothetical modes).

5.1 Retarded protons

Retarded protons were discovered in 1962 at JINR (Dubna) by Karnaukhov with his collaborators [43], who found in the

process of bombarding nickel foil with $^{20}_{10}$Ne ions that a proton emitter with a half-life $T_{1/2} = 24$ s is produced. A similar phenomenon was discovered practically simultaneously by Barton et al. [44].

The mechanism of emission of retarded protons is similar to that described in Section 4.2 for the emission of delayed neutrons. The diagram illustrating emission of retarded protons is depicted in Fig. 6 [45].

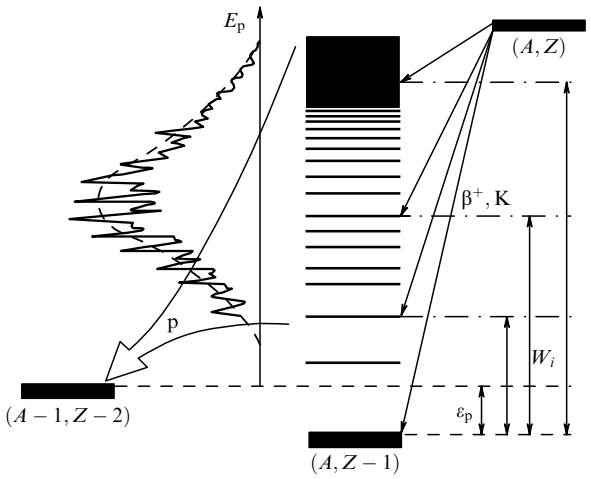

Figure 6. Diagram of emission of retarded protons [45]: (A, Z) stands for the mother β^+-active nucleus, $(A, Z-1)$ for the daughter nucleus with an excitation energy W_i exceeding the proton binding energy ε_p, and p indicates the delayed proton transitions to the nucleus $(A-1, Z-2)$.

Usually a neutron-deficient nucleus (A, Z) passes through β^+-decay or electron capture into the ground or excited state of the daughter nucleus $(A, Z-1)$, whose excitation energy W_i is released through the emission of γ-quanta or internal conversion electrons. However, near the proton instability limit the excitation energy W_i of the nucleus $(A, Z-1)$ may exceed the energy of separation of the proton from this nucleus (the binding energy $\varepsilon_p < W_i$). In this case, in addition to β^+-decay and emission of γ-quanta and conversion radiation, there can be emission of protons from the ith level of the nucleus $(A, Z-1)$. And since this possibility emerges only after the β^+-transition of the nucleus (A, Z) is completed, the emission of protons by the nucleus $(A, Z-1)$ is delayed by the time of this β-transition (emission of the proton proper occurs very fast).

The energy of the retarded protons is $T_p = W_i - \varepsilon_p$, and starting with $T_p = 0.8-1$ MeV this energy can be recorded. At energies of this order of magnitude, the relative probability Γ_p/Γ of retarded proton emission is not very high due to the presence of a Coulomb barrier, whose height is 4 MeV for the light nucleus $^{17}_{10}$Ne but amounts to 15 MeV for $^{179}_{80}$Hg. The relative probability Γ_p/Γ increases with the proton energy, and then drops again due to a decrease in the probability of β-transitions to the high levels of the nucleus $(A, Z-1)$. As a result, the spectrum of retarded protons is represented by a toothed bell-shaped curve (see Fig. 6), with the number of teeth being the number of monochromatic proton groups.

Today more than a hundred emitters of retarded protons are known, and each emits monochromatic protons with several energies (in the case of light nuclei) or a broad energy spectrum (in the case of medium and especially heavy nuclei). For instance, the $^{9}_{6}$C nucleus (actually $^{9}_{5}$B if one recalls Remark 4 in Section 1.2) emits retarded protons with energies amounting to 8.24 and 10.92 MeV ($T_{1/2} = 0.126$ s). Such nuclei have been produced in the reactions $^{10}_{5}$B(p, 2n), $^{7}_{4}$Be(^{3}He, n), and $^{12}_{6}$C(p, p3n). As the emitters get heavier, the number of proton groups increases. For example, the $^{13}_{8}$O nucleus emits four groups of retarded protons with energies ranging from 1.44 to 7.0 MeV ($T_{1/2} = 0.009$ s), while $^{17}_{10}$Ne emits even five groups with energies ranging from 1.68 to 7.04 MeV ($T_{1/2} = 0.108$ s). The fact that the number of proton groups is relatively small for light nuclei makes identifying them a fairly easy task, which enables the study of the energy states of the nucleus $(A, Z-1)$.

For heavier nuclei, starting with $Z \approx 30$, it becomes difficult to resolve the density of levels of the daughter nucleus $(A, Z-1)$ and hence the energy spectrum of the retarded protons. For instance, the spectrum of the retarded protons of $^{181}_{80}$Hg is practically continuous in the energy interval from 3 to 6 MeV, within which, however, there certainly exists a fine structure, which makes it possible to judge the density of nuclear levels at different excitation energies.

The interested reader can find detailed information about retarded protons in the review by Karnaukhov [45], the book by Karnaukhov and Petrov [46], and in Karnaukhov's encyclopedic paper [47].

5.2 Isomeric proton decay

Nuclei that emit protons can be produced (at least theoretically) not only as a result of a preceding β^+-decay but also directly in a nuclear reaction. If such a nucleus is neutron-deficient and its excitation energy is high than the proton binding energy ε_p, it can emit protons, just as in the case with retarded protons. Usually, however, it is impossible to observe this process against the background of the much more probable deexcitation by γ-transitions (and also β^+-decay). One possible exception is the case where there exists an isomeric nucleus that has a metastable level with a large angular momentum, from which a γ-transition is highly unfavored, and if, in addition, the probability of a β^+-transition is not very high for this nucleus.

Such an isomeric nucleus (the only one known so far), a proton emitter, was discovered in 1970 by Jackson et al. and Cerny et al. [48] in the reaction

$$^{54}_{26}\mathrm{Fe(p, 2n)}^{53}_{27}\mathrm{Co}^{*} \qquad (23)$$

and was additionally investigated in 1972 by Cerny et al. [49].

When studying the levels of the excited nucleus $^{53}_{27}$Co* produced in reaction (23) (Fig. 7a) it was found that one of these levels (with an angular momentum of 19/2) is long-lived with $T_{1/2} = 247 \pm 12$ ms and that the probability of proton emission from this level is not low ($\Gamma_p/\Gamma = 0.015$). In these conditions, it became possible to record the emission of protons with an energy of 1.59 ± 0.03 MeV (Fig. 7b).

The researchers used a 35-MeV proton beam extracted from the 88-inch cyclotron at Berkeley. The protons bombarded a $^{54}_{26}$Fe target (840 μg cm^{-2}) obtained through isotope separation. To identify the protons produced in the decay of $^{53}_{27}$Co^{m}, they employed the $\Delta E-E$ method realized through the use of two telescopes with semiconductor detectors 4- and 8-μm (ΔE) and 50-μm (E) thick. Figure 7b shows that 1.59-MeV protons (in the center-of-mass reference frame) produced a sharp peak against the background noise, while the other group of protons corresponding to the formation of

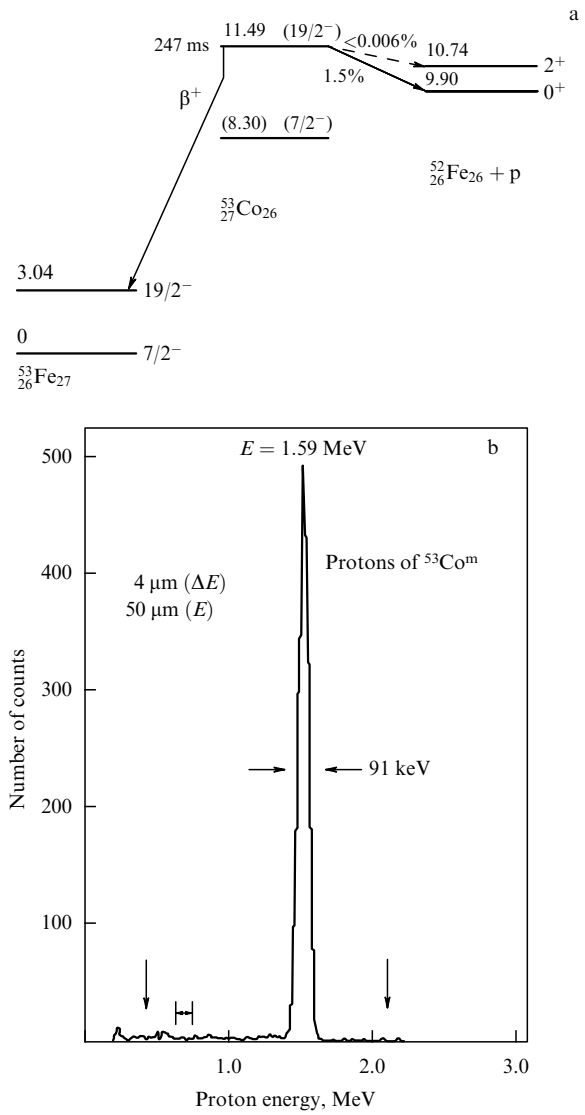

Figure 7. Scheme of isomeric proton decay of the nucleus $^{53}_{27}Co^{m}$ (a), and the energy spectrum of the emitted protons (b).

the $^{52}_{26}Fe$ nucleus in the excited state (Fig. 7a) and for which the second telescope with the 8-μm ΔE-detector was used, is totally absent from the picture. Estimates of the upper bound on its yield, obtained from a comparison with the background level, give a value of the relative probability Γ_p/Γ equal to 6×10^{-5}. Estimates of the proton yield in the main group (1.5%) set the value of the partial half-life $T_{1/2}$ of the isomeric proton decay of $^{53}_{27}Co^{m}$ at roughly 17 s.

5.3 Proton decay of a nucleus from the ground state

The two modes of proton radioactivity that we have just investigated are united by two common features: a small but positive proton binding energy ε_p and, as a result, the possibility of proton emission solely when the excitation energy W of the nucleus is high ($W > \varepsilon_p$). Another possibility of proton emission emerges if the deficit of neutrons in the nucleus is so great that even in the ground state the nucleus is past the proton stability limit ($\varepsilon_p < 0$) and hence the nuclear forces are incapable of holding the proton inside the nucleus. In such a case, the nucleus can, at least in principle, emit protons from the ground state against the intense background produced by β^+-decay.

The mechanism of proton decay is similar to that of α-decay: a tunnelling transition of a proton through the Coulomb barrier (and, possibly, a centrifugal barrier) with a probability determined by the penetrability of the barrier. Since the proton charge is equal to unity and the nuclei emitting protons have smaller values of Z than those emitting α-particles, this barrier is fairly low. From the theoretical viewpoint, proton decay is even simpler than α-decay since there is no problem in forming the emitted particles: in contrast to α-particles, protons exist inside the nucleus ready for emission. However, all attempts to detect proton decay are fraught with a severe experimental difficulty: the strong competition from β^+-decay, because of which one is able to observe proton decay only in exceptional cases, when the β^+-decay manifests itself rather weakly (forbidden β^+-transitions). Calculations have shown that proton emitters are most likely to be found among nuclei with $Z > 50$, which can, theoretically, emit protons with energies $T_p = 0.5-1.5$ MeV and half-lives $T_{1/2} \leqslant 0.1-1$ s that are convenient for recording (the lower bound on $T_{1/2}$ is determined by the possibilities of the experimental method). Here, proton decay has a higher probability of occurring for odd-Z nuclei, in which the last proton is unpaired, i.e. has a smaller binding energy due to the absence of an additional pair interaction which exists between the last even proton and the preceding odd proton.

The first to discover weak proton radioactivity were Karnaukhov and coworkers in 1972 at Dubna (see Ref. [50]) in the reaction

$$^{96}_{44}Ru(^{32}_{16}S,\ p6n)^{121}_{59}Pr\,. \qquad (24)$$

The emitted protons have an energy $T_p = 0.83 \pm 0.05$ MeV and a characteristic half-life $T_{1/2} = 1.4 \pm 0.8$ s.

To clarify the picture we note that the neutron-deficient nucleus $^{121}_{59}Pr$ (which has 20 neutrons *less* than the β-stable isotope of praseodymium $^{141}_{59}Pr$) may be thought of as being a proton-rich nucleus, which has 12 protons *more* than the β-stable nucleus $^{109}_{47}Ag$ with the same number of neutrons (62) as in $^{121}_{59}Pr$. Just the 12th proton is the excessive proton for $^{121}_{59}Pr$, since it has a negative binding energy ($\varepsilon_p < 0$), and proton decay occurs precisely because of this.

Ten years later Hofmann et al. [51] were able to produce a new proton emitter with a very high yield, $^{151}_{71}Lu$, in a reaction with the same nucleus $^{96}_{44}Ru$ but with different bombarding ions $^{58}_{28}Ni$:

$$^{96}_{44}Ru(^{58}_{28}Ni, p2n)^{151}_{71}Lu\,. \qquad (25)$$

What is remarkable about this reaction is that the deficit of neutrons in $^{151}_{71}Lu$, needed for proton decay to occur, is achieved by 'evaporating' only three nucleons, with the result that the reaction cross section is 700 times larger than the cross section of reaction (24), in which seven nucleons must be 'evaporated' to produce the $^{121}_{59}Pr$ nucleus with the necessary neutron deficit.

More than that, the probability of β^+-decay of $^{151}_{71}Lu$ is reduced considerably due to the large difference in the angular momenta of the initial and final nuclei (a forbidden β-transition). In view of these two factors, new possibilities have emerged for a more detailed study of proton decay. Let us discuss this subject in greater detail.

Reaction (25) was studied on the heavy-ion accelerator in Darmstadt (Germany) together with some other reactions in

which nickel ions with energies in the 200 – 400 MeV range were used to bombard the target. The products of the reaction of interest were separated from the beam particles and the products of other reactions by a velocity separator with a 11-m base and were implanted into a device consisting of several position-sensitive surface-barrier detectors that recorded the kinetic energy, the time and location of the implantation of the nuclei, as well as the energy, time, and location of the particles produced in their subsequent decay processes. The use of such a device allowed the researchers to analyze the space – time correlations of chains of events, which made it possible to measure the half-lives (using additional devices, of course).

A telescope with $\Delta E - E$-detectors was used to identify the particles. The reaction-product nuclei were stopped in a thin (25.6 μm) ΔE-detector. The protons and α-particles left the detector and were stopped in a 'thick' (142 μm) detector placed 15 mm behind the ΔE-counter. The intensive production of $^{151}_{71}$Lu in reaction (25) and the recording system described above allowed the researchers to reliably identify the decay protons and to determine their energy T_p and half-life $T_{1/2}$:

$$T_p = 1.231 \pm 0.003 \text{ MeV}, \quad T_{1/2} = 85 \pm 10 \text{ ms}. \qquad (26)$$

Figure 8a depicts the energy spectrum of the particles emitted by a $^{96}_{44}$Ru target bombarded with $^{58}_{28}$Ni ions of energy 261 MeV [at this energy the excitation function of reaction (25) is at its maximum]. The detected proton line resides in the low-energy part of the spectrum at $T_p = 1.23$ MeV (The same line, depicted in Fig. 8b on a linear scale, is magnified to a larger scale.)

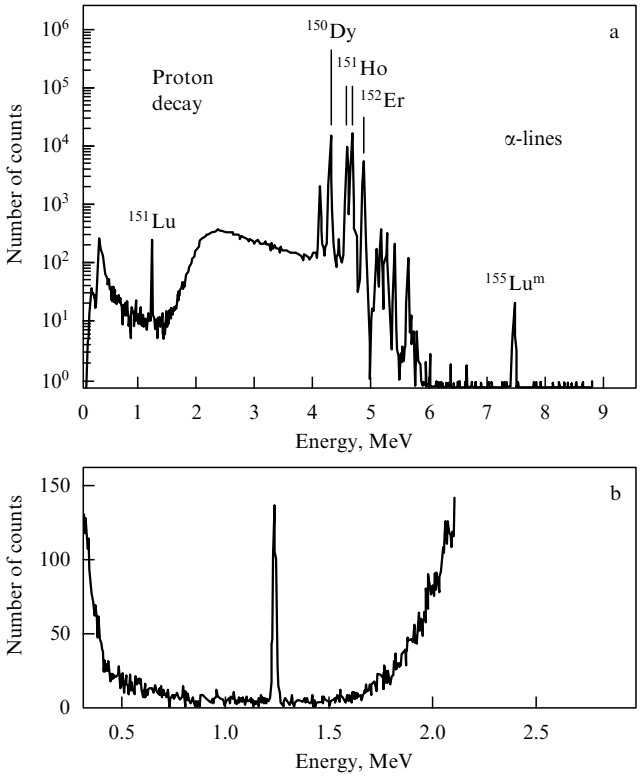

Figure 8. Energy spectra of the particles emitted by a $^{96}_{44}$Ru target bombarded with $^{58}_{28}$Ni ions: (a) relative position of the 1.23-MeV proton line caused by the decay of $^{151}_{71}$Lu and the α-particle lines, and (b) the 1.23-MeV proton line magnified to a larger scale.

The other discrete lines in Fig. 8a correspond to α-transitions of known nuclides. The strongest of these lines, in the 4 – 5 MeV range, belong to the isotopes of the rare-earth elements Dy, Ho, and Er with $N = 84$ (differing by two units from the magic number of neutrons, $N = 82$).

The high-energy α-lines contain the isomeric transition of the $^{155}_{71}$Lu^m nucleus produced in the reaction with the heavier isotopes of $_{44}$Ru, contained in the target in the form of an impurity. The broad maximum between 2 and 4 MeV is produced by α-particles leaving the detector in the opposite direction (back in relation to the α-active nucleus implanted into the detector). The background on the low-energy side of the proton peak is generated primarily by β^+-particles and conversion electrons.

Hofmann et al. [51] paid special attention to the proof of the fact that protons are emitted precisely from the ground state of $^{151}_{71}$Lu and are not of the retarded type. The most convincing argument in favor of this conclusion was the absence of an annihilation γ-quantum (0.511 MeV) and characteristic X-ray radiation, which have to appear, respectively, in β^+-decay and electron capture together with the emission of retarded protons.

Measurements done in the p – γ and p – X coincidence circuits with the statistics of 2400 proton events have shown that the upper limit for the number of coincidences (including random coincidences) does not exceed 5%. This result makes it impossible to interpret the origin of the detected protons as protons retarded after β^+-decay. Additional arguments in favor of the assumption that the detected protons were emitted by the $^{151}_{71}$Lu nucleus in the ground state were obtained from the kinematics of the decay process and from measurements of the reaction's excitation function and the proton energy.

Later on several more proton emitters were produced by reactions in which the target was bombarded by $^{58}_{28}$Ni ions. The proton energies and half-lives for these emitters are listed in Table 1 (for more details see Ref. [47]).

Table 1. Proton emitters with emission starting from the ground state of the nucleus.

Nucleus	T_p, keV	$T_{1/2}$, ms
$^{150}_{71}$Lu	1261 ± 4	$\geqslant 10$
$^{151}_{71}$Lu	1231 ± 3	85 ± 10
$^{147}_{69}$Tm	1117 ± 6	360 ± 80
$^{147}_{69}$Tm	1050 ± 4	560 ± 40
$^{113}_{55}$Cs	958 ± 4	0.033 ± 0.007
$^{109}_{53}$I	811 ± 5	0.109 ± 0.017

According to the data cited in Kadmenskiĭ's recent article [52] (with reference to the paper by Woods and Davids [53]), today we know of more than 30 nuclei that experience proton decay from the ground and isomeric states (from $^{53}_{27}$Co to $^{185}_{83}$Bi). So far, for all the proton-decay nuclei the proton energy is in the 0.5 – 2.0 MeV range. The fraction of proton decay varies from 0.4 to 100%, with β-decay being the main competitor of proton decay for nuclei with $A \leqslant 151$, and α-decay for heavier nuclei. The measured partial proton half-lives lie within the range $17 \times 10^{-6} - 50$ s.

In addition to reviewing the data, Kadmenskiĭ's article [52] presents the main statements of the many-body theory of proton decay of spherical nuclei and of the theory of proton

decay of deformed nuclei (Kadmenskiĭ actively participated in the development of both theories).

5.4 Double-proton radioactivity

The possibility of double-proton radioactivity was predicted 40 years ago by V Gol'danskiĭ [54] (see also his review [55]). His idea was based on the effect of proton pairing (described in Section 5.3), according to which the binding energy of an even proton is higher than that of an odd proton. This means that there exists, at least theoretically, a neutron-deficient nucleus for which the binding energy of the last (even) proton is slightly positive, $\varepsilon_p(A, Z) \geqslant 0$, while that of the penultimate (odd) proton is negative, $\varepsilon_p(A-1, Z-1) < 0$. As a result, the total binding energy of these two protons may prove to be negative:

$$\varepsilon_{2p}(A,Z) = \varepsilon_p(A,Z) + \varepsilon_p(A-1,Z-1) < 0\,, \qquad (27)$$

i.e. such a nucleus is unstable with respect to emission of a proton pair but stable with respect to emission of a single proton.

Similar reasoning concerning the fact that $\varepsilon_{2p} < \varepsilon_p$ may be applied not only to the ground state of a nucleus with even Z but also to the excited state of such a nucleus. Hence, hypothetically, double-proton radioactivity can be observed in the same three modes that were discovered in the case where only one proton is emitted by the nucleus, i.e. double-proton decay, isomeric double-proton decay, and retarded proton pairs. So far only the last mode has been observed in experiments.

In 1980, Gol'danskiĭ [56] identified two concrete nuclei, $^{22}_{13}$Al and $^{26}_{15}$P, whose β^+-decay should lead to the production of emitters of retarded proton pairs, $^{22}_{12}$Mg* and $^{26}_{14}$Si*. Three years later, one of these emitters ($^{22}_{12}$Mg*) was indeed discovered by Cable et al. [57], who employed the 88-inch cyclotron at Berkeley. To produce the neutron-deficient nucleus $^{22}_{13}$Al, the researchers used the interaction of a beam of 110-megavolt doubly charged ions ^{3}He^{2+} and magnesium nuclei $^{24}_{12}$Mg in the reaction

$$^3\mathrm{He} + ^{24}_{12}\mathrm{Mg} \rightarrow ^{22}_{13}\mathrm{Al} + \mathrm{p} + 4\mathrm{n}\,. \qquad (28)$$

The $^{22}_{13}$Al* nuclei produced in reaction (28) were transformed via β^+-decay ($T_{1/2} = 0.07$ s) into highly excited nuclei $^{22}_{12}$Mg* (Fig. 9a), which then emitted retarded proton pairs by the reaction

$$^{22}_{13}\mathrm{Al} \xrightarrow{\beta^+} ^{22}_{12}\mathrm{Mg}^* \rightarrow ^{20}_{10}\mathrm{Ne} + 2\mathrm{p}\,. \qquad (29)$$

To observe and identify the proton pairs, Cable et al. [57] used the telescopes with three silicon detectors $\Delta E1$ (24 μm), $\Delta E2$ (155 μm), and E (500 μm). The detectors $\Delta E1$ and $\Delta E2$ were divided into two parts, each forming two detectors (on the same silicon base). This device, connected to a computer, made it possible to register both protons of the pair simultaneously (with a 20-ns window), to measure and record the energy of each protons in the pair, and to monitor the reactions (28) and (29) by recording the yield of single retarded protons (Fig. 9a) and to estimate the number of accidental coincidences.

Figure 9b depicts the energy spectrum of the proton pairs, with two peaks clearly visible. One peak appears when the value of the total energy of the two protons in the pair is equal to 5.636 ± 0.020 MeV (in the laboratory reference frame), while the other peak is at 4.139 ± 0.020 MeV. The first peak

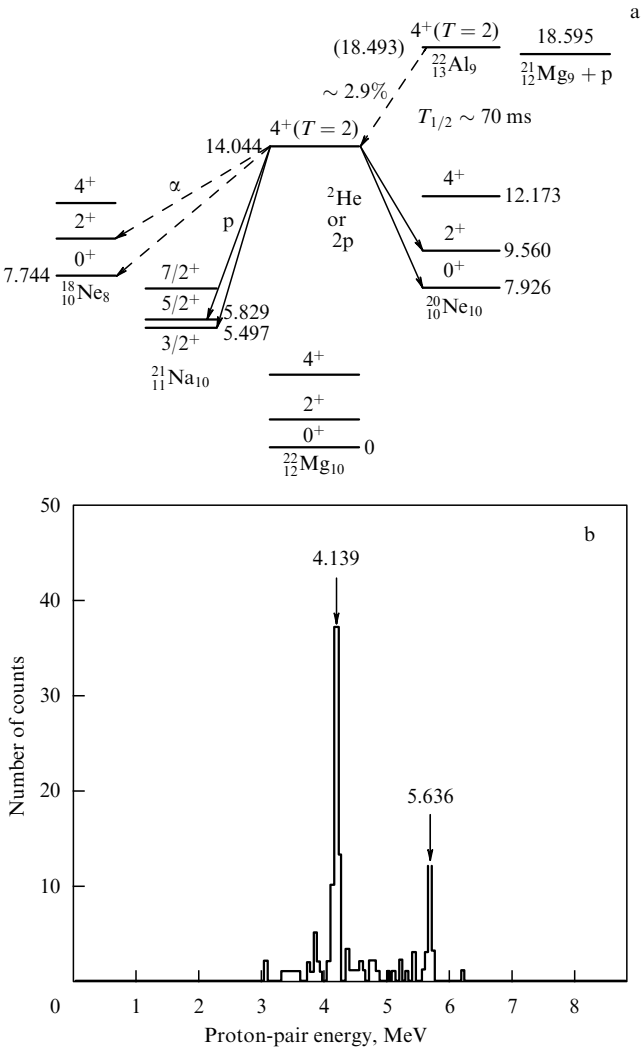

Figure 9. Diagram of emission and the energy spectrum of retarded proton pairs: (a) the likely scheme of partial decay of $^{22}_{13}$Al, and (b) the proton-pair energy spectrum.

corresponds to the 2p-transition from the 14.044-MeV level of the $^{22}_{12}$Mg* nucleus to the ground state of the $^{20}_{10}$Ne nucleus, and the second peak corresponds to the transition to the first excited state (Fig. 9a).

Later, the β^+-active predecessor (also predicted by Gol'danskiĭ [56]) of the potential emitter of proton pairs, $^{26}_{15}$P ($T_{1/2} = 0.02$ s), was discovered, and so was another, $^{35}_{20}$Ca ($T_{1/2} = 0.05$ s).

6. Neutron radioactivity

6.1 General ideas concerning the possibility of neutron radioactivity

As noted earlier, radioactive processes denote spontaneous decays of nuclei accompanied by emission of elementary particles or nuclear fragments in measurable time intervals with current values $\tau \geqslant 10^{-12}$ s (in accordance with the possibility of measuring such time intervals by modern methods). For the radioactive processes described so far, the validity of this condition was guaranteed in different ways. In the case of β-decay, by the weakness (i.e. low rate) of the

corresponding interaction; in the cases of α-decay, spontaneous fission, and proton decay from the ground state, by the presence of a Coulomb (and, possibly, centrifugal) barrier; in the case of γ-transitions, by the small value of the excitation energy and the large difference in the spins of the initial and final states of the nucleus, and, finally, in the case of various delayed processes, by the value of the half-life of the preceding β-transition.

The neutron participates in the strong (i.e. high-rate) interaction and has no electric charge. Hence, a neutron almost instantly (in the course of roughly 10^{-15} s) escapes from a neutron-rich nucleus when $\varepsilon < 0$. For instance, this is the situation with instantaneous neutrons emitted in $\tau_{\text{expt}} < 10^{-14}$ s with fission fragments. As noted earlier, this is not a radioactive process but what is known as an evaporative process, closely resembling the decay of an intermediate (compound) nucleus with the emission of neutrons.

Theoretically, we can speak of neutron radioactivity if, of the above conditions guaranteeing that the lifetime of the radioactive nuclei is measurable, only one of the following two holds: a centrifugal barrier for the neutron in the nucleus is present or the nucleus is formed as a result of a preceding β-decay.

A centrifugal barrier for the neutron emerges if the neutron escaping from the nucleus carries away a finite orbital angular momentum, $l \neq 0$. This is possible (at least in principle), for instance, for isomeric states of nuclei whose excitation energy exceeds the neutron binding energy ($W > \varepsilon_{\text{n}}$). Estimates of the penetrability of the centrifugal barrier show that the lifetime of a neutron isomer may be as long as several tens or even hundreds of seconds. With $W > \varepsilon_{2\text{n}}$, double-neutron decay of an isomeric state is possible (at least theoretically), while with $\varepsilon_{2\text{n}} < 0$ and $l \geqslant 3$ even double-neutron decay of the ground state is possible. So far not one of the above processes has been recorded (for more details see Karnaukhov and Petrov's book [46]). However, the second possibility, the emission of neutrons after β-decay, is realized in nature in even three ways. One of these ways, the emission of single delayed neutrons, has been described in Section 4.2. We will now turn to the other two, which are more exotic.

6.2 Delayed double-neutron radioactivity

In Section 4.2 we said that if, as a result of β^--decay, the final nucleus is produced in an excited state with an excitation energy exceeding the binding energy of the neutron ($W > \varepsilon_{\text{n}}$), the β^--decay of the mother nucleus is followed by the emission of a neutron by the daughter nucleus with the same half-life $T_{1/2}^{(\text{n})} = T_{1/2}^{(\beta^-)}$ and with an energy $T_{\text{n}} = W - \varepsilon_{\text{n}}$ (delayed or β-retarded neutrons).

Similarly, when $W > \varepsilon_{2\text{n}}$, there must be delayed double-neutron radioactivity, i.e. simultaneous emission by the daughter nucleus of two neutrons with $T_{1/2}^{(2\text{n})} = T_{1/2}^{(\beta^-)}$ and $T_{2\text{n}} = W - \varepsilon_{2\text{n}}$. Delayed double-neutron radioactivity was predicted by Gol'danskiĭ [54] in 1960 and discovered experimentally by Azuma et al. [58] in 1979 at CERN in the reaction

$$^{11}_{3}\text{Li} \xrightarrow{\beta^-} {}^{11}_{4}\text{Be} \rightarrow {}^{9}_{4}\text{Be} + 2\text{n} \quad (T_{1/2} = 8.5 \text{ ms}) . \tag{30}$$

The main difficulty encountered by Azuma et al. [58] was that usually $\varepsilon_{2\text{n}} > \varepsilon_{\text{n}}$, i.e. if $W > \varepsilon_{2\text{n}}$, then automatically $W > \varepsilon_{\text{n}}$, and in addition to a pair of delayed neutrons there are many more single delayed neutrons emitted in the process. Obviously, two conditions were to be met if the researchers were to succeed (we mentioned these conditions in the section devoted to delayed double-proton radioactivity): special selection of the nuclear emitters, and a method for separating single- and double-neutron radioactivities.

Fundamentally, there are two criteria by which single neutrons can be distinguished from neutrons in pairs: the energy criterion and the temporal criterion. As mentioned earlier, single delayed neutrons have a certain kinetic energy $T_{\text{n}} = W - \varepsilon_{\text{n}}$ and a characteristic half-life equal to the half-life of the preceding β-transition: $T_{1/2}^{(\text{n})} = T_{1/2}^{(\beta^-)}$. By contrast, for delayed neutrons constituting pairs only the total kinetic energy must be the same, $T_1 + T_2 = W - \varepsilon_{2\text{n}}$, while the energy of each neutron in a pair may vary within the range $0 \leqslant T_{1,2} \leqslant W - \varepsilon_{2\text{n}}$. But the detection of such neutrons is easier because they must escape from the nucleus simultaneously.

Azuma et al. [58] conducted two experiments. The first was planned to study the emission of a single delayed neutron by the ^{11}Li nucleus, while the second was needed to study the emission of delayed neutron pairs. Three ionization chambers filled with ^{3}He and connected in parallel were used to determine the parameters of the delayed neutrons. Such a device made it possible to infer the energy of the neutrons by measuring the energy release in the chamber. The energy Q of the reaction

$$\text{n} + {}^{3}\text{He} \rightarrow {}^{3}\text{H} + \text{p} \tag{31}$$

is equal to 0.864 MeV; the reaction's cross section is at its maximum when the neutrons are thermal ($T_{\text{n}} = 0.025$ eV). As the neutron energy increases, the amount of energy released in reaction (31) grows but the reaction's cross section rapidly decreases. Nevertheless, three neutron peaks in the energy release were detected: at 18 keV, at 80 keV, and at 1.99 MeV (Fig. 10a). Their positions correspond to the well-known level diagram for the ^{11}Be nucleus (Fig. 10b). Two more neutron peaks (at 1.17 MeV and at 1.27 MeV), which were supposed to be present in this scheme, were not observed. The energy range denoted in Fig. 10a by a brace was interpreted by Azuma et al. [58] as a continuum characterizing the emission of a neutron pair.

The proof that delayed neutron pairs are actually emitted was provided by the second experiment. It would seem that the easiest way to solve this problem is to connect several ^{3}He-counters into a coincidence circuit that would record the fact that two neutrons have entered two counters (or one and the same counter) simultaneously. However, such an experimental setup would lead to several serious difficulties (the low efficiency of recording fast neutrons, the fact that it is impossible to distinguish between the entry of one and two neutrons into the same counter, and difficulties with the power supply circuits). Hence, Azuma et al. [58] adopted an approach that at first glance seemed quite unexpected. They purposefully separated in time the neutrons of a pair, which simultaneously escape from the nucleus, lowering their energy to thermal energies by slowing them down. Since this approach is often used in experiments (including those that will be described in Section 8.2), we discuss it here in greater detail.

The researchers employed what is known as a 'long paraffin counter', which is a paraffin cylinder 46 cm in diameter and 60 cm long with eight ^{3}He-counters inside it. The source of delayed neutrons (single and in pairs) was a beam of $^{11}_{3}$Li sent along the cylinder's axis. Clearly, this setup

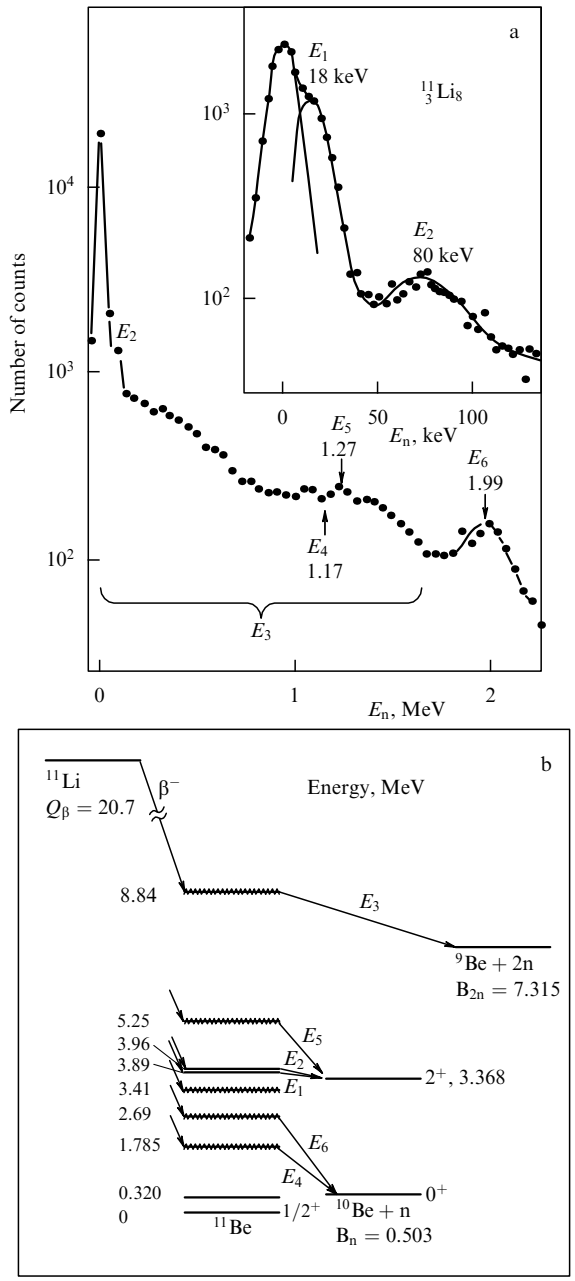

Figure 10. Diagram of emission by the ^{11}Be nucleus of delayed neutron pairs: (a) the spectrum of single delayed neutrons, and (b) the level diagram for the ^{11}Be nucleus.

removes all the difficulties mentioned earlier, since the cross section of reaction (31) sharply increases when thermal neutrons are involved and the detection of both of the neutrons in a pair is separated in time (due to the time difference between delay and diffusion of both of the neutrons in a pair). Furthermore, all the counters can be connected in parallel (since the lifetime of a neutron in the detector, ~ 100 μs, is much longer than the response time of the counter).

The setup operated as follows. The first neutron recorded by one of the counters triggered a 10-MHz 'clock' (opened the 'gate') that counted the time interval Δt to the moment of arrival of the second neutron, which switched off the clock (closed the gate). The process was continued by the next 'first' neutron and stopped by the next 'second' neutron. And so on. The result was the dependence of the number of recorded neutron 'pairs' (the 'first' and 'second' neutrons, which do not necessarily belong to the same true pair) on the time interval Δt between the moments that the two neutrons are recorded (Fig. 11a). It is obvious that if the second neutron is a single delayed neutron or even a background neutron, there will be no correlation between the values of Δt. All such neutrons arrive according to the law of chance, with the values of the time interval between the moments of their arrival distributed randomly (the horizontal straight line in the inset to Fig. 11a, which illustrates the coincidences of the first and second neutrons for $^{9}_{3}$Li emitting only single delayed neutrons).

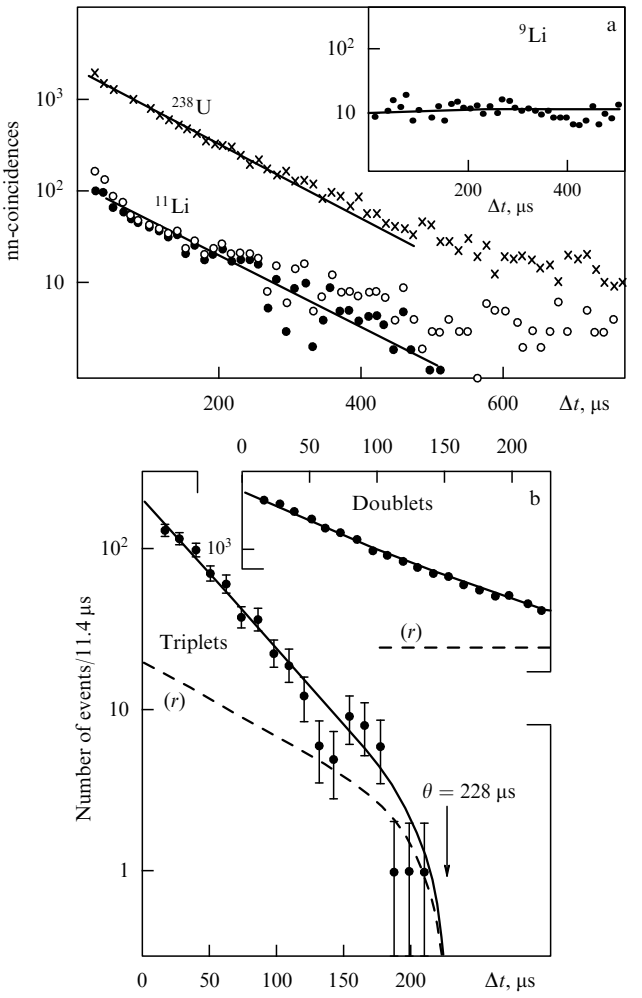

Figure 11. Experimental verification of the existence of delayed (a) double- and (b) triple-neutron radioactivities.

However, if the first and second neutrons constitute a delayed pair and are emitted by the nucleus simultaneously, the distribution of their number in relation to Δt has to exhibit a correlation: small values of Δt will be encountered more often than large values (for neutrons escaping simultaneously the time difference Δt between delay and diffusion of the two neutrons in the pair is more often small than large). The results for ^{11}Li are depicted in the main part of Fig. 11a. Clearly, the number of events in the region of small values of Δt exceeds background level by a factor of ten. A control experiment was conducted with $^{238}_{92}$U, since these nuclei are known to emit two neutrons simultaneously per fission act. We see that the result is a similar correlation curve, which

unequivocally suggests that $^{11}_{3}$Li exhibits delayed double-neutron radioactivity. The equal slopes of both of the curves (for $^{11}_{3}$Li and for $^{238}_{92}$U) characterize the size and design of the paraffin detector (i.e. the nature of diffusion and slowing down of neutrons in this specific detector). The researchers estimate the probability of emission of a delayed neutron pair as being $9 \pm 3\%$ per β-decay event.

Approximately a year later, Detraz et al. [59] discovered a similar phenomenon of emission of delayed neutron pairs for three more neutron-rich nuclei: $^{30}_{11}$Na, $^{31}_{11}$Na, and $^{32}_{11}$Na, with probabilities equal to 1.2, 0.7, and 5.1%, respectively.

6.3 Delayed triple-neutron radioactivity and tritium radioactivity

In 1980, after improving the experimental facility, the same group of researchers at CERN, who discovered delayed double-neutron radioactivity for $^{11}_{3}$Li, reported observing delayed triple-neutron radioactivity for the same nucleus, $^{11}_{3}$Li [60].

The modified facility included a more effective paraffin 4π-detector of neutrons containing 12 ^{3}He-counters connected in parallel. The mean neutron lifetime in the detector, determined from $\beta - \gamma$-coincidences, was found to be equal to 89 ± 1 μs (for an exponential distribution). The time of arrival of individual neutrons at the counters was registered by a special processor to an accuracy of 1 μs and was recorded on magnetic tape for subsequent processing.

Figure 11b depicts the distribution of the time intervals Δt between the arrival at the counters of the first and second neutrons for the events registered as pairs and triples of neutrons within the correlation time of 228 μs (the procedure of obtaining such a distribution was described in detail in Section 6.2). We see that the distribution of time intervals built for neutron triples is steeper than that for neutron pairs, which, obviously, suggests that simultaneous triples of neutrons escaping from the nucleus actually exist (the reader will recall the arguments in Section 6.2).

The question of random triple correlations generated by combinations of single and pair neutrons was analyzed by Azuma et al. [60] separately, and the contribution of these correlations is depicted in Fig. 11b by a dashed curve. Clearly, the contribution is small, i.e. the existence of simultaneous emission of delayed triples of neutrons is proved without doubt. The relative probability of three delayed neutrons being emitted simultaneously is $1.8 \pm 0.2\%$ of the total emission of all the neutrons (1n, 2n, and 3n). The researchers note that the recorded process is the decay of the nucleus into five nuclear particles ($^{11}_{4}\mathrm{Be} \rightarrow 3\mathrm{n} + 2\alpha$).

Another variant of delayed triple-nucleon radioactivity (to be sure, in the form of emission of a three-nucleon nucleus) is the delayed emission of tritium nuclei. Such a phenomenon was discovered in France for the same nucleus $^{11}_{4}$Be produced in the process of β-decay of $^{11}_{3}$Li in an extremely highly excited state ($W = 18.5$ MeV), whose energy exceeds the threshold energy of the process

$$^{11}_{4}\mathrm{Be} \rightarrow {}^{3}_{1}\mathrm{H} + {}^{8}_{3}\mathrm{Li}\,, \qquad |Q| = 15.7 \text{ MeV}. \tag{32}$$

7. Cluster radioactivity

A new period of exotic discoveries feeding the science of radioactive processes started in 1984, when Rose and Jones [61] were able to detect carbon radioactivity. This was a sensation, and yet it was expected. The process of spontaneous emission of clusters by some of the nuclei (nuclear fragments heavier than α-particles) was predicted in 1980 by Sandulescu et al. [62]. It is allowed by all the conservation laws, including the energy conservation law. Therefore, fundamentally, one could expect the existence of cluster decays of heavy nuclei, for which there is an energetically allowed (and actually observed) α-decay with an average energy release of about 5 MeV (a small cluster) or spontaneous fission with an energy release of about 200 MeV (a very large cluster).

This, however, was only true theoretically. Actually, the prediction is in no way trivial or obvious. Indeed, if one tries to extrapolate the mass distribution of fission fragments in the direction of small masses down to cluster values ($A \approx 15-30$), the probability of emerging such fragments has values which are inaccessible to observation. The same result is achieved in the case of simple extrapolation of the α-particle model to cluster decay. Thus, when the problem of the existence of cluster decay is examined more carefully, it seems that there can be nothing between α-decay and spontaneous fission. Overcoming this difficulty required boldness, theoretical intuition, and ingenuity on the part of Sandulescu et al. [62].

7.1 The prediction of cluster radioactivity

Cluster decay was predicted by Sandulescu et al. [62] as a result of realizing two limiting approaches. In the first, cluster decay was studied by analogy with α-decay, i.e. as a process of penetration of the cluster formed in the nucleus through a Coulomb barrier. In this approach, the formation factor was ignored altogether, but the penetrability factor was calculated by employing the method of shell corrections to the decay energy Q. The resulting values were found to be comparable to, and sometimes even larger than, the penetrability factor for α-decay. The researchers used this result to predict a fairly high probability (not only accessible to observation but, as it turned out later, somewhat overvalued) of emerging specific clusters from heavy nuclei ranging from $_{90}$Th to $_{102}$No.

In the second approach, cluster decay was studied as highly asymmetric fission, with a mass distribution of the fragments that acquires (again due to shell effects) new peaks in the vicinity of the masses of the predicted clusters, which can be considered, as in the previous approach, as an indication of cluster decay. The researchers noted that within the second approach they were able, in studying α-decay, to use the liquid drop model with a simple parametrization in the form of two intersecting spheres and to arrive at the results of calculations of the heavy nuclei lifetimes with respect to α-decay that agreed very well with the experimental data at hand. This laid the foundation for the third approach, a unified approach for studying α-decay, cluster radioactivity, and spontaneous fission.

Now, after 20 years have passed since the time of this prediction, although the merit of the *quantitative* content (the values of the decay probabilities, the types of emitted clusters, and the specific nuclear emitters) of this prediction is debatable (see Sections 7.4), its *qualitative* merit is beyond doubt: Sandulescu et al. [62] predicted the existence in nature of a new type of the radioactive process and proposed the first theoretical models for its explanation.

7.2 Carbon radioactivity

When searching for cluster decay, the choice of the initial nucleus and cluster is governed by the value of the decay

energy Q. Obviously, this energy is at its maximum when an especially stable nucleus, at least an even–even one and preferably double magic (see Section 3), is formed in the final state. The search for cluster radioactivity began almost simultaneously in two laboratories, at Oxford (Great Britain) and at the Kurchatov Institute of Atomic Energy (Moscow, Russia), and both groups selected the same variant of decay and the same method, but the Oxford group obtained the results three months earlier than the Moscow group.

Rose and Jones [61], who were the first to discover carbon radioactivity in radium, used the $E-\Delta E$-method. Altogether they detected 11 nuclei of ^{14}C produced in the decay of $^{223}_{88}$Ra ($T_{1/2} = 11.7$ days, $T_\alpha = 5.7$ MeV) via the process

$$^{223}_{88}\mathrm{Ra} \rightarrow {}^{14}_{6}\mathrm{C} + {}^{209}_{82}\mathrm{Pb}\,, \qquad Q = 31.8\ \mathrm{MeV} \tag{33}$$

with the magic nucleus $^{209}_{82}$Pb ($Z = 82$) in the final state. To simplify measurements, they used $^{227}_{89}$Ac ($T_{1/2} = 21$ y) as the source of radioactivity, in which $^{223}_{88}$Ra is in radioactive equilibrium with the actinium decay products. The ratio of the yield of $^{14}_{6}$C nuclei to the yield of α-particles from the same nucleus $^{223}_{88}$Ra proved to be enormously small: $(8.5 \pm 2.5) \times 10^{-10}$. Hence, the researchers paid much attention to the problem of background noise from cosmic rays and multiple pile-up of pulses from α-particles with approximately the same energy release as in the case of $^{14}_{6}$C emission.

The reader will recall that the $E-\Delta E$-method is based on the well-known formula for the energy lost by a heavy charged nonrelativistic particle (charge Z, velocity v, mass M, and kinetic energy T) due to ionization:

$$\frac{\mathrm{d}T}{\mathrm{d}x} \sim \frac{Z^2}{v^2} \sim \frac{Z^2 M}{T}\,, \tag{34}$$

from which it follows that $T\Delta T \sim Z^2 M \sim Z^2 A$, where A is the mass number of the ion.

Usually ΔT is measured in a flat, thin (~ 10 μm) surface-barrier silicon ΔE-detector, the velocity v is measured by the time of flight and distance between two detectors of this kind, and the kinetic energy T by the value of the total energy release in the thick E-detector. An additional factor that helps identify a particle by its charge and mass number is the discreteness of the product Z^2A, in view of which a region with definite values of Z and A is specified in the ΔT, T plane.

Rose and Jones [61] established the cluster charge ($Z = 6$) by comparing the ratio of ionization losses in the ΔE- and E-detectors, which was found to differ considerably for carbon ions and for multiple pile-up of pulses (up to five pulses) from α-particles. Fundamentally, the mass number of the emitted carbon nuclei could be in the range from 12 to 15. To determine it, the researchers measured the total energy release Q, whose calculated value is different for various isotopes of carbon and is at its maximum for ^{14}C ($Q_{^{12}_{6}\mathrm{C}} = 27.7$ MeV, $Q_{^{13}_{6}\mathrm{C}} = 28.8$ MeV, $Q_{^{14}_{6}\mathrm{C}} = 31.8$ MeV, and $Q_{^{15}_{6}\mathrm{C}} = 29.1$ MeV). These measurements were done very thoroughly in view of the difficulty caused by the fact that the ranges of α-particles and carbon ions in the detector are almost the same. After the detectors had been calibrated with α-particles from $^{241}_{95}$Am (which have the same ratio of ionization losses in the ΔE- and E-counters as $^{14}_{6}$C) and corrections for the recoil energy had been introduced, it was found that the measured value of Q corresponds to the decay of $^{223}_{88}$Ra accompanied by $^{14}_{6}$C emission.

It is interesting that Rose and Jones [61] arrive at the same conclusion without measuring the energy release but by simply comparing the Gamow factors characterizing the penetrability of the Coulomb barrier for decays of $^{223}_{88}$Ra in which $^{12}_{6}$C, $^{13}_{6}$C, $^{14}_{6}$C, and $^{15}_{6}$C are emitted. Such a comparison has shown that the $^{14}_{6}$C nuclei have the best Gamow factor (the ratio of this Gamow factor to the Gamow factor for an α-particle was found to be in the $10^{-5}-10^{-3}$ range). With such a Gamow factor, the magnitude of the observed effect, $(8.5 \pm 2.5) \times 10^{-10}$, yields a reasonable value of approximately $10^{-6}-10^{-4}$ for the formation factor attendant to the emitted fragment ^{14}C (again in comparison to the formation factor for an α-particle). The Gamow factors for the other carbon isotopes are five to six orders of magnitude smaller than that for ^{14}C (and approximately equal to each other). When compared with the observed effect, such small values lead to an unacceptably large value of the formation factor (including the value of the formation factor for the alpha-like nucleus $^{12}_{6}$C): $0.1-10$! Thus, even such simple reasoning shows that $^{223}_{88}$Ra emits exactly $^{14}_{6}$C nuclei.

The discovery of carbon radioactivity was confirmed in the same year (1984) by the already mentioned group in Moscow (Russia) headed by Ogloblin [63] and the Orsay group (France) headed by Gales [64]. Ogloblin's group employed the same $E-\Delta E$-method with the same radioactive source $^{227}_{89}$Ac, but the energy calibration of the $E-\Delta E$-spectrum was done with $^{14}_{7}$N and $^{12}_{6}$C beams produced by the cyclotron at the Kurchatov Institute of Atomic Energy. The results of these measurements were seven events corresponding to process (33), which made it possible to obtain a value of $(7.6 \pm 3.0) \times 10^{-10}$ for the ratio of the $^{14}_{6}$C yield to the α-particle yield.

Gales's group also used the same type of radioactive source ($^{227}_{89}$Ac), a magnetic spectrometer with a superconducting magnet to separate the $^{14}_{6}$C nuclei, and an $E-\Delta E$-telescope calibrated with a $^{14}_{6}$C beam. The results of these measurements were 11 events of decay of $^{223}_{88}$Ra accompanied by $^{14}_{6}$C emission, which produced a value of $(5.5 \pm 2.0) \times 10^{-10}$ for the ratio of the $^{14}_{6}$C yield to the α-particle yield. Thus, all three values obtained in 1984 agree to within experimental error, which conclusively confirms the authenticity of the effect. Somewhat later, Kutshera et al. [65] (Argonne National Laboratory, USA) recorded a decay by the process (33), while Price et al. [66] discovered the emission of $^{14}_{6}$C in two isotopes of radium, $^{222}_{88}$Ra and $^{224}_{88}$Ra.

To detect the $^{14}_{6}$C nuclei, Price et al. [66] employed a polycarbon film sensitive to particles with $Z > 2$, which made it possible to identify tracks of $^{14}_{6}$C against a background of α-particles with up to 6×10^{10} α-particles per cm^2. Furthermore, the use of plastic detectors allowed the researchers to substantially increase the solid angle within which cluster decay can be registered.

7.3 Neon, magnesium, and silicon radioactivities

One year after the discovery of carbon radioactivity, Barwick et al. [67] detected the emission of neon nuclei ($^{24}_{10}$Ne) by $^{232}_{92}$U, accompanied by the production of the double-magic nucleus $^{208}_{82}$Pb ($Z = 82$, $N = 126$) in the final state:

$$^{232}_{92}\mathrm{U} \rightarrow {}^{24}_{10}\mathrm{Ne} + {}^{208}_{82}\mathrm{Pb}\,, \qquad Q = 62.3\ \mathrm{MeV}. \tag{35}$$

To detect $^{24}_{10}$Ne nuclei, the researchers used Cronar, a plastic film sensitive only to particles with $Z > 6$, which made it possible to work with this film against a background of α-particles with up to 2×10^{11} α-particles per cm^2. The film was irradiated in the course of one month with a source of $^{232}_{92}$U

whose activity was 0.5 mCi. This was followed by etching the irradiated film in a NaOH solution over the course of several hours. The film was studied under a microscope at a magnification in several hundred times.

The method by which the particles were identified is based on the idea that the intensity of etching along the track is greater than in the nonirradiated parts of the film and depends on the specific energy losses $\mathrm{d}E/\mathrm{d}x$. Hence, each type of particles is characterized by a curve representing the dependence of etching intensity on the residual range. Beams of $^{18}_{8}$O and $^{20}_{10}$Ne ions irradiating the film were used to calibrate the measurement method.

The $^{24}_{10}$Ne nuclei were identified (31events) by the size of the range, $R = 32.8 \pm 0.23$ μm, which almost coincided with $R_{\text{theor}} = 33.2$ μm, which follows from the reaction's Q. The yield of the $^{24}_{10}$Ne nuclei proved to be lower by a factor of 1000 than in the case of carbon radioactivity: the ratio of the $^{24}_{10}$Ne yield to the α-particle yield was $(2 \pm 0.5) \times 10^{-12}$. Later neon radioactivity was discovered in several other nuclei in processes accompanied by the production of magic nuclei in the final state:

$$^{233}_{92}\mathrm{U} \to {}^{24}_{10}\mathrm{Ne} + {}^{209}_{82}\mathrm{Pb} \quad (Z = 82)\,, \tag{36}$$

$$^{234}_{92}\mathrm{U} \to {}^{24}_{10}\mathrm{Ne} + {}^{210}_{82}\mathrm{Pb} \quad (Z = 82)\,, \tag{37}$$

$$^{231}_{91}\mathrm{Pa} \to {}^{24}_{10}\mathrm{Ne} + {}^{207}_{81}\mathrm{Tl} \quad (N = 126)\,, \tag{38}$$

$$^{230}_{90}\mathrm{Th} \to {}^{24}_{10}\mathrm{Ne} + {}^{206}_{80}\mathrm{Hg} \quad (N = 126)\,. \tag{39}$$

New modes of cluster radioactivity were discovered at the end of the 1980s: magnesium radioactivity with the emission of $^{28}_{12}$Mg nuclei was discovered in $^{234}_{92}$U, $^{238}_{94}$Pu, and $^{236}_{94}$Pu, and silicon radioactivity with the emission of $^{32}_{14}$Si nuclei was discovered in the $^{238}_{94}$Pu nucleus:

$$^{234}_{92}\mathrm{U} \to {}^{28}_{12}\mathrm{Mg} + {}^{206}_{80}\mathrm{Hg} \quad (N = 126)\,, \tag{40}$$

$$^{238}_{94}\mathrm{Pu} \to {}^{28}_{12}\mathrm{Mg} + {}^{210}_{82}\mathrm{Pb} \quad (Z = 82)\,, \tag{41}$$

$$^{236}_{94}\mathrm{Pu} \to {}^{28}_{12}\mathrm{Mg} + {}^{208}_{82}\mathrm{Pb} \quad (Z = 82, \quad N = 126)\,, \tag{42}$$

$$^{238}_{94}\mathrm{Pu} \to {}^{32}_{14}\mathrm{Si} + {}^{206}_{80}\mathrm{Hg} \quad (N = 126)\,. \tag{43}$$

The characteristic features of all the processes discussed above are the very large partial half-lives, $T^{\text{cl}}_{1/2} = 10^{14} - 10^{17}$ y, and the very low yields, $\Gamma_{\text{cl}}/\Gamma_\alpha \approx 10^{-14}$.

To illustrate the discovery of magnesium radioactivity, we briefly discuss the work of Ogloblin et al. [68], which in view of the importance of its second (review) part will be taken up in greater detail in Section 7.4. The first part of that paper, which is devoted to the experiment, describes the discovery of magnesium radioactivity of the $^{236}_{94}$Pu nucleus that follows process (42). The detectors were lavsan films irradiated by a specially prepared plutonium target (66 % $^{236}_{94}$Pu + 34 % $^{238}_{94}$Pu) over 690 days. So as not to overload the film with the α-particle background whose ultimately allowed level equals 10^{12} α-particles per cm^2, each film was irradiated for no longer than 115 days. The procedure used in film treatment and the ideas invoked in identifying the particles were developed by S Tretyakova and V Mikheev (JINR, Dubna). These two researchers contributed substantially to the development of the method of registering clusters with solid-state (film and glass) track detectors [69, 70]. The films were calibrated with beams of $^{20}_{10}$Ne, $^{26}_{12}$Mg, and $^{27}_{13}$Al ions accelerated on the U-300 cyclotron (JINR) to energies in the range 1.6 – 3.0 MeV per nucleon. Scanning all the films showed that out of a large number of tracks left by α-particles, fission fragments, and other particles only two were found to belong to $^{28}_{12}$Mg, and it was impossible to assign these two tracks to any background process (Fig. 12a).

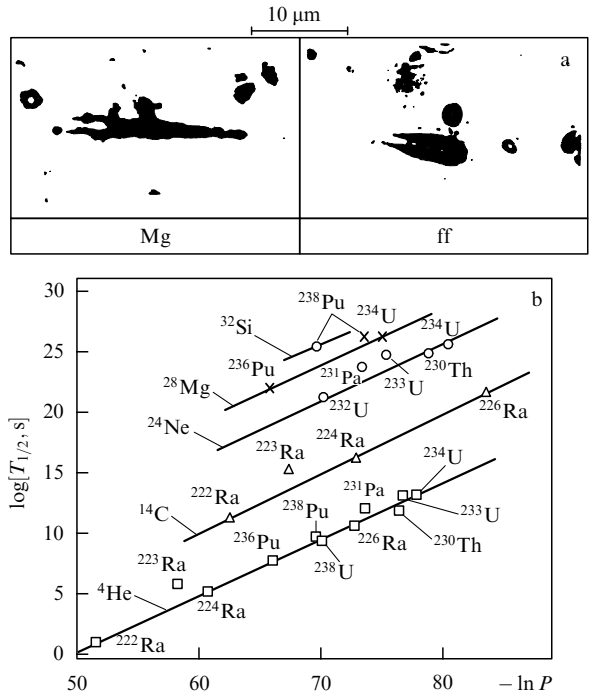

Figure 12. Cluster radioactivity: (a) the micrograph of a magnesium cluster (Mg) compared against fission fragments (ff), and (b) the dependence of the half-life $T_{1/2}$ on the penetrability P of the barrier.

Decay process (42) was identified by the energy release ($Q = 70 \pm 3$ MeV) and corroborated by calculating the relative probability of emission of different magnesium isotopes by the $^{236}_{94}$Pu and $^{238}_{94}$Pu nuclei. For all the variants of decay except (42), this probability proved to be smaller by five to six orders of magnitude. The discovered effect corresponds to a partial half-life $T^{\text{cl}}_{1/2} = 1.5 \times 10^{14}$ y and $\Gamma_{\text{cl}}/\Gamma_\alpha = 2 \times 10^{-14}$. The interested reader may refer to the review by Zamyatnin et al. [71], which describes the experimental method and the details of processing the data, as well as the general state of affairs in this problem as of the year 1990.

7.4 The mechanism of cluster radioactivity

The second (review) part of the paper by Ogloblin et al. [68] presents the first systematic analysis of all the statistical material gathered by the date of publication (1990) on 4 kinds of clusters and 11 different nuclear emitters. The data give an idea of the mechanism of cluster decay. The results of the analysis are depicted in Fig. 12b for 13 cases of cluster decay (two nuclei were found to have two clusters each) in the form of curves representing the dependence of $\log T^{\text{cl}}_{1/2}$ on $\ln P$, where P is the penetrability of the Coulomb barrier. Clearly, the experimental points for all even – even nuclei lie on parallel straight lines, so that the dependence is similar to that obtained in the simplest theory of α-decay

when explaining the Geiger – Nuttall law (the lower straight line in Fig. 12b). The experimental points for odd nuclei lie somewhat above straight lines, which is likewise typical of α-decay.

Thus, the experimental findings suggest that in the domain occupied by nuclei that exhibit cluster radioactivity, the mechanism of such radioactivity is, probably, close to that of α-decay. The resulting parallel straight lines can be interpreted as a generalized Geiger – Nuttall law, which makes it possible to predict the values of $T_{1/2}^{\mathrm{cl}}$ for new nuclear emitters of the clusters mentioned earlier. Furthermore, the relative position of the straight lines clearly shows that the probability of emitting a cluster reduces by five to six orders of magnitude as the cluster mass increases by ten nucleon masses. An attempt can be made to use this empirical dependence to predict the partial half-lives of the not yet discovered heavier clusters (assuming that the 'α-particle' emission mechanism still works). For example, this approach was used by Novatskiĭ and Ogloblin [72] to predict the position of the 'magnesium' straight line (Fig. 12b) and even the point on it where the decay by process (42) occurs, just before the first magnesium cluster had been discovered.

We have seen what conclusions can be drawn from the experimental results. But what does the theory say? In Section 7.1 we noted that in 1980, i.e. four years before the discovery of carbon radioactivity, Sandulescu et al. [62] outlined three ways in which cluster decay can be theoretically described — by analogy with α-decay, by examining highly asymmetric spontaneous fission, and by examining the combination of all three modes of radioactivity mentioned earlier. After the discovery of cluster decay, the development of all three approaches to the theoretical description of the new mode of radioactivity intensified.

Not having the space to describe all the research in this field, we will mention only the main ideas of some of the papers and also will discuss the specific features of each way of describing cluster decay.

The 'α-decay' model of cluster radioactivity (known as the microscopic approach) is set up (e.g. see Refs [73 – 75]) by analogy with the theory of α-decay, in which the probability of α-decay is the product of the formation factor for an α-particle built from the nucleons of a nucleus and the penetrability factor of the Coulomb (and centrifugal) barrier. When estimating this penetrability factor, we must take into account the collision frequency between an α-particle and the barrier and the penetrability of the latter (see Section 2.1). The most difficult problem of the theory is to estimate the formation factor, which in the first theoretical descriptions of α-decay was not evaluated at all and was assumed to be the same for a certain category of nuclei (e.g. even – even in the ground and weakly excited states). Modern theories of α-decay attempt to evaluate the formation factor on the basis of the properties of the nucleons in the nucleus (e.g. the pair interaction mentioned in Section 5.3), but the problem still remains extremely difficult.

As we move from α-decay to cluster radioactivity, the problem of estimating the formation factor becomes even more complicated because of the need to study the process of formation in the nucleus (more precisely, near its surface) of a correlated group of two to three dozen nucleons instead of four nucleons, as in the case of α-decay. For the same reason the problem of estimating the barrier's penetrability factor becomes more complicated as well (obviously, this factor must depend on the size, shape, and nucleon composition of the escaping cluster, the shape of the barrier, and the collision frequency). Naturally, each of these difficulties reduces the cluster emission probability of a given nucleus in relation to the probability of α-decay, while ignoring them (as was the case in the first generalized theories of α-decay) leads to overvaluing the probability. Modern 'α-particle' models have provided a fairly accurate description of the probability of cluster decay for the nuclei already studied.

Let us take the example of the 'α-particle' approach to cluster decay used by Biendowske and Walliser [75], who generalized the theory of α-decay to cluster radioactivity by employing the (semiclassical) WKB approximation (see Section 2.1), according to which $\lambda = vPD$, with

$$v = \frac{v}{2R_i}\,, \quad P = P_\alpha^{(A_{\mathrm{cl}}-1)/3)}\,, \tag{44}$$

$$D = \exp\left\{ -2\int_{R_i}^{R_0} \mathrm{d}R \frac{2M}{h^2}\left[U(R) - Q\right]^{1/2}\right\}. \tag{45}$$

Here v is the cluster velocity inside the barrier, determined by the kinetic energy ($Mv^2/2 = 25A_{\mathrm{cl}}$ MeV); R_i and R_0 are the inner and outer turning points; P and P_α are the formation factors for the cluster and α-particle; A_{cl} is the cluster's mass number, M the reduced mass, Q the decay energy, and $U(R)$ the semiempirical heavy-ion potential normalized to elastic scattering under the assumption that $l = 0$. The values of λ calculated by Biendowske and Walliser [75] are in good agreement with the available experimental data.

In the second group of theoretical models (known as the macroscopic approach), the emission of a cluster is interpreted as a highly asymmetric spontaneous fission. This approach was developed by Poenaru et al. [76, 78, 79], Yi-Jin Shi and Swiatecki [77], Pik-Pichak [80], and others. For instance, Poenaru et al. [76] and Yi-Jin Shi and Swiatecki [77] developed a model of partially overlapping spheres of different masses, with the shape of the smaller sphere not changing in the course of the entire process. For the deformation parameter Poenaru et al. [76] took the distance R between the centers of the spheres; the height of the barrier in the region of overlap was calculated via a quadratic dependence on R (with allowance for Coulomb and nuclear forces). The potentials used beyond the region of overlap are the Coulomb and the centrifugal. Yi-Jin Shi and Swiatecki [77] took for the deformation parameter of the fissioning system the overall length L, which is equal to the diameter D_0 of the daughter nucleus at the beginning, the sum of the diameters of the fragments, $D_1 + D_2$, at the moment when the fragments touch each other, and the distance between the outer edges of their surface before and after separation. When $L \geqslant D_1 + D_2$, the deformation energy is determined by the decay energy, Coulomb repulsion, and nuclear attraction of the fragments. When $L \leqslant D_1 + D_2$, the deformation energy decreases by a power law from the value $L(D_1 + D_2)$ it has at the moment of touching to zero at $L = D_0$. The barrier's penetrability was calculated in the standard WKB approximation both in the case of α-decay and in the case of emission of ^{14}C nuclei.

To make the results agree better with the experimental data, Poenaru et al. in Ref. [76] (and later in the works of the same group of researchers in Refs [78, 79]), when estimating the penetrability of the barrier, added the zero-oscillation energy E to the decay energy Q. This zero-oscillation energy was calculated by the empirical formula $E = 0.13A_{\mathrm{cl}}$ MeV, where A_{cl} is the mass number of the cluster (the small sphere).

The two groups of researchers, whose works we are discussing at this point, Refs [76, 77], assumed that in the process of transforming the system from the initial nucleus to two final nuclei the mass coefficient is equal to the reduced mass of the system at the end of separation. Normalization was done on the basis of numerous data on α-decay and of the data on emission of $^{14}_{6}$C from $^{223}_{88}$Ra gathered just before the two groups did their research.

The above model predicted more or less adequately (undervalued by a factor of approximately ten) the value of $T_{1/2}$ for neon radioactivity (discovered later), so that the assumption that the cluster does not change its shape when penetrating through the barrier can, probably, be considered fairly true up to $Z = 10$. However, both groups of researchers believe that in a more sophisticated theory the model of two intersecting spheres will be replaced by a more complicated one.

The model of intersecting spheres was made more sophisticated by Pik-Pichak [80] who selected the distance between the centers of mass of the fragments formed, which are strongly deformed initially, for the main physical coordinate, instead of the distance between the intersecting spheres being invariant in shape. He noted that since cluster decay usually amounts to the emission of neutron-rich nuclei, the ratio Z/A remains almost unchanged in the process of fragment formation, which justifies the use of the 'fission' approach. Furthermore, since he assumed that initially the future fission fragments are strongly deformed with respect to their final shape, the effective mass coefficient (estimated on the basis of the hydrodynamic model of a homogeneous incompressible perfect fluid) at the beginning of the process is considered to be several times greater than after separation (when it is equal to the reduced mass). In his calculations, Pik-Pichak [80] did not introduce the zero-oscillation energy, which, he believes, leads to violation of the energy conservation law.

The calculations of half-lives in this model yield for nuclei that have been studied so far somewhat larger values (which still are in good agreement with the experimental data) than those obtained by Poenaru et al. [76, 79].

Finally, as noted earlier, there is a third approach to the problem of explaining cluster decay, viz. an attempt to set up a unified model that describes all three radioactive processes described above, namely, α-decay, spontaneous fission, and cluster emission (e.g. see the earlier work by Sandulescu et al. [62] and the later work by the same group of researchers, Ref. [81]). The basis for this theory is the idea of highly asymmetric spontaneous fission in the case of cluster radioactivity and of maximum asymmetry in the case of α-decay. The researchers believe that the usual line of reasoning in which fission is described by the macroscopic liquid drop model with microscopic shell corrections does not work here because it does not allow for describing processes that involve different charge densities and highly asymmetric masses of the fragments if one of the fragments is assumed to be a cluster or, the more so, an α-particle. Hence, Sandulescu et al. [62] used (probably for the first time) the liquid drop model mentioned earlier with a very simple parametrization in the form of two intersecting spheres, and phenomenological expressions for calculating shell corrections. This model interprets α-decay as maximally asymmetric fission resulting in the formation of a very light fragment with definite nucleon composition (2p + 2n) and mass (m_α). The calculated values of $T^{\alpha}_{1/2}$ proved to be in good agreement, over a very wide range of α-emitters, with the experimental data. Furthermore, as mentioned earlier, this asymmetric-fission approach made it possible to predict cluster decay (true, with an overvalued probability of such decay occurring). In later works of this group of researchers (see Refs [76, 78, 79, 81, 82]), the results of theoretical predictions agreed with the available experimental findings to an even higher degree of accuracy.

Generally speaking, all three approaches to the theoretical description of the new mode of radioactivity give a satisfactory prediction of the respective probability for nuclei that have already been studied, which at first glance seems incredible because of the differences in these approaches. A possible explanation, as noted by Ogloblin et al. [68], is that the decay mechanism does not play an important role for the nuclei studied so far, since the decay probability is primarily determined by the released energy Q.

Novatskiĭ and Ogloblin [72] believe that differences in the predictions of these three approaches will manifest themselves only for very far transuranium elements, where the relative role of spontaneous fission among other decay channels becomes significant. As noted in Section 4.4, the probability of spontaneous fission depends on the fissionability parameter Z^2/A. Hence, if the mechanism of cluster decay is similar to that of spontaneous fission, then at a certain value of Z^2/A there must appear a sizable jump in the curve representing the theoretical dependence of the cluster decay probability on Z^2/A.

Novatskiĭ and Ogloblin [72] found that this jump would appear for $Z^2/A > 36.5$, i.e. for even–even neutron-deficient nuclei heavier than $^{232}_{92}$U. For not very heavy nuclei, this may be $^{236}_{94}$Pu or $^{240}_{96}$Cm, while for heavier nuclei a candidate for such a nucleus is $^{244}_{98}$Cf. One such nucleus, $^{236}_{94}$Pu, as noted in Section 7.3, has already been studied, and the corresponding point lies on the magnesium straight line (Fig. 12b). However, the straight line exhibits no break at the point corresponding to $^{236}_{94}$Pu, which has $Z^2/A = 37.44 > 36.5$. We see that for the time being all the statistics gathered by 1990 support the α-particle mechanism of cluster decay. However, they are not sufficiently complete to permit a final decision. New experiments are needed, involving nuclei with larger values of Z^2/A. We will devote the next section to this aspect.

7.5 Cluster decay of curium

We have just noted how important it would be to discover cluster decay in a nucleus heavier than plutonium and with the emission of a cluster heavier than ^{32}Si. The closest candidate for such a nucleus whose decay one can hope to detect is the curium isotope $^{242}_{96}$Cm. All modern models predicted that according to the amount of released energy Q the most probable decay of $^{242}_{96}$Cm is that in which the cluster ^{34}Si is emitted and the double-magic nucleus $^{208}_{82}$Pb is produced:

$$^{242}_{96}\mathrm{Cm} \rightarrow {}^{34}_{14}\mathrm{Si} + {}^{208}_{82}\mathrm{Pb} \quad (Z = 82\,, \quad N = 126)\,. \qquad (46)$$

The first experimental search for the decay of $^{242}_{96}$Cm was described in 1991 – 1993 by Mikheev et al. [83] and was carried out by a Dubna – Moscow collaboration. However, the researchers were only able to make an estimate of the lower bound on the partial half-life: $T_{1/2} > 6 \times 10^{15}$ y. The next experiment, whose results were published by Ogloblin and coworkers in 1999 – 2000 [84], was begun by the same collaboration in 1996 and was successfully concluded in 1998 – 1999. Not only was a decay that followed process (46) discovered but as a result of this experiment hopes were raised

for solving the difficult problem of the mechanism of cluster decay.

The isotope $^{242}_{96}$Cm was produced through separating it chemically from $^{241}_{95}$Am bombarded by neutrons on the research reactor IR-8 of the Russian Research Centre 'Kurchatov Institute'. The experimenters used two radioactive sources containing 0.228 and 0.168 mg of $^{242}_{96}$Cm and four sets of track-recording phosphate glass detectors mounted on the inner surfaces of copper hemispheres 190 mm in diameter. For protection from the fragments of spontaneous fission, the detectors were covered by a 10.3-μm thick aluminium foil or by a 20.0-μm thick polymer film. The bombardment was carried out in vacuum chambers filled with methane under a pressure of 70 and 7.5 Torr, respectively. The detection efficiency (in a solid angle of 2π) was 0.73. To calibrate the detectors, the researchers used the beam of $^{28}_{14}$Si ions accelerated on the cyclotron of the Russian Research Centre 'Kurchatov Institute' (Moscow), beams of ions $^{30}_{14}$Si and $^{32}_{16}$S of the Lognaro tandem (Italy), and the products of spontaneous decay of ^{248}Cm. Altogether four bombardment sessions were conducted with an overall duration of 292 days. The procedure of developing and identifying the tracks was similar to that described in Section 7.3, but instead of the alkali NaOH the researchers used the acid HF and selected the etching time in such a way so as to suppress the appearance of tracks of clusters lighter than $^{34}_{14}$Si.

As a result of scanning, the researchers found 15 tracks, and identification showed that the tracks were caused by particles with a charge $Z = 14$. Extremely thorough individual processing of the features of each track made it possible to obtain the energy spectrum of the recorded events in the form of a *single* peak without any additional events between the peak and the recording threshold. Such a peak can only be caused by the cluster decay $^{242}_{96}\text{Cm} \rightarrow ^{34}_{14}$ Si. The value of the energy at the maximum of the peak, 81.0 ± 3.0 MeV, is in satisfactory agreement with the value 82.97 MeV that follows from the calculated value of Q for this decay. Estimate of the partial half-life for process (46) led to the value $T_{1/2} = (1.4^{+0.5}_{-0.3}) \times 10^{23}$ s, which agrees with most predictions of the theoretical models (with the exception of the 'α-particle' model) and semiempirical systematics.

Earlier we noted that in the vicinity of $Z^2/A > 36.5$ one can expect the 'α-particle' mechanism of cluster decay to be replaced by the 'fission' mechanism. Lately the validity of this supposition has been boosted substantially by the discovery of cold spontaneous fissions in $^{252}_{98}$Cf [85], in which the fission fragments are produced not in the excited state, as they are in ordinary spontaneous fission, but in the ground state, i.e. in the same way as clusters are. Comparison of the properties of cold and ordinary spontaneous fissions of $^{252}_{98}$Cf shows that the probability of emission of a cold fragment is several orders of magnitude lower than that of a 'hot' fragment.

Pik-Pichak's calculations [80] of all possible modes of the $^{242}_{96}$Cm decay by the cold fission scheme showed a comparable probability of cluster decay at $A = 90-110$ (the fission range) and $A \approx 35$, with the last calculated value almost coinciding with the experimental value of the emission probability of the discovered cluster ^{34}Si. These coincidences make it possible to assume that adiabatic models are more or less realistic. Notice that estimates of the emission probability of clusters with $A \approx 100$, made with nonadiabatic models (e.g. see Biendowske and Walliser's results [75] corroborated by Furman [86]), produce values that are several orders of magnitude smaller (see below).

Even more convincing are two systematics of experimental results presented in Fig. 13. Figure 13a basically repeats the data in Fig. 12b, from which the validity of the generalized Geiger–Nuttall law (i.e. a nonadiabatic model of the 'α-particle' type) followed up to $A \approx 30$ (a linear increase in $\log T_{1/2}$ with cluster mass). The main new findings in Fig. 13a in comparison to Fig. 12b are the two straight lines passing through the new experimental points that correspond to the $^{242}_{96}$Cm decay by the process (46) and the decay of $^{228}_{90}$Th by the process

$$^{228}_{90}\text{Th} \rightarrow ^{20}_{8}\text{O} + ^{208}_{82}\text{Pb} \qquad (Z = 82\,, \quad N = 126)\,, \tag{47}$$

and the theoretical straight line that passes through the point corresponding to the decay of $^{242}_{96}$Cm by the scheme

$$^{242}_{96}\text{Cm} \rightarrow ^{108}_{44}\text{Ru} + ^{134}_{52}\text{Te} \qquad (N = 82)\,. \tag{48}$$

Figure 13a shows that the arrangement of the straight line representing decay scheme (47) approximately corresponds to the previous generalized Geiger–Nuttall type law. As for the second experimental straight line representing (46), it does

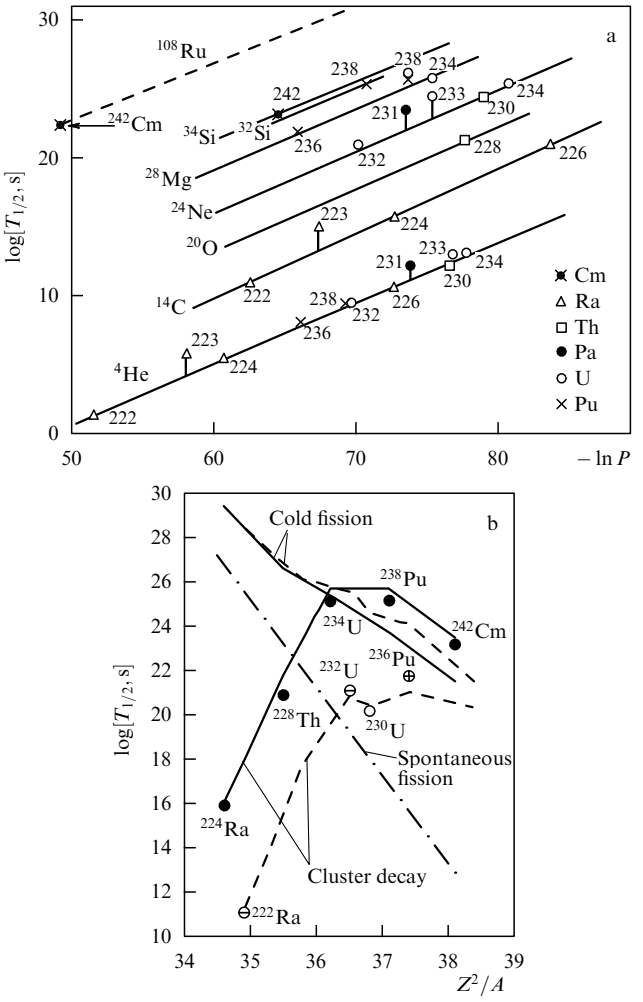

Figure 13. New findings on cluster decay: (a) comparison of the decay $^{242}_{96}\text{Cm} \rightarrow ^{34}_{14}$Si (experiment) with the decay $^{242}_{96}\text{Cm} \rightarrow ^{108}_{44}$Ru (theory), and (b) the dependence of $\log T_{1/2}$ on Z^2/A for even–even cluster emitters in comparison to $\log T_{1/2}$ for cold spontaneous fission and ordinary spontaneous fission.

not satisfy such a law because it is shifted upward (in relation to the straight line corresponding to the decay $^{238}_{94}\mathrm{Pu} \rightarrow {}^{32}_{14}\mathrm{Si}$) by a disproportionately small distance.

Calculations show that as the mass number of the cluster grows, this discrepancy substantially increases, which can be seen from the position of the theoretical straight line corresponding to the decay of the same nucleus $^{242}_{96}\mathrm{Cm}$ by process (48). The value of $\log T_{1/2}$ for this decay mode almost coincides with the experimental value of $\log T_{1/2}$ for the decay $^{242}_{96}\mathrm{Cm} \rightarrow {}^{34}\mathrm{Si}$, while the straight line itself corresponding to the decay process (48) is positioned only 5 to 6 orders of magnitude higher than the straight line attendant to decay scheme (46), instead of the expected 40 or so orders of magnitude that the generalized Geiger – Nuttall law would provide. Thus, Fig. 13a apparently suggests that starting with the cluster mass number $A \approx 35$, the cold-fission type adiabatic mechanism begins to play a more important role than the nonadiabatic 'α-particle' type mechanism.

Additional arguments in favor of the fission mechanism follow from examining Fig. 13b taken from Ref. [84], which is augmented with the empirical dependence of $\log T_{1/2}$ for ordinary spontaneous fission on the fissionability parameter Z^2/A [72]. The dependence is valid for all even–even nuclei for which cluster decays have been observed and is given for the sake of comparison with the behavior of cold fission. We see that cold fission exhibits the same dependence on Z^2/A as ordinary spontaneous fission (the probability of cold fission, however, is several orders of magnitude lower). As for the probability of cluster decay, for nuclei emitting light clusters the behavior of this probability differs entirely from the fission dependence, but for $^{238}_{94}\mathrm{Pu}$ and $^{242}_{96}\mathrm{Cm}$ nuclei it follows the fission dependence.

Thus, the experimental data and the results of calculations suggest that in the vicinity of $A \approx 35$ the cluster decay mechanism probably changes from the nonadiabatic 'α-particle' mechanism to the cold-fission type adiabatic mechanism.

8. Double β-decay

In this section we discuss a mode of radioactivity that is probably the most exotic of all the modes discussed. We are speaking of double β-decay (2β-decay). Indeed, 65 years ago, when the existence of such a decay was predicted, the very idea that such a process could exist seemed to be exotic. Then, for many decades, exceptionally difficult experiments were carried out, experiments in which the most exotic conditions were met (for instance, some experiments were done deep underground). Finally, in modern times, 2β-decay has been (partially) detected using devices and facilities which, thanks to their huge size and unique properties, can also be considered as entirely exotic.

Double β-decay is a process in which a nucleus emits two electrons (or positrons) simultaneously. The theory of such processes distinguishes between two modes of 2β-decay: two-neutrino 2β-decay (2β2ν), and neutrinoless 2β-decay (2β0ν). Two-neutrino 2β-decay was predicted by Goeppert-Mayer [87] in 1935, while neutrinoless 2β-decay was predicted by Majorana [88] in 1937.

[6] In addition to ν_e and $\tilde{\nu}_e$, there exit in nature the muon neutrino (ν_μ) and the muon antineutrino ($\tilde{\nu}_\mu$), and also the tauon neutrino (ν_τ) and the tauon antineutrino ($\tilde{\nu}_\tau$).

2β2ν-decay is allowed by the (V – A)-variant of the theory of weak interaction and the Standard Model of electroweak interaction as an extremely weak second-order effect that follows the reactions

$$2n \rightarrow 2p + 2e^- + 2\tilde{\nu}_e \quad \text{or} \quad 2p \rightarrow 2n + 2e^+ + 2\nu_e\,, \qquad (49)$$

where ν_e is the electron neutrino, and $\tilde{\nu}_e$ the electron antineutrino.[6] In all these processes $\tilde{\nu}_e \neq \nu_e$. They differ in the leptonic number (ν_e has $+1$, and $\tilde{\nu}_e$ has -1), helicity (ν_e has left-handed helicity, and $\tilde{\nu}_e$, right-handed), and in the nature of the interaction in which the lepton-number conservation law is satisfied. In both processes in (49) this law is satisfied by the very fact that the electron has a leptonic number equal to $+1$, a positron has a leptonic number equal to -1, and the two nucleons have a zero leptonic number. A similar rule holds in other process in which a neutrino and an antineutrino are involved, e.g. in the collisional process $\tilde{\nu}_e + p \rightarrow n + e^+$ used in 1953 to experimentally prove the existence of the electron antineutrino.

Today several nuclei are known to exhibit 2β2ν-decay, which has been proved without doubt in experiments (see Section 8.1). The decay process is depicted schematically in Fig. 14a, where W^- stands for the weak-interaction quantum, the W-boson (discovered in 1982); the W^+-boson participates in the 2β-decay process in which two positrons ($2e^+$) are produced.

Neutrinoless 2β-decay is beyond the scope of the Standard Model of electroweak interaction. According to E Majorana, such a process is possible if ν_e and $\tilde{\nu}_e$ are truly neutral particles ($\tilde{\nu}_e = \nu_e$), which requires violation of the lepton-number conservation law. Here, there are left neutrinos ($\nu_e^l \equiv \tilde{\nu}_e^l$) and right neutrinos ($\nu_e^r \equiv \tilde{\nu}_e^r$). The process of 2β0ν-decay is depicted schematically in Fig. 14b and involves no real neutrinos. The antineutrino emitted by the first neutron is absorbed as a neutrino by the second neutron, so that in the final state there are two pairs of particles instead of three:

$$2n \rightarrow 2p + 2e^- \quad \text{or} \quad 2p \rightarrow 2n + 2e^+\,. \qquad (50)$$

This feature identifies 2β0ν-decay as a *two-particle* process in which the total energy of the two electrons (positrons) must be the same in all the decay events with the nuclei of a given kind. It is this feature that makes detection of 2β0ν-decay possible. However, the process has yet to be discovered in experiments. Only lower bounds on the half-life have been obtained, and these allow the estimation of the upper bounds on the Majorana neutrino mass (see Section 8.2).

8.1 Two methods for searching 2β-decay. The first experiments

The search for 2β-decay begins with selecting the appropriate nuclei for which 2β-decay is possible, at least in principle. Usually these nuclei are chosen from the most stable even–even (and, sometimes, magic) nuclei (A, Z) for which the β-transition to the neighboring (with respect to charge) nuclei (A, $Z\pm1$) is forbidden (either by energy conservation law or by selection rules) but the 2β-transition to nuclei (A, $Z \pm 2$) differing in charge by two units is allowed by energy conservation law. An example of the first type is the triplet of nuclei $^{116}_{48}\mathrm{Cd}$, $^{116}_{49}\mathrm{In}$, and $^{116}_{50}\mathrm{Sn}$ in which the β-transition $^{116}_{48}\mathrm{Cd} \xrightarrow{\beta^-} {}^{116}_{49}\mathrm{In}$ is forbidden by energy conservation law since $M_{\mathrm{Cd}} < M_{\mathrm{In}}$ but, in view of the fact that $M_{\mathrm{Cd}} > M_{\mathrm{Sn}}$, the 2β-transition $^{116}_{48}\mathrm{Cd} \xrightarrow{2\beta^-} {}^{116}_{50}\mathrm{Sn}$ is energetically allowed. An exam-

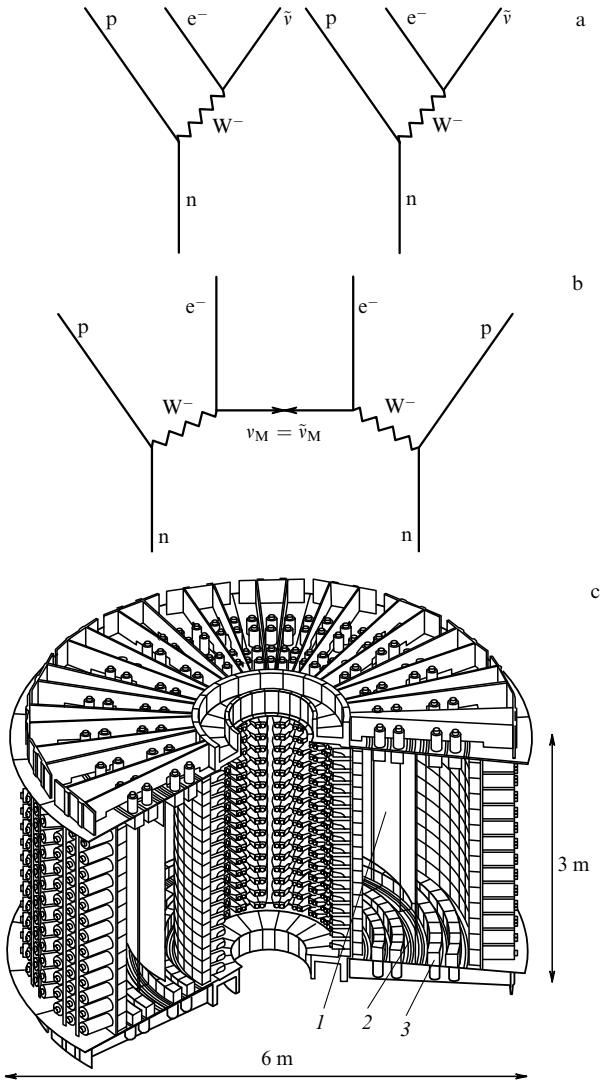

Figure 14. Feynman diagrams for two-neutrino (a) and neutrinoless (b) 2β-decays, and (c) the modern experimental device NEMO-3 for studying them: *1*, the foil that is the source of 2β-decay; *2*, track detectors, and *3*, scintillators.

ple of the second type is the triplet of nuclei $^{48}_{20}$Ca, $^{48}_{21}$Sc, and $^{48}_{22}$Ti, in which the nuclei belonging to the first pair differ substantially in their angular momenta.

Fundamentally, there are two approaches to searching for double β-decay: by detecting the daughter substance, and by recording an electron pair. The first approach has been used in geochemical surveys of ores containing $^{130}_{52}$Te and $^{82}_{34}$Se, which may undergo 2β-decay by the following schemes

$$^{130}_{52}\mathrm{Te} \xrightarrow{2\beta^-} {}^{130}_{54}\mathrm{Xe} \quad \text{and} \tag{51}$$

$$^{82}_{34}\mathrm{Se} \xrightarrow{2\beta^-} {}^{82}_{36}\mathrm{Kr}\,. \tag{52}$$

Knowing the age of the ore and measuring the amount of emanating chemically inert gas, one can estimate the value of the half-life. For $^{130}_{52}$Te, the first to obtain a result by this method (already in 1949) was Inghram and Reynolds [89]:

$$T_{1/2}(^{130}_{52}\mathrm{Te}) = 1.4 \times 10^{21}\ \mathrm{y}. \tag{53}$$

Much later (in 1992) this value was refined by Bernatowicz et al. [90]:

$$T_{1/2}(^{130}_{52}\mathrm{Te}) = (2.7 \pm 0.1) \times 10^{21}\ \mathrm{y}, \tag{54}$$

and for $^{128}_{52}$Te a year later Bernatowicz et al. [91] found the huge value

$$T_{1/2}(^{128}_{52}\mathrm{Te}) = (7.7 \pm 0.4) \times 10^{24}\ \mathrm{y}. \tag{55}$$

For 2β-decay of the $^{82}_{34}$Se nucleus, in 1969 Kirsten et al. [92] arrived at the value

$$T_{1/2}(^{82}_{34}\mathrm{Se}) = (1.37 \pm 0.28) \times 10^{20}\ \mathrm{y}. \tag{56}$$

Naturally, this method does not distinguish between 2β2ν-decay and 2β0ν-decay.

The second approach is aimed at recording the electrons produced in 2β-decay. These electrons have to meet certain conditions: they must escape from a single point (the 'same' nucleus) and must have certain energies and directions of flight. This method allows one, in principle, to distinguish between 2β2ν-decay and 2β0ν-decay if the researcher is able to identify the peak corresponding to the energy of the 2β-transition. Experiments conducted according to the second approach are exceptionally complicated due to a very low probability of the process (on the scale of one significant event in a week) and difficulties in fighting with background noise, in view of which they are carried out deep underground to eliminate as much as possible the cosmic component of the noise. Furthermore, the researchers took special measures to lower the level of proper radioactive background noise from the laboratory and the detector itself. Below we will describe three types of modern facilities used to obtain the most striking estimates of $T_{1/2}(2\beta2\nu)$ and $T_{1/2}(2\beta0\nu)$. In two of these the working medium combines two functions — an emitter of 2β-activity and its detector. The third allows the use of different sources of 2β-activity.

8.2 Modern 2β-decay detectors

The first facility we are going to discuss is the Time Projection Chamber (TPC). The working medium (of the emitter and the detector) in it is 180 litres of 62.5% enriched $^{136}_{54}$Xe that is kept at a pressure of 5 atm [93]. The facility is supplied with a special device that identifies pairs of electron tracks starting at the same point, records two projections of their coordinates, and measures the third projection by the time of drift of ionization electrons in the chamber. To reduce the level of background noise, the facility was installed in the St. Gotthard Tunnel, Switzerland, which runs at a depth of 3000-m water equivalent. Furthermore, the facility is protected by a shield consisting of lead (30-cm thick) and copper (5-cm thick) and a neutron shielding. The resolving power of the facility at $E = 2.5$ MeV is $\Delta E/E = 0.066$. The researchers give two half-life estimates as the results of their experiments:

$$T_{1/2}(2\beta2\nu) \geqslant 5.6 \times 10^{20}\ \mathrm{y}, \tag{57}$$

$$T_{1/2}(2\beta0\nu) \geqslant 4.2 \times 10^{23}\ \mathrm{y}. \tag{58}$$

The second modern facility for studying 2β-decay in which the working medium also combines two functions, emitter and detector, uses $^{76}_{32}$Ge enriched up to 86%. Five detectors of this type with an overall mass of 11.5 kg of $^{76}_{32}$Ge,

built by the Heidelberg – Moscow collaboration [94, 95], are operational in the laboratory under Gran Sasso d'Italia at a depth of 3500-m water equivalent.

The germanium detector has the best resolving power ($\Delta E \approx 1$ keV for crystals of moderate sizes). The researchers arrived at the following estimates for 2β2ν- and 2β0ν-decays of $^{76}_{32}$Ge:

$$T_{1/2}(2\beta 2\nu) = (1.7^{+0.13}_{-0.11}) \times 10^{21} \text{ y}, \tag{59}$$

$$T_{1/2}(2\beta 0\nu) > 6.4(10.0) \times 10^{24} \text{ y}. \tag{60}$$

In 1995 this was the most exact estimate of the value of $T_{1/2}(2\beta 0\nu)$. Since then the value has been refined substantially (see Section 8.3).

In contrast to the above two facilities, the distinctive feature of the Neutrino Experiment with Molybdenum (NEMO) facility is the mutual independence of the source and detector, which enables the properties of different 2β-active nuclei to be studied. The NEMO collaboration has built three variants of the detector: NEMO-1, NEMO-2, and NEMO-3 [96]. NEMO-1 and NEMO-2 occupied an underground laboratory in Frejus (France) at a depth of 4000-m water equivalent, and was used for a thorough study of background noise (NEMO-1) and for obtaining preliminary estimates of the half-lives of $^{100}_{42}$Mo and $^{116}_{48}$Cd (NEMO-2). The sources of 2β-decay in the detector of NEMO-2 were 1 m by 1 m by 40 μm foil plates whose surfaces had been covered with a thin layer (40 μm) of $^{100}_{42}$Mo enriched up to 98.4% (172 g) or $^{116}_{48}$Cd enriched up to 93.2% (152 g). Detection was done using 20 layers of Geiger counters, with 32 counters in each layer, positioned vertically and horizontally. The energy and time of flight were measured using two exterior rows consisting of 8×8 plastic counters.

The measurements produced the following values for the half-lives of $^{100}_{42}$Mo and $^{116}_{48}$Cd:

$$T^{\text{Mo}}_{1/2}(2\beta 2\nu) = (0.95 \pm 0.04_{\text{stat}} \pm 0.09_{\text{sys}}) \times 10^{19} \text{ y}, \tag{61}$$

$$T^{\text{Mo}}_{1/2}(2\beta 0\nu) \geqslant 6.4 \times 10^{21} \text{ y}, \tag{62}$$

$$T^{\text{Cd}}_{1/2}(2\beta 2\nu) = (3.4 \pm 0.4_{\text{stat}} \pm 0.3_{\text{sys}}) \times 10^{19} \text{ y}. \tag{63}$$

At present the third variant, the NEMO-3 detector, is being completed. It is a device of monstrous proportions: six meters in diameter and three meters high (Fig. 14c), and this huge volume is jam packed with electronics. The source of 2β-activity in NEMO-3 will be the central cylindrical thin (50 μm) foil with an area of 20 m^2, covered with 10 kg of the 2β-active isotope $^{100}_{42}$Mo. The space on both sides of the foil is occupied by 6180 Geiger counters and 1920 plastic scintillation counters. The planned resolving power of NEMO-3 at $E = 1$ MeV is $\Delta E/E = 13-14.5\%$. To discard false 2β-events, among which, possibly, are $(e^+ - e^-)$-pairs produced by high-energy γ-quanta on the capture of neutrons, a 30-G magnetic field can be switched on in the device. An iron shield (20-cm thick) and neutron shielding will be used to reduce the level of background noise. In addition to $^{100}_{42}$Mo, there are plans to use other isotopes (such as $^{82}_{34}$Se, $^{96}_{40}$Zr, and $^{116}_{48}$Cd) as sources of 2β-activity.

8.3 Results

Today there is a large group of sources of 2β-activity with half-lives exceeding 10^{21} y ($^{48}_{20}$Ca, $^{76}_{32}$Ge, $^{82}_{34}$Se, $^{100}_{42}$Mo, $^{116}_{48}$Cd, $^{130}_{52}$Te, $^{136}_{54}$Xe, and $^{150}_{60}$Nd), and some of these sources have been studied by more than one group of researchers. The results play a very important role in developing the theory. The experimental values of $T_{1/2}(2\beta 2\nu)$ allow the predictions of the Standard Model of electroweak interaction to be checked, which makes it possible to calculate the matrix elements characterizing the probability of this process. So far no group of researchers has obtained experimental values for $T_{1/2}(2\beta 0\nu)$. However, the established lower bounds on this quantity make it possible to estimate the upper bound on the Majorana neutrino mass and to get an idea about the extent to which the lepton-number conservation law is violated in 2β0ν-decay and about the possibility that right-handed charged currents exist. In 1995, the most exact estimate of the upper bound on the Majorana neutrino mass was derived from Eqn (62) by the Heidelberg – Moscow collaboration consisting of the Russian Research Centre 'Kurchatov Institute' (the V I Lebedev laboratory) and the Max Planck Institute of Nuclear Physics (the H V Klapdor-Kleingrothaus laboratory):

$$m^{\text{M}}_{\nu_e} < 0.6 \text{ eV}. \tag{64}$$

Since then this collaboration has produced the most precise results for $T_{1/2}(2\beta 0\nu)$ and $m^{\text{M}}_{\nu_e}$. Modern estimates (1999) are as follows [97]

$$T_{1/2}(2\beta 0\nu) \geqslant 5.7 \times 10^{25} \text{ y} \quad (90\,\%),$$

$$m^{\text{M}}_{\nu_e} \leqslant 0.2 \text{ eV}. \tag{66}$$

This remarkable result was achieved to a great extent due to modifications in the experimental apparatus for separating the pulses from electrons and pulses from γ-quanta by their shapes. In the future, the collaboration intends to build a detector on the base of 1000 kg of enriched germanium $^{76}_{32}$Ge, which will raise the sensitivity still higher.

In addition to $T_{1/2}(2\beta 2\nu)$ and $T_{1/2}(2\beta 0\nu)$, some researchers have measured the half-lives for various modes of 2β-decay with allowance made for hypothetical particles, majorons M^0:

$$(A, Z) \to (A, Z+2) + 2\text{e}^- + \text{M}^0, \tag{67}$$

$$(A, Z) \to (A, Z+2) + 2\text{e}^- + 2\text{M}^0. \tag{68}$$

The interested reader can find more details on 2β-decay in, say, Ref. [98].

9. Processes in nuclear physics forbidden by parity conservation law

9.1 Weak nucleon – nucleon interaction

The atomic nucleus consists of nucleons which participate in all three types of nuclear interaction: strong, electromagnetic, and weak. The first two obey the law of conservation of spatial parity P, i.e. they are described by reflection-symmetrical wave functions

$$|\Psi(-x, -y, -z)|^2 = |\Psi(x, y, z)|^2, \tag{69}$$

which implies that these functions must be either even or odd:

$$\Psi(-x, -y, -z) = \pm\Psi(x, y, z). \tag{70}$$

Spatial parity is not conserved in weak interactions, with the result that the corresponding wave function cannot be classified as odd or even. Since the atomic nucleus consists of nucleons, it can participate in all nuclear interactions (as the constituent nucleon can), i.e. in the most general form the wave function of the nucleus must reflect the properties of these interactions. This means that to describe strong and electromagnetic processes the nuclear wave function must contain a principal even or odd part, but on the whole (with allowance made for the weak interaction) it cannot be either odd nor even.

Clearly, these requirements are met if the wave function of the nucleus is written in the form

$$\Psi_{\rm n} = \Psi_{\rm reg} + F\Psi_{\rm irreg}, \tag{71}$$

where $\Psi_{\rm reg}$ and $\Psi_{\rm irreg}$ are reflection-symmetrical wave functions of different parity, and $F \approx 10^{-7}$ is a factor characterizing the relative intensity of the weak interaction in comparison to the strong. Indeed, the structure of formula (71) shows that although the first principal part of the wave function, $\Psi_{\rm reg}$, is assumed to satisfy the parity conservation law, the total wave function on the whole does not:

$$\Psi_{\rm n}(-x,-y,-z) = \pm\Psi_{\rm reg}(x,y,z) \mp F\Psi_{\rm irreg}(x,y,z) \neq$$
$$\neq \pm\Psi_{\rm n}(x,y,z). \tag{72}$$

Naturally, when describing strong and electromagnetic processes in the leading approximation (as if the weak interaction was 'switched off'), the second term in formula (71) can be ignored and the corresponding solutions will satisfy the parity conservation law. This property manifests itself in experiments in the reflection symmetry of the observed processes (there will be no odd powers in the series expansion of the angular distribution function in $\cos\Theta$, where Θ is the angle between the particle momentum and a selected direction in space). However, according to the same formula taken in the general form, there may be certain fine effects caused by the participation of the weak interaction in strong and electromagnetic processes. Experimental proof that such a phenomenon exists in the electromagnetic process was found in 1964–1966, and in the strong process in 1970 and 1978.

9.2 Parity-violation effects in γ-transitions

The reader will recall that γ-quanta are characterized mainly by their energy E, the multipolarity l, and their nature (electric or magnetic). The emission probability of γ-quanta depends very strongly on the energy (increases with energy), the multipolarity (decreases with increasing l), and the nature of the γ-quanta (at equal energies and multipolarities, electric γ-quanta are emitted approximately a hundred times more often than magnetic γ-quanta).

Electric and magnetic γ-quanta satisfy different selection rules in parity P:

$$\frac{P_{\rm i}}{P_{\rm f}} = (-1)^{l_{\rm E}}, \quad \frac{P_{\rm i}}{P_{\rm f}} = (-1)^{l_{\rm M}+1}, \tag{73}$$

where $P_{\rm i}$ and $P_{\rm f}$ are the parities of the initial and final nuclei, and $l_{\rm E}$ and $l_{\rm M}$ are the multipolarities of the electric and magnetic γ-quanta, respectively. Equation (73) implies, for instance, that an E1 transition is possible exclusively between nuclear states with different parities, while an M1 transition is possible between nuclear states with the same parities. This means, according to the structure of formula (71), that a γ-transition with a given multipolarity, forbidden by the parity conservation law for the principal part $\Psi_{\rm reg}$ of the wave function, must be allowed for the second term, $F\Psi_{\rm irreg}$. Thus, if $\Psi_{\rm reg}$ allows for electric γ-transitions, then $\Psi_{\rm irreg}$ allows for magnetic γ-transitions, and vice versa. This implies that in the case where both types of γ-quanta of a given multipolarity (say, E1 and M1) are emitted, they may interfere with each other, and the pertinent interference effect will be proportional to F. Experimentally, this effect manifests itself in the asymmetry of the γ-quanta emission with respect to the polarization direction of the nuclei.

Since $F \approx 10^{-7}$ (and, of course, there is no way in which this value can be increased), the effect is very weak and experiments that would reveal it are extremely sophisticated. This difficulty can be partially resolved by selecting a γ-transition that heightens the interference effect at the expense of decreasing the contribution to interference that the principal part of the wave function, $\Psi_{\rm reg}$, provides. Three types of heightening are distinguished here: kinematic, structural, and dynamic, whose compound action can in some cases result in an amplification coefficient $R \approx 10^3$. In such a case the scale of the effect will be not $F \approx 10^{-7}$ but $a = RF \approx 10^{-4}$, which can be measured (albeit with difficulty) in experiments.

The first to discover the asymmetry in the emission of γ-quanta with respect to the spin of a polarized nucleus were Abov et al. [99] at the Institute of Theoretical and Experimental Physics (Moscow) in 1964. They selected the $^{113}_{48}$Cd nucleus which has a large theoretical amplification coefficient $R \sim 10^3$ and a large cross section of thermal-neutron capture. Figure 15a depicts the level diagram for the ^{114}Cd* nucleus which forms after the ^{113}Cd nucleus captures polarized thermal neutrons. We see that the main γ-transition for this nucleus is M1, while the (theoretically) stronger E1 transition is forbidden by parity conservation law. The experiment was conducted using a facility with two scintillation spectrometers around NaI(Tl) crystals and photomultipliers (Fig. 15b), which made it possible to measure the asymmetry of emission of γ-quanta. As a result of such measurements, the asymmetry coefficient was found to be equal to

$$a = -(4.1 \pm 0.8) \times 10^{-4}, \tag{74}$$

where the 'minus' sign corresponds to preferable emission of γ-quanta in the direction opposite to that of the neutron's spin. The value of a in formula (74) yields the following experimental estimate: $F = 2 \times 10^{-7}$.

A similar result was obtained in 1966 at the Leningrad Physico-Technical Institute by Lobashev et al. [100], who discovered that the γ-radiation emitted by the $^{181}_{73}$Ta nucleus is circularly polarized. Their results prove that the nucleon–nucleon interaction potential V contains a term $V_{\rm par.nonconserv}$ that does not conserve spatial parity.

9.3 α-decay forbidden by parity conservation law

In contrast to the case of γ-quanta, where both components of the wave function, $\Psi_{\rm reg}$ and $\Psi_{\rm irreg}$, may be responsible for the different types of radiation (electric and magnetic), in view of which there emerges an interference effect proportional to F, in the case of α-decay this situation is impossible, since there can be only one type of α-particle with an intrinsic parity $P = +1$. Alpha decay can be allowed by parity conservation law either for $\Psi_{\rm reg}$ or for $\Psi_{\rm irreg}$. If $\Psi_{\rm reg}$ is responsible for the allowed α-decay, the probability of parity-forbidden α-decay

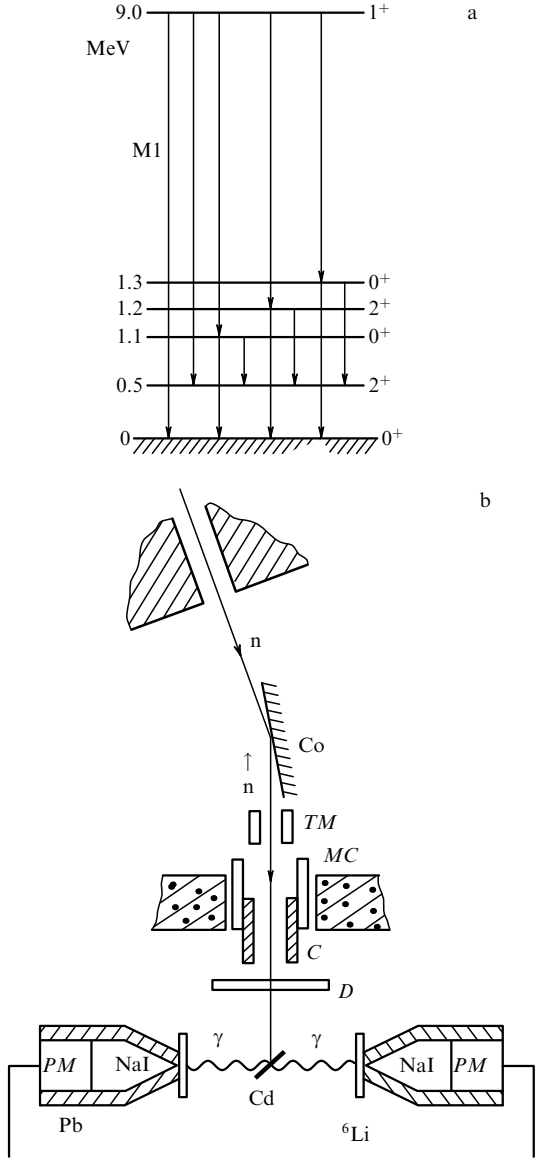

Figure 15. Level diagram for the $^{114}_{48}Cd^{*}$ nucleus (a), and the layout of experimental facility for studying the forbidden γ-transition (b): n, the beam of thermal neutrons; Co, cobalt mirror; *TM*, turning magnet; *MC*, magnetic circuit; *D*, depolarizer; Cd, cadmium target; NaI, scintillation spectrometer; *PM*, photomultipliers; Pb, lead, and *C*, collimator.

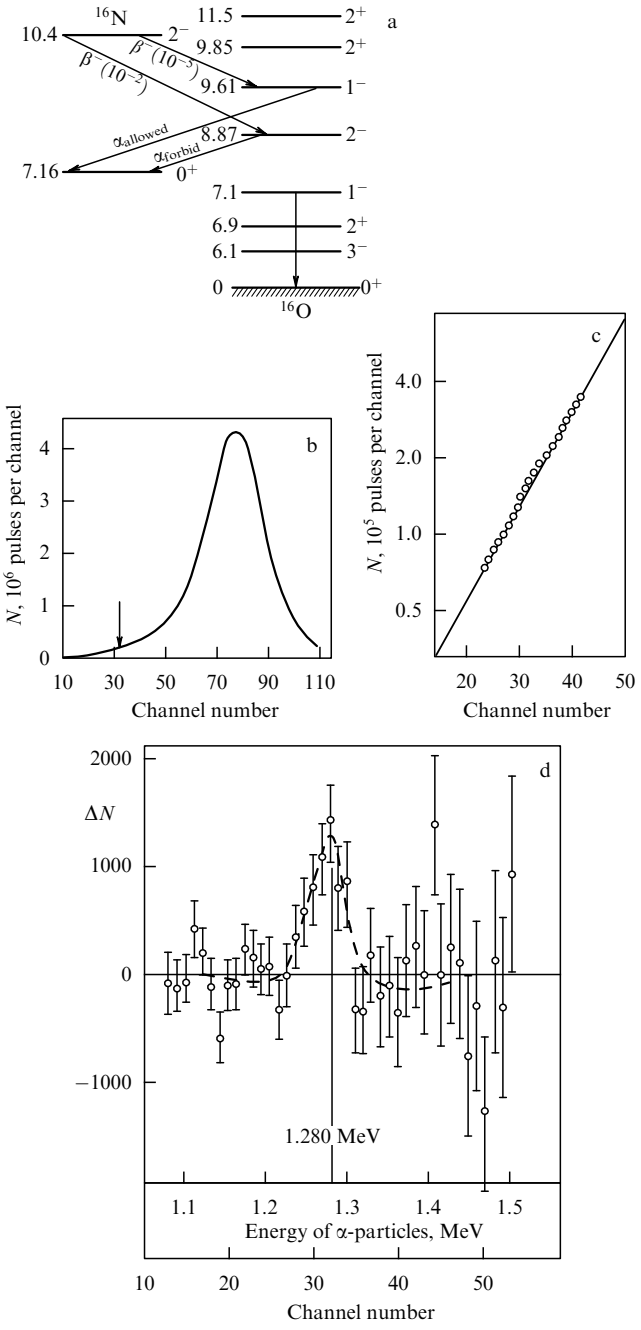

Figure 16. Forbidden α-transitions: (a) level diagram for the $^{16}_{7}N$ and $^{16}_{8}O$ nuclei, (b) general form of the spectrum of allowed α-particles (the arrow indicates the place where the α-particles will 'land' after a forbidden transition), (c) general form of the spectrum of forbidden α-particles against the background of the allowed α-particles, and (d) the difference effect.

will be proportional to $F^2|\Psi_{\text{irreg}}|^2 \approx 10^{-14}$, which offers no hope for ever detecting it in experiments. However, here, too, a certain heightening factor may help, which, as in the case of γ-quanta, amounts to suppressing the effect of the α-transition allowed by parity conservation law.

The first α-transition forbidden by parity conservation law was discovered in 1970 by Hättig et al. [101] for the ^{16}O nucleus. Figure 16 depicts the level diagrams for the $^{16}_{8}O$ nucleus and the $^{16}_{7}N$ nucleus attendant to the former through β-transitions. The researchers compared the probabilities of α-transitions from the 9.61- and 8.87-MeV levels. Clearly, the first is allowed by the law of conservation of spatial parity P, and the second is forbidden. Indeed, in the case of α-decay, this law requires that the parity of the initial state, P_i, and that of the final state, P_f, be linked through the relation

$$P_i = P_f(-1)^{l_\alpha}, \qquad (75)$$

where l_α is the angular momentum carried away by the α-particle. In the α-transition from the 9.61-MeV level with angular momentum and parity 1^- to the 7.16-MeV level with angular momentum and parity 0^+, the parity of the initial state is $P_i = -1$, the parity of the final state is $P_f = +1$, and $l_\alpha = 1$, i.e. condition (75) is met (an allowed α-transition). In the α-transition from the 8.87-MeV level to the 7.16-MeV level, P_i and P_f also have different signs, but $l_\alpha = 2$, so that condition (75) is not met (a forbidden transition). Let us compare the probabilities of these transitions.

An estimate of the penetrability of the Coulomb barrier for the α-transition from the 9.61-MeV level yields $\Gamma_{\alpha\ \text{allowed}} \approx 10^4$ eV, i.e. $\tau = \hbar/\Gamma \approx 10^{-19}$ s. The estimate of $\Gamma_{\alpha\ \text{forbid}}$ took into account the contribution to $F\Psi_{\text{irreg}}$ (8.87 MeV) of the adjacent levels with the same angular momentum but opposite (allowed) parity. The impurity amplitude F_i was calculated by perturbation theory for each ith 2^+ level:

$$F_i = \frac{< i2^+|V_{\text{par.nonconserv}}|8.87\ 2^- >}{E_i - 8.87}\,. \tag{76}$$

Allowance for the values of F_i yields $\Gamma_{\alpha\ \text{forbid}} = 10^{-10}$ eV, i.e. $\tau \approx 10^{-5}$ s. We see that, indeed, the ratio

$$\frac{\Gamma_{\alpha\ \text{forbid}}}{\Gamma_{\alpha\ \text{allowed}}} = 10^{-14}\,, \tag{77}$$

which, of course, is impossible to detect in experiments. However, there are several factors that make the situation not so hopeless: the different probabilities of formation of the 9.61- and 8.87-MeV levels in the preceding β-decay, the difference in the energies of the two α-particles, competition between the γ-transitions from the 8.87-MeV level, etc. The outcome of all this is an increase of the magnitude of the sought effect from 10^{-14} to 5×10^{-5} (see below). Such a magnitude can already be detected in experiments, although, as we will now see, this is extremely difficult.

The experiment was done with gaseous ^{15}N under a pressure of 1 atm. The gas was bombarded by 3-MeV deuterons:

$$\mathrm{d} + {}^{15}\mathrm{N} \rightarrow {}^{16}\mathrm{N} + \mathrm{p}\,. \tag{78}$$

The ^{16}N produced in this reaction left the target through thin capillaries into a small ($\sim 2\,\mathrm{cm}^3$) low-pressure (7 mm Hg) detector chamber, which registered the α-particles from ^{16}O that were produced in the β-decay of ^{16}N. Pulses from the detector were amplified and fed to a 4×128-channel analyzer. The accuracy with which the energy of the α-particles was determined was ±10 keV.

Figure 16b gives the general form of the spectrum of α-particles registered by the detector. The broad peak corresponds to an allowed α-transition, and the arrow indicates the place (channel N 32) where the α-particles produced in a forbidden transition will occur. Estimates made with allowance for the shift of this position in relation to the center of the peak show that such α-particles constitute less than 1% of the overall number of α-particles registered in this region.

Registering such a small effect required using a special method for processing the data, a method that merits special attention because it is so original. Out of the entire spectrum a section was initially isolated, extending from channel N 13 to channel N 53, and for this section an approximating exponential curve was built over all channels except Nos 30–34 (these are the channels into which the forbidden α-particles were expected to fall). Then all the experimental points including those for channels Nos 30–34 were plotted on this curve. Naturally, all deviations from the exponential curve could be detected only in this narrow section and only as a barely noticeable bulge above the approximating curve (Fig. 16c). To make this effect pronounced in the range of channels Nos 13 to 53 ($E_\alpha = 1.1$–1.5 MeV), the difference ΔN between the experimental values and the approximating curve was plotted against the energy of the α-particles and channel number (Fig. 16d). We see that the effect of the forbidden α-transition clearly manifests itself in the form of a peak encompassing a region of seven channels rather than five. This is experimental proof of the existence of α-transitions forbidden by parity conservation law.

Altogether the experimenters registered $N_\alpha(8.87) = 7 \times 10^3$ α-particles forbidden by parity conservation law against the background of $N_\alpha(9.61) = 1.3 \times 10^8$ α-particles allowed by the same law, i.e. the scale of recorded effect amounted to 5×10^{-5}, which is a substantial achievement.

The ratio $N_\alpha(8.87)/N_\alpha(9.61)$ must satisfy a simple formula that allows for the probability Y_β of formation of the corresponding levels in the β-decay of ^{16}N (the yields of the corresponding β-particles) and the total (α-particle and radiative) widths of these levels:

$$\frac{N_\alpha(8.87)}{N_\alpha(9.61)} = \frac{Y_\beta(8.87)}{Y_\beta(9.61)}\,\frac{\Gamma_\alpha(8.87)}{\Gamma_\alpha(8.87) + \sum\Gamma_\gamma(8.87)} \times \frac{\Gamma_\alpha(9.61) + \sum\Gamma_\gamma(9.61)}{\Gamma_\alpha(9.61)}\,. \tag{79}$$

If we allow for the fact that $\sum\Gamma_\gamma(8.87) \approx 10^{-3}$ eV, which is much larger than $\Gamma_\alpha(8.87) \approx 10^{-10}$ eV, and $\Gamma_\alpha(9.61) \approx 10^4$ eV, which is much larger than any possible value of $\sum\Gamma_\gamma(9.61)$, then formula (79) becomes simpler and produces the following expression for $\Gamma_{\alpha\ \text{forbid}}$:

$$\Gamma_{\alpha\ \text{forbid}}(8.87) = \frac{N_\alpha(8.87)}{N_\alpha(9.61)}\,\frac{Y_\beta(9.61)}{Y_\beta(8.87)}\sum\Gamma_\gamma(8.87)\,. \tag{80}$$

Plugging the measured values of $N_\alpha(8.87)$ and $N_\alpha(9.61)$ and the values of the probabilities known from other experiments into (8), i.e. $Y_\beta(8.87) = (1 \pm 0.2) \times 10^{-2}$, $Y_\beta(9.61) = (1.19 \pm 0.10) \times 10^{-5}$, and $\sum\Gamma_\gamma(8.87) = (2.7 \pm 0.5) \times 10^{-3}$ eV, we obtain

$$\Gamma^{\text{expt}}_{\alpha\ \text{forbid}} = (1.8 \pm 0.8) \times 10^{-10}\ \text{eV}\,, \tag{81}$$

which agrees with available theoretical predictions.

9.4 Fission forbidden by parity conservation law

Another exotic result concerning strong processes forbidden by parity conservation law was obtained in 1978 by Danilyan [102] of the Institute of Theoretical and Experimental Physics (Moscow), who discovered asymmetry in the emission of the fission products by polarized uranium and plutonium nuclei. Again the scale of the effect is of order 10^{-4} but, in contrast to the two previous cases, here the asymmetry exists in the direction of motion of large fragments consisting of many dozens of nucleons. What is exotic about this effect is the fact that it *should have not appeared at all*. The thing is that, in contrast to γ-radiation and α-decay, the fission process is characterized by a huge number (10^7–10^{10}) of final states, since the fission fragments formed possess a very broad spectrum of masses, kinetic energies, spins, etc. It would seem that any initial asymmetry would even out and disappear. Nevertheless, the effect has been detected and on a scale (10^{-4}) such that for the number of states $N \approx 10^8$–10^{10} it should have completely disappeared, since $\Delta N/N = \sqrt{N}/N = 10^{-5}$–$10^{-4}$.

The experiment involved a polarized beam of thermal neutrons from the heavy-water reactor of the Institute of Theoretical and Experimental Physics (Fig. 17). The fission fragments were recorded by a fission chamber with a

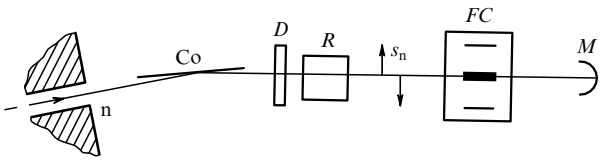

Figure 17. Experimental setup for detecting fission fragments forbidden by parity conversion law: n, neutron beam; Co, cobalt mirror; *D*, depolarizer; *R*, device used to reorient the neutron spin s_n; *FC*, fission chamber, and *M*, monitor.

discriminator, which made it possible to separate light and heavy fragments. The chamber's target consisted of an aluminium substrate covered on both sides with a thin layer (100 μg cm^{-2}) of uranium ($^{233}_{92}$U and $^{235}_{92}$U) oxide or plutonium ($^{239}_{94}$Pu) oxide. The fission fragments were registered by silicon surface-barrier detectors for two orientations of the neutron spin (in the direction in which a fragment moves or in the opposite direction). Each detector could simultaneously register light fragments and heavy fragments, separating them by their energy (difficulties associated with the overlap of fragments in energy and cutting off the background did not appear). Spin reorientation and detector polarity reversal were done by the law of chance. Measurements involving a depolarized beam of neutrons were used for control.

The gained effect for the fissioning isotopes of uranium and plutonium was as follows

$$^{234}_{92}\mathrm{U}: \quad (2.8 \pm 0.3) \times 10^{-4}\,, \tag{82}$$

$$^{236}_{92}\mathrm{U}: \quad (1.37 \pm 0.35) \times 10^{-4}\,, \tag{83}$$

$$^{240}_{94}\mathrm{Pu}: \quad (-4.8 \pm 0.8) \times 10^{-4}\,, \tag{84}$$

where the 'minus' sign corresponds to a deficiency in light fragments in the direction of the neutron spin. Other experiments conducted later confirmed the existence of this effect (see the literature cited in Ref. [102]).

The exotic feature of this effect was explained by Sushkov and Flambaum [103] by the special shape of the double-humped fission barrier (see Fig. 5a in Section 4.5). According to this model, near the second potential-energy minimum it is preferable (energetically) for the nucleus to be in a strongly deformed asymmetric pear-shaped state. And since, as the saddle point is passed, all the excitation energy is spent to deform the nucleus, this deformation must be 'optimal', i.e. the only one possible. Thus, despite the large number of channels in the initial stage (a hot compound nucleus) and final stage (a multitude of fragments), fission proceeds through one channel (or, possibly, a few channels) determined by the intermediate cold stage.

10. Decays of the simplest nuclei (nucleons) and the properties of the simplest antinuclei

At the beginning of our review we agreed not to discuss the radioactivity of elementary particles. However, there is a pair of particles for which we must make an exception. These particles are constituents of all atomic nuclei and are bound there by nuclear forces. One is the proton (p) and the other is the neutron (n). And in this (nuclear) sense (if we ignore the difference caused by electromagnetic interaction), the two particles are quite identical. This becomes especially evident in nuclear physics when we compare what is known as mirror nuclei, which differ in that all protons are replaced by neutrons and vice versa ($^3_1$H^2 and $^3_2$He^1, $^7_3$Li^4 and $^7_4$Be^3, and other pairs), and in particle physics when we compare proton – proton, neutron – neutron, and neutron – proton interactions.

In a somewhat formal but convenient language it is said about mirror nuclei that they form isotopic doublets of nuclei with the same vector of isotopic spin $T = 1/2$ but with different projections of this spin, whose value is determined by the half-difference of the numbers of protons and neutrons in a given nucleus ($+1/2$ for $^3_2$He^1 and $^7_4$Be^3, and $-1/2$ for $^3_1$H^2 and $^7_3$Li^4). The fact that mirror nuclei have the same isotopic spin means that their nuclear properties are equivalent, while the fact that their projections of the isotopic spin are different means that their electromagnetic properties differ.

The constituent parts of nuclei, i.e. protons and neutrons, also form an isotopic doublet of nuclear-equivalent particles, nucleons, and this doublet is characterized by the isotopic spin $T = 1/2$ as well. Here, the projection of the proton's isospin is $T_\xi = +1/2$, and that of the neutron, $T_\xi = -1/2$. In terms of isotopic spin, the nuclear equivalence of the proton and neutron is called isotopic invariance (i.e. the independence of nuclear interaction from the isospin projection).

As noted earlier, nucleons occupy a special place among the huge number of elementary particles because they are the simplest elements of any atomic nucleus 'pasted' together by nuclear forces. In other words, the proton and the neutron are themselves the simplest mirror atomic nuclei, whose properties will be considered here within the scope of the nuclear physics subject of the review.

10.1 β-decay of the neutron

Due to the difference in the electromagnetic properties of the neutron and the proton, the former is somewhat heavier than the latter:

$$m_\mathrm{n} - m_\mathrm{p} \approx 2.5 m_\mathrm{e}\,, \tag{85}$$

where $m_\mathrm{e} = 0.51$ MeV is the electron mass. Hence, the β-decay of the neutron by the following scheme is allowed by energy conservation law:

$$\mathrm{n} \to \mathrm{p} + \mathrm{e}^- + \tilde{\nu}_\mathrm{e}\,. \tag{86}$$

In weak interaction theory, the β-transition between n and p is a superallowed transition, i.e. it occurs with the highest probability for the given energy of the β-transition. Since the difference in masses between the neutron and the proton is small, the expected lifetime of the neutron is not short. Weak interaction theory predicted a lifetime of about 30 min. Measuring such a lifetime for an immobile radioactive target of some sort is not a particular problem. However, what makes the β-decay of the neutron so exotic is that as long as a neutron is free it is always moving and all measurements must be done in flight, but the velocity v even of the relatively slow thermal neutrons emitted in large quantities by nuclear reactors is approximately 2.2 km s^{-1}. If the size of the device for studying neutron decay is of order $l = 10$ cm, a neutron will spend about $l/v = 5 \times 10^{-5}$ s in it, i.e. the probability of registering the neutron is only

$$\omega = \frac{5 \times 10^{-5}}{30 \times 60} = 3 \times 10^{-8}\,. \tag{87}$$

The first experiments on measuring the neutron lifetime were conducted in 1948 – 1950 by Snell and Miller [104]

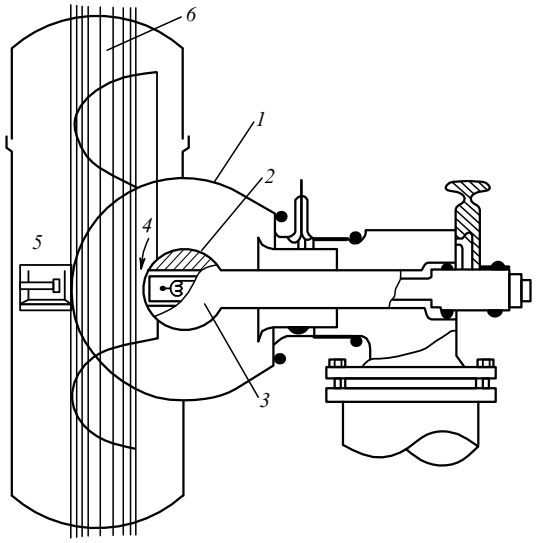

Figure 18. Schematic of the first measuring device constructed by Spivak and Sosnovskiĭ [105] for detecting the β-decay of neutrons: *1* and *3*, spherical electrodes; *2*, proportional counter; *4*, counter window covered by a thin film; *5*, α-gun, and *6*, beam of thermal neutrons.

(USA), Spivak and Sosnovskiĭ [105] (USSR), and Robson [106] (Canada). Figure 18 depicts the schematic of the first device of Spivak and Sosnovskiĭ. The device consisted of two spherical electrodes *1* and *3* to which a high voltage (20 kV) was applied. Inside electrode *3* there was a proportional counter *2* with a window covered by a thin film *4*. The operation of the counter was monitored by an α-gun *5*. The hatched area *6* indicates the beam of thermal neutrons, whose decay products, protons, were deflected inside the device by an electric field in the direction of an electrode *3*, and a fraction of these protons landed in the counter. Knowing the intensity of the neutron beam, the geometry of the device, and the number of recorded protons makes it possible to estimate the neutron lifetime. The first measurements of all three groups of researchers yielded values ranging from 10 to 20 min. Subsequently, Spivak's group used a similar beam method to refine this value. In 1978 they found that (the results were published later in Ref. [107])

$$\tau_n = 891 \pm 9 \text{ s}. \tag{88}$$

The other groups of researchers obtained similar values for τ_n.

In addition to the beam method, there is one more (direct) method of measuring the neutron lifetime by the decrease in the number of ultracold neutrons *contained* in special vessels, which according to the graphic terminology introduced by Ya B Zel'dovich are sometimes called neutron bottles. Here, the exotic feature consists in the existence of a remarkable property, discovered in 1959 by Zel'dovich [108], of ultracold neutrons: total internal reflection from the vacuum (air)–matter boundary for all angles of incidence, thanks to which ultracold neutrons can exist very long periods of time (theoretically, several thousand seconds) by 'bouncing off' the walls of the vessel without being absorbed. Neutrons possess this property at energies lower than a certain threshold energy, which depends on the material of the wall but is approximately 10^{-7} eV.

Note, however, that the realization of this extremely beautiful theoretical idea proved to be very difficult. And although its verification was obtained fairly soon and by 1968 Shapiro's group [109] was able to store ultracold neutrons for 30 s, the central problem, viz. the production of vessels for prolonged storage of ultracold neutrons, due to technical difficulties required many years to solve. The main reason for the leakage of ultracold neutrons was the presence of almost unremovable hydrogenous contaminants on the vessel walls. Inelastically colliding with hydrogen, ultracold neutrons get heated to thermal energies, with the result that they lose their property of total internal reflection and freely pass through the vessel walls.

After these difficulties were resolved by various methods, among which was the covering of the inner walls of the vessels with films not containing hydrogen and the cooling of the vessels to very low ($\sim$ 15 K) temperatures, the storing time for ultracold neutrons was gradually increased to 60 min, which exceeds the neutron lifetime severalfold. In such conditions losses during storage were reduced to 3% of the number of neutrons lost due to decay. This enabled Mampe et al. [110], in 1993, to measure the neutron lifetime by the natural decrease in the number of neutrons in a vessel with an accuracy of several seconds:

$$\tau_n = 882.6 \pm 2.7 \text{ s}. \tag{89}$$

Since then the accuracy in determining τ_n has been increased. In 1998, Morozov's group (Russian Research Centre 'Kurchatov Institute') published the most precise value of the neutron lifetime [111]:

$$\tau_n = 885.4 \pm 0.9_{\text{stat}} \pm 0.4_{\text{sys}} \text{ s}. \tag{90}$$

The need to know the exact value of the neutron lifetime τ_n stems from the fact that the decay constant $\lambda^{00}_{\tau_n}$ of the neutron's β-decay can be calculated from the neutron lifetime and the lifetimes of β-active nuclei with $(0^+ - 0^+)$-transitions (for these nuclei, just as for the neutron, the values of the matrix elements determining the probability of β-decay are known). The decay constant, which plays an important role in weak interaction theory in general, is further remarkable in that it can be determined from other parameters of the neutron β-decay, precisely from the angular correlations between the neutron spin $\boldsymbol{\sigma}_n$ and the momenta $\mathbf{p}_e$ and $\mathbf{p}_{\tilde{\nu}_e}$ of the decay products. Knowing the angular correlations $\mathbf{p}_e\mathbf{p}_{\tilde{\nu}_e}$, $\boldsymbol{\sigma}_n\mathbf{p}_e$, $\boldsymbol{\sigma}_n\mathbf{p}_{\tilde{\nu}_e}$, and $\boldsymbol{\sigma}_n[\mathbf{p}_e\mathbf{p}_{\tilde{\nu}_e}]$ makes it possible to obtain another, correlation, value of the decay constant λ_c characterizing the neutron's β-decay.

Within the generally accepted (V−A)-variant of weak interaction theory, the two constants $\lambda^{00}_{\tau_n}$ and λ_c should have the same value. If they were different, it would mean a deviation of the theory from this variant, e.g. due to the presence of a small admixture of the (V+A)-variant ('right-handed currents'). Before 1990, the experimental values of these constants coincided to within measurement errors. However, beginning with 1990, the accuracy of the experiments increased so markedly that it became possible to speak of a slight (of order 3σ) difference. This problem has been discussed in many papers, whose authors estimated the contribution of the right-handed currents, the mass of the hypothetical right W-boson, and other parameters of the theory. Lately certain factors have been established that indicate that the values of the two constants are closer than believed earlier. According to modern estimates made by Mostovoy [112], the difference does not exceed 0.5%. More

details about the properties of ultracold neutrons (e.g. the discovery of a new anomaly in their storage at roughly 10 K) and the β-decay of the neutron can be found in Ref. [113].

10.2 Hypothetical decays of nucleons with violation of the baryon-number conservation law

Today it is known that all three types of interaction characterizing nuclear processes, the strong, the electromagnetic, and the weak, are of a general gauge nature, i.e. satisfy the general principle of local gauge symmetry which must be related to a symmetry group wider than SU(2) in the isotopic symmetry mentioned earlier, SU(3) in the octet symmetry describing ordinary and strange particles, and SU(2)×U1 in the electroweak interaction theory. A possible candidate for such a group is SU(5) which encompasses quarks and leptons on an equal basis. The corresponding theory is called Grand Unification. It allows for transitions between quarks and leptons, i.e. processes that violate baryon- and lepton-number conservation laws ($\Delta B = 1$, $\Delta L = -1$) but in which the difference $B - L$ is preserved. In particular, this theory allows for decays of nucleons by the following processes

$$\mathrm{p} \to \mathrm{e}^+ + \pi^0\,, \quad \mathrm{p} \to \mathrm{e}^+ + \pi^+ + \pi^-\,, \tag{91}$$

$$\mathrm{n} \to \mathrm{e}^+ + \pi^-, \quad \mathrm{n} \to \pi^0 + \tilde{\nu}_\mathrm{e}\,. \tag{92}$$

In all these processes, the rule $B - L = \text{const}$ is observed.

Theory gives the following estimate for the proton lifetime: $10^{31} - 10^{33}$ y, and a similar result holds for the neutron. However, the neutron here is not free but is bound in the nucleus, i.e. it does not decay by process (86). Obviously, looking for processes with such huge lifetimes is an extremely difficult task. The experiments are conducted in deep (up to 7.6-km water equivalent) underground laboratories with detectors that weigh several thousand tons and contain several thousand photomultipliers and other electronic gadgets. It is assumed that the decay of a nucleon can be detected by the Cherenkov radiation set up by the charged decay products in the water of the detector. Today approximately a dozen laboratories are searching for nucleon decays, and only a lower bound on the time of neutron decay with $\Delta B = 1$ is known:

$$\tau_\mathrm{n}^{\Delta B=1} > 10^{32} \text{ years}. \tag{93}$$

It will be a sensation if even one event of a nucleon decay with $\Delta B = 1$ is discovered, as well as an exotics.

10.3 Antinucleons. Production and interaction. Decay of the antineutron

The remarkable story of the positron discovery is well known. In 1928, P Dirac derived his famous relativistic quantum-mechanical equation for an electron. The equation predicted correct values for the electron's spin and magnetic moment (previously there were difficulties in determining the latter) and, what is more important, the existence of a particle that is charge-conjugate to the electron, the positron.

According to Dirac, the positron would have the same mass, spin, and lifetime as the electron but opposite values of the electric charge and magnetic moment. A particle with such properties came to be known as an antiparticle. In 1932, the electron's antiparticle, the positron, was discovered in cosmic rays, and in several years the charge conjugation principle was corroborated by the discovery of two further particle–antiparticle pairs: in 1936–1938 the muons μ^+ and μ^- were discovered, and in 1947, the pions π^+ and π^-. Thus, nature proved to be symmetric with respect to the existence of particles and antiparticles, which according to the charge conjugation principle, as in the case of the electron and positron, must have (and do indeed have) equal masses, spins, and lifetimes. Later, however, it was proved that in the weak interaction the charge symmetry is violated, but the prediction of the symmetry of nature with respect to the existence of particles and antiparticles with identical values of m, $\boldsymbol{\sigma}$ and τ remain valid, since it is a corollary of another, more general theorem, the CPT theorem proved in 1954–1955 by G Luders and W Pauli.

According to the CPT theorem, in any interaction the product of three inversions, charge inversion C (charge conjugation operation), spatial inversion P (mirror conjugation), and temporal inversion T (time reversal), is an invariant. The CPT theorem is based on Lorentz invariance and the correct relationship between spin and statistics, i.e. it is valid for all theories for which the causality principle holds. In accordance with this theorem, in any particle–antiparticle pair (including pairs yet to be discovered), the particle and antiparticle not only have opposite electric charges and magnetic moments but also other signed quantum numbers should be opposite (e.g. the baryonic and leptonic numbers discussed earlier are equal to $+1$ for particles, and -1 for antiparticles). For instance, the antiproton and antineutron should have the same values of the baryonic number ($B = -1$), and the positron and antineutrino will have $L = -1$ as the leptonic number. In normal processes (in contrast to the exotic processes discussed in Section 10.2) these numbers must be conserved. Hence, when an antiproton ($\tilde{\mathrm{p}}$) meets a proton (p), the two annihilate, and the mass and energy of these particles transform into the mass and energy of several other particles (usually pions, rarely kaons, still more rarely γ-quanta) that have zero as the baryonic number:

$$\tilde{\mathrm{p}} + \mathrm{p} \to n\pi \quad (-1 + 1 = 0)\,. \tag{94}$$

For low-energy antiprotons and protons, the average value of $\bar{n}$ is 5 and the average energy carried away by a single pion is 200–250 MeV. As the energy of the interacting $\tilde{\mathrm{p}}$ and p increases, the number of pions produced in the annihilation process increases and reaches nearly 30 at energies 2×270 GeV. In vacuum, the antiproton is just as stable as the proton, but our world consists of atoms, i.e. protons, neutrons, electrons, which are all *particles*. In view of this any antiproton and antineutron (as well as a positron) arriving from outer space is sure to collide with the appropriate particle and the two will annihilate. This fact complicates observation of cosmic antinucleons (although special cases in which cosmic antiprotons were probably observed have been recorded since 1947). Hence to prove the existence of antinucleons, the following specially designed accelerator experiment was done.

The antiproton was discovered by E Segre and coworkers (see Ref. [114]) in 1955 at Berkeley. The researchers used the Bevatron, an accelerator that produced protons with energies up to 6.3 GeV. The reaction employed was

$$\mathrm{p} + \mathrm{p} \to \tilde{\mathrm{p}} + 3\mathrm{p} \tag{95}$$

having a structure determined by the same baryon-number conservation law ($1 + 1 = -1 + 3$) and a threshold of 5.6 GeV.

The facility used to discover the antiproton is schematically depicted in Fig. 19a. The copper target *CT* in the Bevatron chamber was bombarded with protons whose energies ranged from 4.3 to 6.2 GeV (the reaction threshold of the production of an antiproton on a nucleus is reduced to 4.3 GeV due to the Fermi motion of nucleons in the nucleus). The produced antiprotons and π^--mesons (there were 60,000 times more π^--mesons than antiprotons) were fed into a magnetic channel, which consisted of deflecting magnets *M1* and *M2* and focusing lenses *L1* and *L2* and was tuned to transmit negative 1.19-GeV/*c*-momentum particles to the detecting device.

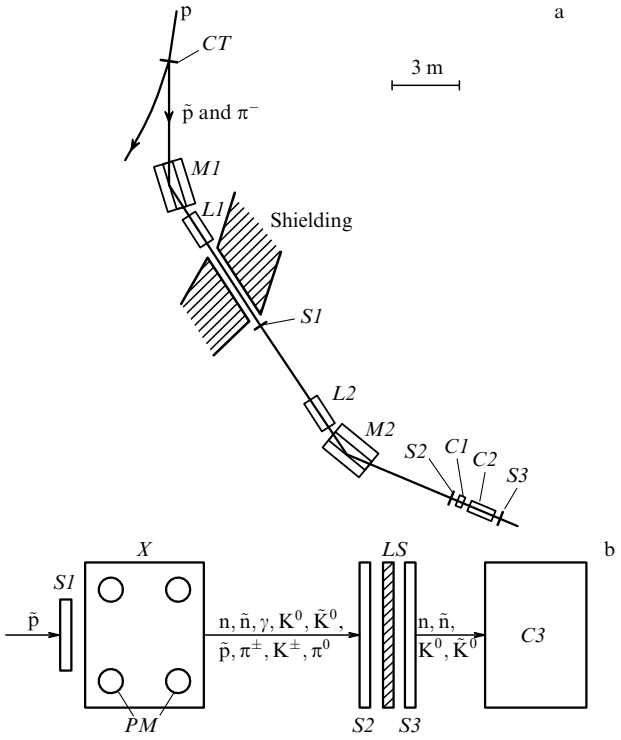

Figure 19. Layout of the facility for studying the production of antinucleons. (a) Antiproton production: p, beam of protons with energies ranging from 4.3 to 6.2 GeV; *CT*, copper target; $\tilde{p}$ and π^-, produced antiprotons and π^--mesons; *M1* and *M2*, deflecting magnets; *L1* and *L2*, magnetic focusing lenses; *S1*, *S2*, and *S3*, scintillation counters, and *C1* and *C2*, Cherenkov counters. (b) Antineutron production: $\tilde{p}$, beam of antiprotons; *S1*, *S2*, and *S3*, scintillation counters; *X*, converter; *PM*, photomultipliers; *LS*, lead screen, and *C3*, Cherenkov counter.

The detecting device consisted of two scintillation counters, *S1* and *S2*, separated by a distance of 12 m, which made it possible to determine the time of flight of the antiproton (51×10^{-9} s) and the π^--meson (40×10^{-9} s); two Cherenkov counters, *C1* and *C2*, with the latter tuned to register antiprotons with (for a given momentum) a value of $\beta = v/c$ (v is the particle's velocity, and c is the speed of light in vacuum) ranging from 0.75 to 0.78, and *C1* to select particles with $\beta > 0.79$, i.e. beam-entering ($\beta = 0.99$) and scattered π^--mesons, and a scintillation counter *S3* that confirmed the absence of scattering of the particle registered in the counter *C2*. Altogether 60 antiprotons were registered in the first experiment.

In subsequent experiments, in which a much larger number of produced antiprotons were registered, all the expected antiproton characteristics were confirmed ($m_{\tilde{p}} \equiv m_p$, $\boldsymbol{\sigma}_{\tilde{p}} = \boldsymbol{\sigma}_p = 1/2$, $\tau_{\tilde{p}} = \tau_p$, and $\boldsymbol{\mu}_{\tilde{p}} = -\boldsymbol{\mu}_p$), and antiproton beams were formed in the biggest accelerators of that time (Brookhaven, Serpukhov, Batavia, Geneva). Somewhat later, in 1981, two accelerators with energies amounting to 2×31.4 GeV and 2×270 GeV were built at CERN, which enabled researchers to use the entire energy of both colliding particles (i.e. to conduct experiments in their center-of-mass system).

The fact that there were antiproton beams made it possible to study the proton–antiproton interaction cross section ($\sigma_{\tilde{p}p}$) as a function of energy and to compare it with the energy dependence of the proton–proton interaction cross section (σ_{pp}). It was found that the two differ substantially at relatively low energies, which can be explained by the sizable contribution to $\sigma_{\tilde{p}p}$ of a new process, annihilation. At $p_{lab} = 5$ GeV/c, $\sigma_{\tilde{p}p} = 65$ mb, while σ_{pp} amounts to only 41 mb. As the energy increases, the relative contribution of annihilation to $\sigma_{\tilde{p}p}$ drops and the difference between the two interaction cross sections decreases (and so do the interaction cross sections); at $p_{lab} = 50$ GeV/c, the values of the cross sections are 44 and 39 mb, respectively. When p_{lab} is higher than 50 GeV/c, σ_{pp} begins to increase, while $\sigma_{\tilde{p}p}$ first continues decreasing and then, starting at $p_{lab} = 2 \times 10^2$ GeV/c, also increases. As a result, the two cross sections at $p_{lab} = 2 \times 10^3$ GeV/c are almost the same: $\sigma_{\tilde{p}p} = \sigma_{pp} = 42$ mb. This results confirms the Pomeranchuk theorem [115] proved in 1958, which states that the total cross section both for scattering of a particle by a given target particle and for scattering of its antiparticle by the same target particle at ultrarelativistic energies must be the same.

Antineutrons ($\tilde{n}$) were discovered in 1956 by Cork et al. [116], who employed for their production the process of charge exchange in the antiproton–nucleon interaction:

$$\tilde{p} + p \to \tilde{n} + n, \qquad \tilde{p} + n \to \tilde{n} + n + \pi^-. \tag{96}$$

The experimenters used a beam of antiprotons whose intensity was 5 to 10 antiprotons per minute. The beam was formed in the Bevatron using two deflecting magnets and five focusing magnetic lenses. The antineutrons were produced in the converter *X* with a liquid scintillator that was scanned by four photomultipliers (Fig. 19b). In addition to reactions (96), there may be annihilation in the converter, accompanied by the production of pions and K-mesons and also γ-quanta, with a powerful energy pulse of approximately 1 GeV being emitted in the process. Furthermore, an antiproton may pass through the converter without undergoing nuclear interaction, spending only some of its energy (about 50 MeV) on ionization of the converter's material. It is the energy release that makes it possible (in the first approximation) to discriminate the processes (96), in which it is, obviously, lower than 50 MeV. A more reliable detection of antineutrons occurs in the lead-glass Cherenkov counter *C3* scanned by 16 photomultipliers, with the pulse of light produced in the counter being so large as to indicate the annihilation of an antineutron. Here, to clear the Cherenkov counter *C3* from background noise which could emerge because of antiproton annihilation products in the converter ($\pi^\pm, K^\pm, \gamma, \pi^0$), a system of two scintillation counters *S2* and *S3* was included, connected in anticoincidence circuit, with a lead screen *LS* between them. Special measures were taken to eliminate powerful spurious pulses from the pile-up of several pulses caused by neutrons and/or K^0-mesons that are not blocked by

the system of counters *S2* and *S3*. As a result, the average number of observed antineutrons was 0.003 ñ for each p̃. The reliability of detecting antineutrons was corroborated by a system of check experiments. Today we can confirm that the antineutron has the same mass and spin as the neutron and decays by the charge-conjugate process

$$\tilde{n} \to \tilde{p} + e^+ + \nu_e \qquad (97)$$

with the same half-life as the neutron. The magnetic moment of the antineutron is equal in magnitude and opposite in sign to that of the neutron (i.e. it is positive), while the baryonic charge is negative, as processes (96) imply.

In conclusion of this topic we note that the antiproton and antineutron (just as the proton and the neutron) form an isotopic doublet of antiparticles with an isotopic spin vector $T = 1/2$ but with opposite (in relation to the nucleons) signs of the projections ($T_\varsigma^{(\tilde{p})} = -1/2$, and $T_\varsigma^{(\tilde{n})} = +1/2$). The interaction between antinucleons is the same as the interaction between nucleons (to within some fine weak-interaction features, which we will not discuss here).

10.4 Antideuteron, antihelium III, and antitritium

Experimental proof of the existence of antiprotons and antineutrons and of the symmetry in their properties makes it possible to assume that there are antinuclei with properties similar to those of the respective nuclei. The first 'complex' nuclei (complex in comparison to the antiproton), antideuteron, was discovered by L Lederman's group at BNL with the help of a mass spectrometer placed near the beryllium target in the accelerator. The antideuteron consists of an antiproton and an antineutron, i.e. it has a baryonic number $B = -2$, an electric charge $Z = -1$, its mass coincides with that of the deuteron, and its spin is equal to unity.

In 1970, a group of researchers headed by Yu D Prokoshkin used the Serpukhov accelerator to prove the existence of an antinucleus more complex than the antideuteron, the $^3_2\widetilde{\mathrm{He}}$ antinucleus, which is composed of two antiprotons and one antineutron, i.e. having $B = -3$, $Z = -2$, and $M(^3_2\widetilde{\mathrm{He}}) = M(^3_2\mathrm{He})$ (see Ref. [117]).

The experimental facility consisted of 50 fast detectors: Cherenkov and scintillation counters and nanosecond electronics. The nuclei of antihelium III were discriminated by their charge $Z = -2$ and velocity β. The charge was found from the ionization and intensity of the Cherenkov radiation, and the velocity was found by using threshold and differential Cherenkov counters and from the time of flight. Altogether 2×10^{11} particles passed through the facility, among which only five antinuclei of ^{3}He were identified. This ratio (4×10^{10}:1) shows how difficult the experiment was (the similar ratio in the experiment on registering an antiproton was 6×10^4:1).

Approximately the same ratio of background to operative particles (10^{11}:1) was found in the experiment in which another antinucleus, antitritium $^3_1\widetilde{\mathrm{H}}$, was detected. This experiment proved to be even more complicated than the previous one since the charge of $^3_1\widetilde{\mathrm{H}}$ is $Z = -1$, i.e. coincides with the charge of most background particles (π^-- and K^--mesons). The proof that the antinucleus $^3_1\widetilde{\mathrm{H}}$ exists was obtained in the collective work of V I Rykalin's group and V I Petrukhin's group at Dubna (see Ref. [118]).

Since it was impossible to discriminate $^3_1\widetilde{\mathrm{H}}$ antinuclei by the charge, their selection was done by the velocity β, which is uniquely related to the mass of the antinucleus and the momentum, to which the magnetic channel was tuned. To this end a system of Cherenkov counters was used and the time-of-flight technique with several path lengths was employed. The experiments were done in conjunction with a computer and nanosecond electronics. Altogether 3.7×10^{11} particles passed through the facility, among which only four tritium antinuclei were identified. The tritium antinucleus has $B = -3$, $Z = -1$, and $M(^3_1\widetilde{\mathrm{H}}) = M(^3_1\mathrm{H})$. Naturally, the lifetime and radioactivity of antitritium have yet to be measured. Comparison of the intensity of the antinucleus *production* with $B = -2$ and $B = -3$ shows that it decreases by a factor of 10^4 as $|B|$ increases one unit. Hence, the search for antinuclei heavier than $^3_2\widetilde{\mathrm{He}}$ and $^3_1\widetilde{\mathrm{H}}$ should be extremely complicated. The authors of this article know of no attempts in this direction. However, the results obtained so far are solid proof that nature is symmetric with respect to the existence of matter and antimatter, since all the necessary constituents (positrons, antiprotons, antineutrons, and antinuclei) of antimatter exist.

11. The last exotic feature (so far)

11.1 A lyrical introduction

Finally we would like to relate the most up-to-date exotic discoveries in nuclear physics, the experimental proof of the existence of the famous superheavy, fairly stable element 114, whose salient properties had been predicted in the nuclear shell model (see Section 3), and the discovery of the even heavier element 118. We note immediately that the exotic feature is peculiar: it does not amount to discovering new phenomena; rather, we will talk about ordinary α-decays and spontaneous fission. However, the very experiments that led to the discovery of elements 114 and 118 are indeed fantastic: events whose cross sections were only 1 pb, i.e. 10^{-36} cm^2, were registered! Here, reliable identification required the use of a sort of 'time machine', which enabled travelling into the past and into the future to gather the several stages of these events that successively occurred at a given point in space but at different moments in time into a unique chain.

For instance, the Dubna group, moving step by step back in time, was able to study the 'family-tree' of the isotope of the 114th element, $^{289}114$. First they discovered its 'great-granddaughter', which left the most noticeable trace of its vital activity (spontaneous-fission fragments with a kinetic energy of roughly 170 MeV); then the less energetic 'granddaughter' that underwent α-decay with an energy release amounting to roughly 9 MeV; then one more α-decay with approximately the same energy release signaled the existence of a 'daughter', and, finally, the $^{289}114$ nucleus was identified by another α-decay process with slightly higher energy liberation. What also helped in this search was the fact that the 'ancestor' and all his 'descendents' occupied the same small 'house' of size 1.6 mm and did not leave it.

The 118th element, discovered at Berkeley, was found to have even more 'descendents'. Here, in addition to a 'great-granddaughter', the researchers found a 'great-great-granddaughter', a 'great-great-great-granddaughter', and a 'great-great-great-great-granddaughter'! And all occupied a 'house' that was even smaller.

After this lyrical introduction, which we just could not refrain from writing and for which, we believe, the reader will excuse us, we will tell the story of how everything actually happened.

11.2 Discovery of the 114th element

At the end of 1998 and the beginning of 1999, a group of JINR researchers headed by Yu Ts Oganessian discovered two isotopes of the superheavy 114th element, $^{289}114$ and $^{287}114$ [119, 120]. Both isotopes were produced by bombarding plutonium targets ($^{244}_{94}$Pu and $^{242}_{94}$Pu, respectively) in the heavy-ion accelerator U-400 with a beam of $^{48}_{20}Ca^{5+}$ ions. Calculations (see Ref. [121]) showed that in such conditions the synthesis of the sought nuclei with highest probability followed the reactions

$$^{48}_{20}\mathrm{Ca} + {}^{244}_{94}\mathrm{Pu} \rightarrow {}^{292}114 \rightarrow {}^{289}114 + 3\mathrm{n}\,, \tag{98}$$

$$^{48}_{20}\mathrm{Ca} + {}^{242}_{94}\mathrm{Pu} \rightarrow {}^{290}114 \rightarrow {}^{287}114 + 3\mathrm{n}\,, \tag{99}$$

which lead, with a cross section of approximately 1 pb, to the production of the recoil nuclei $^{289}114$ and $^{287}114$, which emerge after three neutrons have evaporated from the weakly excited (about 30 MeV above the Coulomb barrier) compound nuclei $^{292}114$ and $^{290}114$.

In the second half of 1999, a new bombardment of a plutonium target $^{244}_{94}$Pu with 236-MeV ions of $^{48}_{20}$Ca was carried out. After processing the data from this experiment, a new, third, isotope of the 114th element was discovered, $^{288}114$ [122]. The production reaction was as follows

$$^{48}_{20}\mathrm{Ca} + {}^{244}_{94}\mathrm{Pu} \rightarrow {}^{292}114 \rightarrow {}^{288}114 + 4\mathrm{n}\,. \tag{100}$$

11.2.1 The first isotope of the 114th element, $^{289}114$. In the first paper on this subject, Oganessian et al. [119] reported the results of an experiment that used 98.6% enriched ^{244}Pu as a target and a 236-MeV beam of $^{48}_{20}Ca^{5+}$ ions with an intensity of $4 \times 10^{12}\ \mathrm{s}^{-1}$. Altogether 5.2×10^{18} ions passed through the target in 40 days of irradiation.

The produced recoil nuclei of the 114th element were separated from the beam particles and other nuclear reactions by a system of magnets and an electrostatic separator VASSILISSA, passed through a time-of-flight device, and entered a semiconductor silicon position-sensitive detector placed in the focal plane of the separator, where they left spatial, energy, and time marks. The products of the decay of the implanted recoil nuclei (α-particles or spontaneous-fission fragments) also left their marks (the exact place in the detector, the released energy, and the moment in time), which were recorded by a computer. If a nucleus of the 114th element landing in the detector undergoes a series of successive transformations (a chain of α-decays ending in spontaneous fission), all of these occur in the same place in the focal plane of the device. Developing the position-fixed events (i.e. events registered by a definite strip of the position-sensitive detector) backward in time (from fission fragments to α-decays and to the recoil nucleus), the full pattern of decays of a given isotope of the 114th element can be reconstructed if the entire chain of events fits into the detector without losses to edge effects.

It was this total pattern for a single event that was registered in the experiment on synthesizing the isotope $^{289}114$:

$$^{289}114 \xrightarrow[\substack{9.71\,\mathrm{Mev}\\30.4\,\mathrm{s}\\(3\text{–}20\,\mathrm{s})}]{\alpha} {}^{285}112 \xrightarrow[\substack{8.67\,\mathrm{MeV}\\15.4\,\mathrm{min}\\(30\text{–}300\,\mathrm{min})}]{\alpha} {}^{281}110 \xrightarrow[\substack{8.83\,\mathrm{MeV}\\1.6\,\mathrm{min}\\(2\text{–}20\,\mathrm{min})}]{\alpha} {}^{277}108 \xrightarrow[\substack{172\,\mathrm{MeV}\\16.5\,\mathrm{min}}]{} \mathrm{s.f.} \tag{101}$$

This decay scheme shows that the isotope $^{289}114$ underwent an α-decay 30.4 s after the moment it entered the detector and that all subsequent decays occurred even less rapidly, so that the entire duration of the decay chain amounted to 34 min (for different stages the figures in parentheses give the estimated values of the half-lives, which were calculated using the values of the measured energy [123]). What is really important is that all the five signals (absorption of the primary nucleus, three successive α-decays, and spontaneous fission) were registered inside a spatial region of size 1.6 mm, which, as shown by check measurements of definitely correlated events, undoubtedly suggests that the signals are correlated. According to estimates, the probability of a random correlation that imitates a registered event is 5×10^{-5}.

Oganessian et al. [119] noted that the lifetimes of the new nuclides in the chain, especially those of $^{285}112$ and $^{281}110$, are approximately 10^6 times longer than that of the well-known nuclei $^{277}112$ and $^{273}110$ [124, 125], which have eight neutrons less. This fact (together with the earlier data of Oganessian et al. [126] for $^{283}112$) can be considered as the first experimental proof of the existence of elevated stability in the realm of superheavy elements.

11.2.2 The second isotope of the 114th element, $^{287}114$. The second isotope of the 114th element, $^{287}114$, was discovered by Oganessian's group (see Ref. [120]), who used a similar device but with a different target ($^{242}_{94}$Pu enriched up to 97%). The beam energy at the center of the target was 235 ± 2 MeV, which corresponded to an excitation energy $E = 33.5$ MeV of the produced compound nucleus. The total number of ions that passed through the target in 32 days of irradiation was 7.5×10^{18}.

The theoretical study of Myers and Swiatecki [127] suggested that the most probable decay scheme of the compound nucleus $^{290}114$ that forms as a result of fusion of $^{48}_{20}$Ca and $^{242}_{94}$Pu is the evaporation of three neutrons accompanied by production of the isotope $^{287}114$. The extraction of the $^{287}114$ nuclei was done using the electrostatic separator VASSILISSA mentioned earlier (Fig. 20a). The search for $^{287}114$ was done by the same 'back-in-time' method used in discovering the isotope $^{289}114$ and led to two decay chains

$$^{287}114 \xrightarrow[\substack{10.29\,\mathrm{MeV}\\1.32\,\mathrm{s}}]{\alpha} {}^{283}112 \xrightarrow[\substack{195\,\mathrm{MeV}\\9.3\,\mathrm{min}}]{} \mathrm{s.f.}\,, \tag{102}$$

$$^{287}114 \xrightarrow[\substack{2.3\,\mathrm{MeV}\\14.4\,\mathrm{s}}]{\alpha} {}^{283}112 \xrightarrow[\substack{165\,\mathrm{MeV}\\3.8\,\mathrm{min}}]{} \mathrm{s.f.} \tag{103}$$

(in the second case, the α-particle escaped from the detector and left behind only a fraction of its energy).

The experimental data provide the means for approximate estimates of the half-lives for $^{287}114$ [$T_{1/2}^{(\alpha)} = (5.5^{+10}_{-2})$ s] and $^{283}112$ [$T_{1/2}^{(\mathrm{s.f.})} = (180^{+170}_{-60})$ s]. Myers and Swiatecki [127] note that the properties of the daughter element $^{283}112$ produced in the α-decays of $^{287}114$ are close to those of the same isotope $^{283}112$ produced earlier by Oganessian et al. [126] directly in the reaction

$$^{48}_{20}\mathrm{Ca} + {}^{238}_{92}\mathrm{U} \rightarrow {}^{286}112 \rightarrow {}^{283}112 + 3\mathrm{n}\,. \tag{104}$$

In both cases, spontaneous fission with half-lives of several minutes and close fragment energies (180 – 200 MeV) was registered.

The half-life of $^{287}114$ is several times shorter than that of $^{289}114$ due to the smaller number of neutrons (the distance

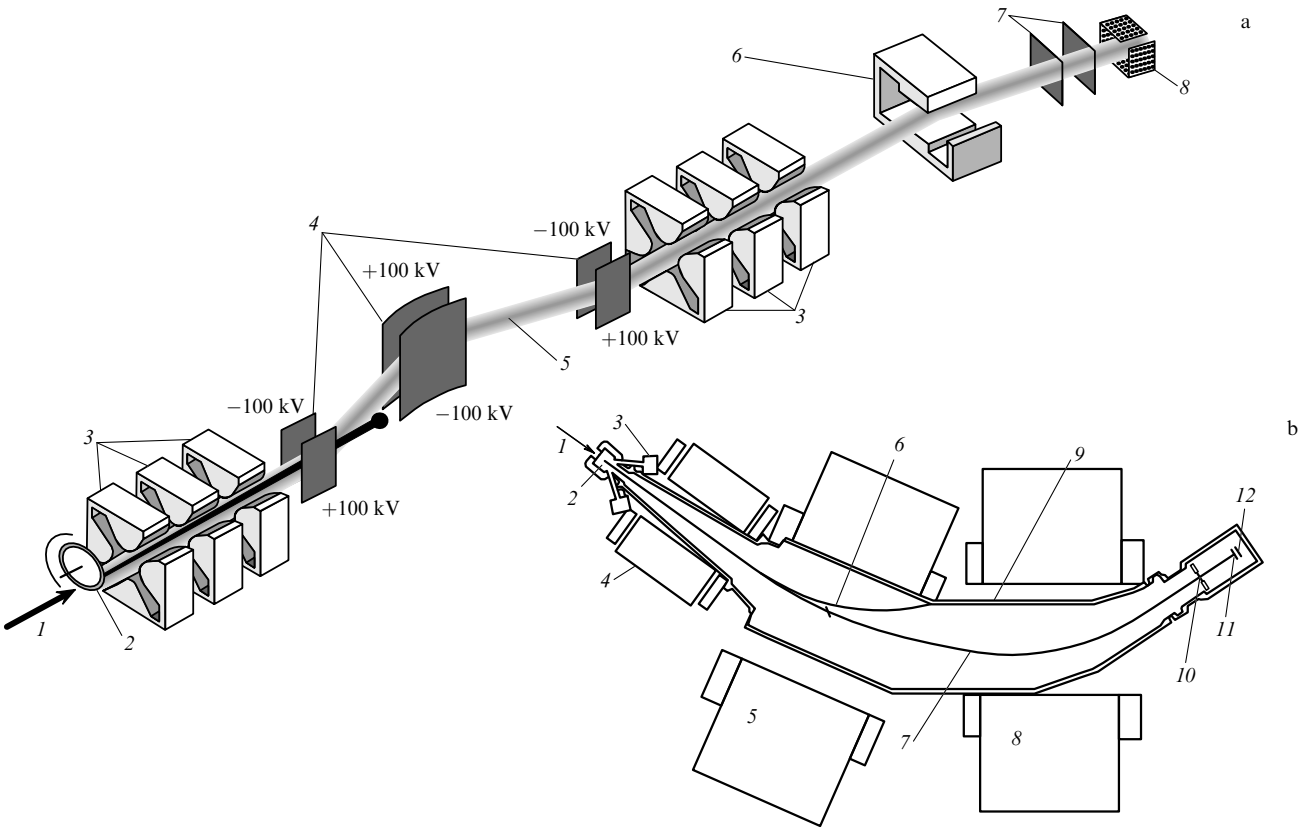

Figure 20. Layouts of the facility used to discover new superheavy elements. (a) VASSILISSA electrostatic separator with which element 114 was discovered at Dubna: *1*, ^{48}Ca beam; *2*, ^{242}Pu target; *3*, quadrupole magnetic focusing mechanism; *4*, electrostatic displacement mechanism; *5*, recoil atoms; *6*, magnetic displacement; *7*, time-of-flight detector; *8*, position-sensitive detector. (b) Gas-filled separator used at Berkeley to discover element 118 (additional explanations are given in the main text): *1*, beam; *2*, target position; *3*, monitoring detectors; *4*, quadrupole magnet; *5*, magnet with nonuniform field; *6*, beam path; *7*, path of recoil atoms (EVR); *8*, magnet with uniform field; *9*, vacuum chamber; *10*, recording device PPAC; *11*, silicon detector in the focal plane; *12*, Punch-through detector.

being greater from the double-magic nucleus ^{298}114). The production cross section for the isotope ^{287}114 in the 3n-evaporation channel amounts to $(2.5^{+4.5}_{-1})$ pb.

11.2.3 The third isotope of the 114th element, ^{288}114. To produce the third isotope of element 114, the Dubna experimenters again reverted to a $^{244}_{94}$Pu target and bombarded it with ions of $^{48}_{20}$Ca, whose energy was roughly 236 MeV [122]. Altogether 1.0×10^{19} ions passed through the target in 60 days of irradiation. Estimates of the excitation energy of the produced compound nucleus ^{292}114 made with allowance for energy losses of the ions in the target, small variations of the target thickness, and variations in the beam energy in the course of bombardment, led to values in the range 31.5 – 39 MeV, which corresponds to evaporation of three or four neutrons from the compound nucleus [127]. For the two registered events in which the new isotope was detected, the beam energy at the target's center (236 MeV) corresponded to 36 – 37 MeV of the excitation energy of the compound nuclei, which is sufficient for the evaporation of four neutrons. The corresponding chains of events were as follows

$$^{292}114^{*} \xrightarrow{4n} {}^{288}114 \xrightarrow[\substack{9.87\,\text{MeV}\\0.77\,\text{s}\\(1.4\,\text{s})}]{\alpha_1} {}^{284}112 \xrightarrow[\substack{9.21\,\text{MeV}\\10.3\,\text{s}\\(37\,\text{s})}]{\alpha_2} {}^{280}110 \xrightarrow[\substack{221\,\text{MeV}\\14.3\,\text{s}}]{} \text{s.f.}, \tag{105}$$

$$^{292}114^{*} \xrightarrow{4n} {}^{288}114 \xrightarrow[\substack{9.80\,\text{MeV}\\4.58\,\text{s}\\(1.4\,\text{s})}]{\alpha_1} {}^{284}112 \xrightarrow[\substack{9.13\,\text{MeV}\\18.0\,\text{s}\\(37\,\text{s})}]{\alpha_2} {}^{280}110 \xrightarrow[\substack{213\,\text{MeV}\\7.4\,\text{s}}]{} \text{s.f.} \tag{106}$$

(The figures in parentheses are estimated values of the half-lives.) Spatial marks for all the stages in the first chain lie within 0.5 mm, and in the second within 0.4 mm. The production cross section for the new nucleus ^{288}114 was approximately 1 pb. The observed chain events agree perfectly with the predictions of macro- and microscopic theories [123].

11.3 Discovery of the 118th element

Soon after the discovery of the first two isotopes of the 114th element at Dubna, news came from Berkeley of the discovery of the 118th element [128]. The search for elements resided so far from the region of superheavy elements studied previously ($Z \leqslant 112$), where the production cross sections were of order 1 pb, was undertaken in connection with theoretical predictions of an exceptionally large cross section of cold synthesis

$$^{86}_{36}\text{Kr} + {}^{208}_{82}\text{Pb} \rightarrow {}^{294}118 \rightarrow {}^{293}118 + \text{n} \tag{107}$$

(670 pb), and a long chain of α-decays for the produced nucleus ^{293}118, with estimates of the energies of the α-particles and half-lives [129]. This reaction was indeed discovered, but

its cross section proved to be much smaller (2.2 pb) than the prediction. Nevertheless, the value is two to three orders of magnitude larger than could be expected from extrapolations of the existing experimental data on lighter elements.

Reaction (107) was studied on the 88-inch cyclotron at Berkeley. The energy of the beam of ions of $^{86}_{36}$Kr at the center of the target was 449 MeV. Altogether 2.3×10^{18} ions passed through the target in the two bombardment sessions that lasted for two weeks. The experimenters used a new helium-filled separator schematically depicted in Fig. 20b. The separator consists of a vacuum chamber with two monitors at the entrance, three magnets (one quadrupole and two dipole) that form the path of the nuclei of element 118, a plane-parallel avalanche counter PPAC which recorded the time, energy, and coordinates x and y of particles, and a 300-μm 16-strip silicon detector with an active area of 80×35 mm into which the nuclei of the 118th element got implanted. The silicon detector was placed in the focal plane at a distance of 29 cm from the PPAC counter, which made it possible to measure the time of flight of the nuclei of element 118. At the exit of the separator there was a Punch-through detector which cut off the particles that passed through the detector placed in the focal plane.

The efficiency of the detector in transmitting and implanting the nuclei of element 118 was calculated by the Monte Carlo method and amounted to 75%. The same value for the separator efficiency was obtained through an experimental check via the reaction

$$^{86}_{36}\mathrm{Kr} + {}^{116}_{48}\mathrm{Cd} \rightarrow {}^{202}_{84}\mathrm{Po}\,, \tag{108}$$

which produces a number of α-active isotopes of polonium after the evaporation of several neutrons. The efficiency of the PPAC counter in distinguishing between the nuclei of the 118th element and the beam particles that had landed in the focal plane was 99%.

Altogether, in the course of bombardment, three decay chains were registered, each containing up to seven links, which with a high probability can be associated with the successive stages of decay of the 118th element:

$$^{293}118 \xrightarrow[\substack{12.37\,\mathrm{MeV}\\261\,\mu\mathrm{s}}]{\alpha_1} {}^{289}116 \xrightarrow[\substack{11.63\,\mathrm{MeV}\\1243\,\mu\mathrm{s}}]{\alpha_2} {}^{285}114 \xrightarrow[\substack{11.31\,\mathrm{MeV}\\0.708\,\mathrm{ms}}]{\alpha_3} {}^{281}112 \xrightarrow[\substack{2.41\,\mathrm{MeV}\\1.201\,\mathrm{ms}}]{\alpha_4}$$

$$^{277}110 \xrightarrow[\substack{10.18\,\mathrm{MeV}\\5.738\,\mathrm{ms}}]{\alpha_5} {}^{273}108 \xrightarrow[\substack{9.78\,\mathrm{MeV}\\1.203\,\mathrm{s}}]{\alpha_6} {}^{269}106\,, \tag{109}$$

$$^{293}118 \xrightarrow[\substack{12.41\,\mathrm{MeV}\\212\,\mu\mathrm{s}}]{\alpha_1} {}^{289}116 \xrightarrow[\substack{2.39\,\mathrm{MeV}\\1207\,\mu\mathrm{s}}]{\alpha_2} {}^{285}114 \xrightarrow[\substack{3.04\,\mathrm{MeV}\\0.741\,\mathrm{ms}}]{\alpha_3} {}^{281}112 \xrightarrow[\substack{10.67\,\mathrm{MeV}\\1.750\,\mathrm{ms}}]{\alpha_4}$$

$$^{277}110 \xrightarrow[\substack{1.33\,\mathrm{MeV}\\2.139\,\mathrm{ms}}]{\alpha_5} {}^{273}108 \xrightarrow[\substack{9.47\,\mathrm{MeV}\\2.107\,\mathrm{s}}]{\alpha_6} {}^{269}106 \xrightarrow[\substack{2.87\,\mathrm{MeV}\\21.53\,\mathrm{s}}]{?}\,, \tag{110}$$

$$^{293}118 \xrightarrow[\substack{?\\<120\,\mu\mathrm{s}}]{\alpha_1} {}^{289}116 \xrightarrow[\substack{3.46\,\mathrm{MeV}\\310\,\mu\mathrm{s}}]{\alpha_2} {}^{285}114 \xrightarrow[\substack{11.38\,\mathrm{MeV}\\1.047\,\mathrm{ms}}]{\alpha_3} {}^{281}112 \xrightarrow[\substack{10.69\,\mathrm{MeV}\\0.939\,\mathrm{ms}}]{\alpha_4}$$

$$^{277}110 \xrightarrow[\substack{10.19\,\mathrm{MeV}\\4.919\,\mathrm{ms}}]{\alpha_5} {}^{273}108 \xrightarrow[\substack{2.16\,\mathrm{MeV}\\1.810\,\mathrm{s}}]{\alpha_6} {}^{269}106 \xrightarrow[\substack{8.74\,\mathrm{MeV}\\43.10\,\mathrm{s}}]{?}\,. \tag{111}$$

The researchers noted that α_4 in the first chain, α_2, α_3, α_5, and $\alpha(\beta)_7$ in the second, and α_2 and α_6 in the third left only a fraction of their energy in the detector, while α_1 in the third chain was not registered at all due to the fact that its characteristic half-life proved to be shorter than the detector's dead time. The nature of the decay of the last nuclei in the second and third chains (α or β?) was not established. The positions of the coordinate marks for all the links of the first chain lie within a 0.6-mm interval, those for the second chain lie within a 1-mm interval, and those for the third chain within a 0.3-mm interval, which does not exceed the spread obtained through calibration measurements.

To verify the reliability of their results, the researchers estimated the probability of the compound nucleus ^{294}118 emitting an α-particle or proton instead of a neutron and found that the values were 1/60 and 1/2000, respectively. The emission of two neutrons is forbidden by energy conservation law. Thus, the results can be considered as proof of synthesis of the isotope ^{293}118 of the new superheavy element 118 and its decay products ^{289}116, ^{285}114, ^{281}112, ^{277}110, ^{273}108, and ^{269}106. Averaging the data over all three chains, the researchers obtained the following values for the respective half-lives: 120^{+180}_{-60} μs for ^{293}118, 600^{+860}_{-300} μs for ^{289}116, 580^{+870}_{-290} μs for ^{285}114, 890^{+1300}_{-450} μs for ^{281}112, $3.0^{+4.7}_{-1.5}$ ms for ^{277}110, and $1.2^{+1.7}_{-0.6}$ s for ^{273}108.

To finalize the discussion devoted to the discovery of elements 114 and 118, we would like to express not only our admiration of the achievements but also our regret that all the chains discovered at Dubna and Berkeley did not reach the region of well-studied nuclei. Therefore, strictly speaking, the last links in the chains (and hence the first ones) have not yet been fully identified, although in all the cases considered it is difficult to give an alternative explanation of the results achieved. In any case, the Dubna group was able to prove that there is a stability island in the vicinity of the 114th element, while the Berkeley group proved that it is already possible to produce elements heavier than element 114. It appears that the old question of where the Periodic Table ends (see Section 4.4) once again becomes greatly important, the more so that according to recent theoretical calculations by Rutz et al. [130] and Cwiok et al. [131] the stability maximum may occur near $Z = 120$ or even $Z = 126$.

12. Conclusions

In this review we attempted to tell the story of all the known exotic (rare, unexpected, forbidden, forgotten, etc.) modes of radioactivity of atomic nuclei and some other processes and phenomena of nuclear physics that have not, we believe, been sufficiently covered in the general-physics literature or even in the special literature, and also to give an idea of the newest achievements in this field (discovery of elements 114 and 118, detection of the cluster decay of curium, attainment of a uniquely low bound on the Majorana electron neutrino mass, etc.). Furthermore, for continuity reasons and to simplify the reading of the new material, at the beginning of the review we gave a brief survey of the history of the discoveries of natural and artificial radioactivity.

What should one expect in the near future in this field of research, i.e. will there be new discoveries or will our knowledge about the already discovered processes concerning other nuclei grow only quantitatively?

Possibly, double-proton radioactivity from the ground or isomeric state or maybe similar neutron or double-neutron radioactivity will be found.

In the area of cluster radioactivity one can expect the discovery of new, heavier clusters and progress in the

discovery of heavier nuclear emitters of clusters. In the latter case there is the unresolved problem of the possible change of the mechanism of cluster radioactivity of nuclei with a large fissionability parameter Z^2/A (although recent data suggest that the solution is close).

In the area of double β-decay considerable progress has been achieved in detecting its two-neutrino variant ($2\beta2\nu$), whose measured half-lives ($T_{1/2} > 10^{21}$ y) correspond to the results of calculations done in the Standard Model of electroweak interaction. However, so far not a single event of neutrinoless double β-decay ($2\beta0\nu$) has been registered, i.e. the problems of violation of the lepton-number conservation law and the nature of the neutrino mass (Dirac or Majorana) have yet to be resolved. The best estimate of the Majorana neutrino mass is $m_\nu^{(M)} < 0.2$ eV [$T_{1/2}(2\beta0\nu) \geqslant 5.7 \times 10^{25}$ y!].

One can only wonder whether nucleon decay with violation of the baryon-number conservation law will be discovered. Scientists in a goodly dozen laboratories, deep underground and equipped with supersensitive detectors, are wrestling with this problem. So far the estimates for the nucleon lifetime with respect to decay with $\Delta B = 1$ yield $T_{1/2} > 10^{32}$ y. Finally, new superheavy elements are sure to be discovered.

The authors would like to express their deep gratitude to P A Krupchitskiĭ, who read the entire manuscript and made many useful remarks, to A A Ogloblin for discussing the material in the section devoted to cluster radioactivity, to V I Lebedev, Yu A Mostovoĭ, and L N Bondarenko for supplying new materials, and to V N Tikhonov and A F Sustavov for the help they provided in writing the review.

References

1. Becquerel A *C. R. Acad. Sci.* **122** 501 (1896)
2. Curie P, Curie M Rapport presente on Congr. Internal. de Phys., t3 (1900)
3. Curie M *C. R. Acad. Sci.* **130** 76 (1900)
4. Rutherford E *Phys. Z.* **4** 235 (1903); *Philos. Mag.* **5** 177 (1903)
5. Geiger H, Nuttall J M *Philos. Mag.* **22** 613 (1911)
6. Gamow G *Z. Phys.* **51** 204 (1928)
7. Condon E U, Gurney R W *Nature* (London) **122** 439 (1928); *Phys. Rev.* **33** 127 (1929)
8. Joliot F, Curie I *J. Phys. Radium* **4** 494 (1933)
9. Curie I, Joliot F *C. R. Acad. Sci.* **198** 254 (1934)
10. Fermi E *Nature* (London) **133** 572, 898 (1934)
11. Alvarez L W *Phys. Rev.* **52** 134 (1937)
12. Mukhin K N *Eksperimental'naya Yadernaya Fizika* (Experimental Nuclear Physics) Book 1, Part 1: *Svoĭstva Nuklonov, Yader i Radioaktivnykh Izlucheniĭ* (Properties of Nucleons, Nuclei, and Radioactive Radiations) 5th ed. (Moscow: Energoatomizdat, 1993)
13. Kurchatov I V, Kurchatov B V, Mysovskiĭ L, Rusinov L *C. R. Acad. Sci.* **200** 1201 (1935)
14. Weizsacker C *Naturwissenschaften* **24** 813 (1936)
15. Goeppert-Mayer M *Phys. Rev.* **75** 1966 (1949); **78** 16, 22 (1950)
16. Hahn O, Strassmann F *Naturwissenschaften* **26** 756 (1939); **27** 11 (1939)
17. Fermi E et al. *Ric. Sci.* **5** (7–10) (1934); *Nature* (London) **134** 668 (1934)
18. Curie I, Savitch P *C. R. Acad. Sci.* **206** 906 (1938); *J. Phys. Radium* **9** 355 (1938)
19. Meitner L, Frisch O R *Nature* (London) **143** 239, 471 (1939)
20. Hahn O, Strassmann F *Naturwissenschaften* **27** 89 (1939)
21. Frenkel J *Phys. Rev.* **55** 987 (1939)
22. Bohr N, Wheeler J *Phys. Rev.* **56** 426 (1939)
23. Frisch O R *Nature* (London) **143** 276 (1939)
24. Joliot F *C. R. Acad. Sci.* **208** 241, 647 (1939)
25. Von Halban H, Joliot F, Kowarski L *Nature* (London) **143** 470, 1680 (1939)
26. Roberts R, Meyer R, Wang R *Phys. Rev.* **55** 510 (1939)
27. Petrzhak K A, Flerov G N *Zh. Eksp. Teor. Fiz.* **10** 1013 (1940); *Dokl. Akad. Nauk SSSR* **28** 500 (1940); *Phys. Rev.* **58** 89 (1940); *J. Phys.* **3** 275 (1940); *Usp. Fiz. Nauk* **25** 171 (1941)
28. Zel'dovich Ya B, Khariton Yu B *Zh. Eksp. Teor. Fiz.* **9** 1425 (1939); *Usp. Fiz. Nauk* **23** 329 (1940); *Zh. Eksp. Teor. Fiz.* **10** 29, 477, 831 (1940); *Usp. Fiz. Nauk* **25** 381 (1941)
29. Snell A H *Phys. Rev.* **72** 541 (1947)
30. McMillan E, Abelson R H *Phys. Rev.* **57** 1186 (1940)
31. Seaborg G T et al. *Phys. Rev.* **69** 366, 367 (1946)
32. Kennedy J W et al. *Phys. Rev.* **70** 555 (1946)
33. Polikanov S M et al. *Zh. Eksp. Teor. Fiz.* **42** 1464 (1962) [*Sov. Phys. JETP* **15** 1016 (1962)]
34. Perelygin V P et al. *Zh. Eksp. Teor. Fiz.* **42** 1472 (1962) [*Sov. Phys. JETP* **15** 1022 (1962)]
35. Flerov G N et al. *Zh. Eksp. Teor. Fiz.* **45** 1396 (1963) [*Sov. Phys. JETP* **18** 964 (1964)]
36. Flerov G N, Druin V A *Struktura Slozhnykh Yader* (The Structure of Complex Nuclei) (Moscow: Atomizdat, 1966)
37. Strutinsky V M *Nucl. Phys. A* **95** 420 (1967)
38. Polikanov S M *Izomeriya Formy Atomnykh Yader* (Nuclear Shape Isomerism) (Moscow: Atomizdat, 1977)
39. Kuznetsov V I, Skobelev N K, Flerov G N *Yad. Fiz.* **4** 99, 279 (1966); **5** 271, 1136 (1967)
40. Belov A G et al., Preprint JINR R15-9759 (Dubna: JINR, 1976)
41. Gangrskiĭ Yu P et al. *Yad. Fiz.* **27** 894 (1978) [*Sov. J. Nucl. Phys.* **27** 475 (1978)].
42. Kuznetsov V I *Fiz. Elem. Chastits At. Yadra* **12** 1285 (1981) [*Sov. J. Part. Nucl.* **12** 511 (1981)]
43. Karnaukhov V A, Ter-Akop'yan G M, Subbotin V G, Preprint JINR R-1072 (Dubna: JINR, 1962); Karnaukhov V A et al. *Zh. Eksp. Teor. Fiz.* **45** 1280 (1963) [*Sov. Phys. JETP* **18** 879 (1964)]; Flerov G N et al. *Zh. Eksp. Teor. Fiz.* **47** 419 (1964) [*Sov. Phys. JETP* **20** 278 (1965)]; *Nucl. Phys.* **60** 129 (1964)
44. Barton R, Mc Pherson R *Bull. Am. Phys. Soc.* **8** 357 (1963); Barton R et al. *Can. J. Phys.* **41** 2007 (1963)
45. Karnaukhov V A *Fiz. Elem. Chastits At. Yadra* **4** 1018 (1973)
46. Karnaukhov V A, Petrov L A *Yadra, Udalennye ot Linii Beta-Stabil'nosti* (Nuclei Far from the Beta Stability Line) (Moscow: Energoizdat, 1981)
47. Karnaukhov V A, in *Fizicheskaya Entsiklopediya* (Physics Encyclopedia) Vol. 4 (Ed.-in-chief A M Prokhorov) (Moscow: Bol'shaya Rossiĭskaya Entsiklopediya, 1994) p. 165
48. Jackson K P et al. *Phys. Lett. B* **33** 281 (1970); Cerny J et al. *Phys. Lett. B* **33** 284 (1970)
49. Cerny J et al. *Nucl. Phys. A* **188** 666 (1972)
50. Bogdanov D D et al. *Yad. Fiz.* **16** 890 (1972)
51. Hofmann S et al. *Z. Phys. A* **305** 111 (1982)
52. Kadmenskiĭ S G, in *Fizika Atomnogo Yadra i Elementarnykh Chastits* (Atomic Nuclei and Elementary Particle Physics) (Proc. 33th Winter Workshop) (St.-Petersburg: Izd. PIYaF, 1999) p. 264
53. Woods P J, Davids C N *Annu. Rev. Nucl. Part. Sci.* **47** 541 (1997)
54. Gol'danskiĭ V I *Zh. Eksp. Teor. Fiz.* **39** 497 (1960) [*Sov. Phys. JETP* **12** 348 (1960)]
55. Gol'danskiĭ V I *Usp. Fiz. Nauk* **87** 255 (1965) [*Sov. Phys. Usp.* **8** 770 (1966)]
56. Gol'danskiĭ V I *Pis'ma Zh. Eksp. Teor. Fiz.* **32** 572 (1980) [*JETP Lett.* **32** 554 (1980)]
57. Cable M D et al. *Phys. Rev. Lett.* **50** 404 (1983)
58. Azuma R E et al. *Phys. Rev. Lett.* **43** 1652 (1979)
59. Detraz C et al. *Phys. Lett. B* **94** 307 (1980)
60. Azuma R E et al. *Phys. Lett. B* **96** 31 (1980)
61. Rose H J, Jones G A *Nature* (London) **307** 245 (1984)
62. Sandulescu A, Poenaru D N, Greĭner W *Fiz. Elem. Chastits At. Yadra* **11** 1334 (1980) [*Sov. J. Part. Nucl.* **11** 528 (1980)]
63. Aleksandrov D V et al. *Pis'ma Zh. Eksp. Teor. Fiz.* **40** 152 (1984) [*JETP Lett.* **40** 909 (1984)]
64. Gales S *Phys. Rev. Lett.* **53** 759 (1984)
65. Kutshera W et al. *Phys. Rev. C* **32** 2036 (1985)
66. Price P B et al. *Phys. Rev. Lett.* **54** 297 (1985)
67. Barwick S W et al. *Phys. Rev.* **31** 1984 (1985)
68. Ogloblin A A et al. *Phys. Lett. B* **235** 35 (1990)

69. Tret'yakova S P *Fiz. Elem. Chastits At. Yadra* **23** 364 (1992) [*Sov. J. Part. Nucl.* **23** 156 (1992)]
70. Tretyakova S P, Mikheev V I *Nuovo Cimento A* **110** 1043 (1997)
71. Zamyatnin Yu S et al. *Fiz. Elem. Chastits At. Yadra* **21** 537 (1990) [*Sov. J. Part. Nucl.* **21** 231 (1990)]
72. Novatskiĭ B G, Ogloblin A A *Vestnik AN SSSR* **1** 81 (1988)
73. Kadmensky S G et al., in *Proc. Int. School on Nuclear Structure* (Alushta, USSR 1985) (Dubna: JINR, 1985) p. 385
74. Iriondo M et al. *Nucl. Phys. A* **454** 252 (1986)
75. Biendowske R, Walliser H *Phys. Rev. Lett.* **61** 1930 (1988)
76. Poenaru D N et al. *J. Phys. G* **10** L183 (1984)
77. Yi-Jin Shi Y S, Swiatecki W J *Phys. Rev. Lett.* **54** 300 (1985)
78. Poenaru D N et al., Preprint JINR E4-84-446 (Dubna: JINR, 1984)
79. Poenaru D N et al. *Phys. Rev. C* **32** 572 (1985)
80. Pik-Pichak G A *Yad. Fiz.* **44** 1421 (1986) [*Sov. J. Nucl. Phys.* **44** 923 (1986)]
81. Poenaru D N et al. *Z. Phys. A-Hadron Nucl.* **325** 435 (1986)
82. Poenaru D N et al. *Atom. Data Nucl. Data Tables* **34** 423 (1986)
83. Mikheev V I et al., FLNR Scientific Report 1991-92. E7-93-57 (Dubna: JINR, 1993) p. 48
84. Ogloblin A A et al., in *Proc. Intern. Conf. SHELL–99* (Dubna, April 1999); *Phys. Rev. C* **61** 034301 (2000)
85. Gönnenwein F *Nucl. Phys. A* **654** 855 (1999)
86. Furman V I Private communication to Ogloblin A A
87. Goeppert-Mayer M *Phys. Rev.* **48** 512 (1935)
88. Majorana E *Nuovo Cimento* **14** 171 (1937)
89. Inghram M G, Reynolds J H *Phys. Rev.* **76** 1265 (1949)
90. Bernatowicz T et al. *Phys. Rev. Lett.* **69** 2341 (1992)
91. Bernatowicz T et al. *Phys. Rev. C* **47** 806 (1993)
92. Kirsten T et al., in *Proc. Intern. Conf. Mass Spectroscopy: Kyoto 1969* (Tokyo, 1970) p. 501
93. Lou K et al., in *Proc. IV Intern. Symposium on Weak and Electromagnetic Interactions in Nuclei* (Osaka, Japan, 12–16 June 1995) (Eds H Ejiri, T Kishimoto, T Sato) (Singapore: World Scientific, 1995) p. 192
94. Klapdor-Kleingrothaus H V, in *Proc. IV Intern. Symposium on Weak and Electromagnetic Interactions in Nuclei* (Osaka, Japan, 12–16 June 1995) (Eds H Ejiri, T Kishimoto, T Sato) (Singapore: World Scientific, 1995) p. 174
95. Balysh A et al. *Phys. Lett. B* **356** 450 (1995)
96. Hubert Ph, in *Proc. IV Intern. Symposium on Weak and Electromagnetic Interactions in Nuclei* (Osaka, Japan, 12–16 June 1995) (Eds H Ejiri, T Kishimoto, T Sato) (Singapore: World Scientific, 1995) p. 184
97. Baudis L et al. *Phys. Rev. Lett.* **83** 41 (1999)
98. Kozlov Yu V, Martem'yanov V P, Mukhin K N *Usp. Fiz. Nauk* **167** 849 (1997) [*Phys. Usp.* **40** 807 (1997)]
99. Abov Yu G, Krupchitsky P A, Oratovsky Yu A *Phys. Lett.* **12** 25 (1964); *Yad. Fiz.* **1** 479 (1965)
100. Lobashev V M et al. *Pis'ma Zh. Eksp. Teor. Fiz.* **3** 268 (1966) [*JETP Lett.* **3** 173 (1966)]
101. Hättig H, Hünchen K, Wäffer H *Phys. Rev. Lett.* **25** 941 (1970)
102. Danilyan G V *Usp. Fiz. Nauk* **131** 329 (1980) [*Sov. Phys. Usp.* **23** 323 (1980)]
103. Sushkov O P, Flambaum V V *Usp. Fiz. Nauk* **136** 3 (1982) [*Sov. Phys. Usp.* **25** 1 (1982)]
104. Snell A H, Miller L C *Phys. Rev.* **74** 1217 (1948)
105. Spivak P E et al., in *Doklady Sovetskoĭ Delegatsii na Mezhdunarodnoĭ Konferentsii po Mirnomu Ispol'zovaniyu Atomnoĭ Energii: Fizicheskie Issledovaniya* (Reports of the USSR Delegation at the Intern. Conf. on Peaceful Uses of Atomic Energy: Physics Studies) (Geneva, 1955) (Moscow: Izd. Akad. Nauk SSSR, 1955) p. 935
106. Robson J M *Phys. Rev.* **77** 747 (1950); **78** 311 (1950)
107. Spivak P E *Zh. Eksp. Teor. Fiz.* **94** (9) 1 (1988) [*Sov. Phys. JETP* **67** 1735 (1988)]
108. Zel'dovich Ya B *Zh. Eksp. Teor. Fiz.* **36** 1952 (1959) [*Sov. Phys. JETP* **9** 1389 (1959)]
109. Shapiro F L *Usp. Fiz. Nauk* **95** 145 (1968) [*Sov. Phys. Usp.* **11** 345 (1968)]
110. Mampe W et al. *Pis'ma Zh. Eksp. Teor. Fiz.* **57** 77 (1993) [*JETP Lett.* **57** 82 (1993)]
111. Arzumanov S et al., in *Proc. Inter. Nuclear Physics Conference* held in Paris, France on 24–28 August 1998, B2, p. 709
112. Mostovoy Yu, Preprint IAE-6040/2 (Moscow: IAE, 1997); Erozolimskiĭ B G, Kuznetsov I A, Mostovoĭ Yu A, Stepanenko I V *Yad. Fiz.* **61** 1418 (1998) [*Phys. Atom. Nuclei* **61** 507 (1998)]
113. Mostovoĭ Yu A, Mukhin K N, Patarakin O O *Usp. Fiz. Nauk* **166** 987 (1996) [*Phys. Usp.* **39** 925 (1996)]
114. Chamberlain O et al. *Phys. Rev.* **100** 947 (1955)
115. Pomeranchuk I Ya *Zh. Eksp. Teor. Fiz.* **34** 725 (1958) [*Sov. Phys. JETP* **7** 499 (1958)]
116. Cork B et al. *Phys. Rev.* **104** 1193 (1956)
117. Antipov Yu M et al. *Yad. Fiz.* **12** 311 (1970)
118. Baldin B Yu et al. *Yad. Fiz.* **20** 694 (1974)
119. Oganessian Yu et al., Preprint JINR E7-99-53 (Dubna: JINR, 1999); Oganessian Yu et al. *Phys. Rev. Lett.* **83** 3154 (1999)
120. Oganessian Yu et al., Preprint JINR E7-99-111 (Dubna: JINR, 1999); Oganessian Yu et al. *Nature* (London) **400** 242 (1999)
121. Postylnik B I, in *Proc. Intern. School-Seminar "Heavy Ion Physics": Dubna–1997* (Singapore: World Scientific, 1998) p. 431
122. Oganessian Yu et al., Preprint JINR E7-99-347 (Dubna: JINR, 1999); submitted to *Phys. Rev. Lett.*
123. Smolanczuk R *Phys. Rev. C* **56** 812 (1997)
124. Lazarev Yu A et al. *Phys. Rev. Lett.* **73** 624 (1994); *Phys. Rev. Lett.* **75** 1903 (1995); *Phys. Rev. C* **54** 620 (1996)
125. Hofmann S et al. *Z. Phys. A* **354** 229 (1996)
126. Oganessian Yu Ts et al., Preprint JINR E7-98-212 (Dubna, 1998); *Eur. Phys. J. A* **5** 63 (1999)
127. Myers W D, Swiatecki W J *Nucl. Phys. A* **601** 141 (1996)
128. Ninov V et al. *Phys. Rev. Lett.* **83** 1104 (1999)
129. Smolanczuk R *Phys. Rev. C* **59** 2634 (1999)
130. Rutz K et al. *Phys. Rev. C* **56** 238 (1997)
131. Cwiok S et al. *Nucl. Phys. A* **611** 211 (1996)